PNNL-13378

Results of Detailed Hydrologic Characterization Tests – Fiscal Year 1999

F. A. Spane, Jr.
P. D. Thorne
D. R. Newcomer

January 2001

Prepared for the U.S. Department of Energy
under Contract DE-AC06-76RL01830

DISCLAIMER

PACIFIC NORTHWEST NATIONAL LABORATORY
operated by
BATTELLE
for the
UNITED STATES DEPARTMENT OF ENERGY
under Contract DE-AC06-76RL01830

Printed in the United States of America

Available to DOE and DOE contractors from the
Office of Scientific and Technical Information,
P.O. Box 62, Oak Ridge, TN 37831-0062;
ph: (865) 576-8401
fax: (865) 576-5728
email: reports@adonis.osti.gov

Available to the public from the National Technical Information Service,
U.S. Department of Commerce, 5285 Port Royal Rd., Springfield, VA 22161
ph: (800) 553-6847
fax: (703) 605-6900
email: orders@ntis.fedworld.gov
online ordering: http://www.ntis.gov/ordering.htm


This document was printed on recycled paper.
(8/00)

PNNL-13378

Results of Detailed Hydrologic Characterization Tests – Fiscal Year 1999

F. A. Spane, Jr.
P. D. Thorne
D. R. Newcomer

January 2001

Prepared for
the U.S. Department of Energy
under Contract DE-AC06-76RL01830

Pacific Northwest National Laboratory
Richland, Washington 99352

Abstract

This report provides the results of detailed hydrologic characterization tests conducted within newly constructed Hanford Site wells during fiscal year 1999. Detailed characterization tests performed included groundwater-flow characterization; barometric response evaluation; slug tests; single-well tracer tests; constant-rate pumping tests; and in-well, vertical flow tests. Hydraulic property estimates obtained from the detailed hydrologic tests include transmissivity; hydraulic conductivity; specific yield; effective porosity; in-well, lateral flow velocity; aquifer-flow velocity; vertical distribution of hydraulic conductivity (within the well-screen section); and in-well, vertical flow velocity. In addition, local groundwater-flow characteristics (i.e., hydraulic gradient and flow direction) were determined for four sites where detailed well testing was performed.

Summary

The Pacific Northwest National Laboratory,[(a)] as part of the Hanford Groundwater Monitoring Project, examines the potential for offsite migration of contamination within underlying aquifer systems. Hydraulic property estimates obtained from the analysis of hydrologic tests are important for evaluating aquifer-flow characteristics (i.e., groundwater-flow velocity) and transport travel time. This report presents test results obtained from the detailed hydrologic characterization program of the unconfined aquifer system conducted for the Hanford Groundwater Monitoring Project during fiscal year (FY) 1999. Hydrologic tests conducted as part of the detailed program include the following:

- slug testing (10 wells tested)
- tracer-dilution tests (4 wells tested)
- tracer-pumpback tests (4 wells tested)
- constant-rate pumping tests (4 wells tested)
- vertical flow, in-well tracer tests (2 wells tested).

Hydraulic property estimates obtained from the detailed hydrologic tests include hydraulic conductivity; transmissivity; specific yield; effective porosity; in-well, lateral, groundwater-flow velocity; aquifer-flow velocity; vertical distribution of hydraulic conductivity; and in-well, vertical flow velocity. In addition, local groundwater-flow characteristics (i.e., hydraulic gradient, flow direction) were determined for four sites that had detailed well testing performed. Pertinent results from the FY 1999 detailed characterization program are summarized below.

Slug-test results provided hydraulic conductivity estimates for the Ringold Formation (gravel Unit E) that range between 0.88 and 9.5 m/d for the nine 200-West Area wells and 24.2 m/d for the Hanford formation at the one 200-East Area well tested. The results fall within the previously reported slug-test values for the Ringold and Hanford formations within the 200-West and 200-East Areas.

The hydraulic conductivity estimates derived from slug tests correspond closely with values obtained from constant-rate pumping tests and fall within the error range commonly reported for slug tests in aquifer characterization studies (i.e., within a factor of ~2 or less). The close correspondence is attributed, in part, to improved analysis methods for slug tests. The close correspondence between slug-test and pumping-test hydraulic conductivity estimates also indicates that the tested formation can be represented as a homogeneous unit at the slug-test or larger scale.

Constant-rate pumping-test results for transmissivity ranged between 66 and 345 m^2/d (average 157 m^2/d). These values fall within to slightly below recently calculated values for the central 200-West Area. The recent estimates were based on the analysis of the induced areal composite pumping/injection effects of the 200-ZP-1 pump-and-treat system, which produced large-scale estimates that range between 230 and 430 m^2/d (average 325 m^2/d).

(a) Pacific Northwest National Laboratory is operated for the U.S. Department of Energy by Battelle.

Pumping-test results also correspond fairly closely for specific yield, ranging between 0.11 and 0.17. These results coincide with previously reported estimates of 0.11 and 0.17 for the 200-West Area. These earlier estimates were based on analyzing the growth and decline of the groundwater mound beneath the 200-West Area associated with wastewater-disposal practices in the area.

Tracer-dilution test results indicated that two of the four sites (i.e., wells 299-W10-26 and -W14-13) exhibited in-well, downward, vertical flow conditions that compromise the results of this characterization test. The indicated flow condition within the wells was corroborated using two additional test methods: in-well vertical tracer tests and electromagnetic flow-meter surveys. The fact that the tracer tests and flow-meter survey were conducted nearly 8 months apart, and still provided consistent results, suggests that the downward vertical flow condition is a persistent characteristic at these well sites.

Estimates for average, in-well, lateral flow velocity from tracer-dilution tests for the two sites not exhibiting vertical flow ranged between 0.012 to 0.170 m/d. The highest value (0.170 m/d) was calculated for well 299-W19-42, which is located near the 200-ZP-1 extraction well pump-and-treat facilities. This well is within the potential radius of influence of the pump-and-treat system, which could produce elevated in-well flow velocities.

A comparison of the observed depth versus velocity profiles from tracer-dilution tests provided information about the permeability distribution within the well-screen sections at two well sites. At well 299-W10-24, the highest flow velocities (and inferred permeabilities) were exhibited near the middle of the screen, with lowest flow velocities indicated near the top. In contrast, well 299-W19-42 exhibited relatively uniform depth well-velocity profiles, indicating homogeneous permeability conditions throughout the well-screen section.

Estimates for effective porosity from the two reportable tracer-pumpback tests ranged between 0.027 and 0.072. This range falls within to slightly below that commonly reported for semiconsolidated to unconsolidated alluvial aquifers of 0.05 to 0.30 and is slightly below the large-scale values for specific yield (0.11 and 0.17) derived from the constant-rate pumping-test results.

Estimates for groundwater-flow velocity within the aquifer from the two reportable tracer-pumpback tests ranged between 0.029 and 0.419 m/d and, generally, are within a factor of 2.5 of the calculated in-well flow velocities. As noted previously for well 299-W19-42, the calculated aquifer-flow velocity estimate (0.419 m/d) at this well site may be elevated as a result of the effects imposed by operation of the adjacent 200-ZP-1 pump-and-treat system.

Groundwater-flow characterization results for the four detailed hydrologic characterization sites, based on trend-surface analysis of surrounding well water-level elevations, provided hydraulic gradients that range between 0.00073 and 0.00184. The trend-surface analysis results also indicated easterly and southerly groundwater-flow directions. The hydraulic gradient and flow-direction calculations are consistent with previous generalizations for these areas.

Acknowledgments

Several Pacific Northwest National Laboratory staff contributed to the performance of the hydrologic tests presented in this report. In particular, Kirk Cantrell provided laboratory and field support for the tracer tests. Bill Webber participated in the performance and data acquisition of some of the field slug tests. The field testing personnel and test equipment support provided by Waste Management, Inc. is also acknowledged.

In addition, Pacific Northwest National Laboratory staff also provided significant contributions to this report's preparation. Technical peer review comments were provided by Tyler Gilmore and Stuart Luttrell. The detailed editorial review given by Bev Johnston is also acknowledged. Thanks are also extended to Signe Wurstner for providing hydrologic testing software support.

Nomenclature

A	=	cross-sectional area within well screen; L^2
b	=	aquifer thickness; L
C	=	tracer concentration in the test interval at time, t; M/L^3
C_o	=	initial tracer concentration in well at the start of the test; M/L^3
C_t	=	average tracer concentration in well at test termination; M/L^3
Δh_w	=	water-level change over the last hour; L
Δh_{ai}	=	barometric pressure change over the last hour; L
Δh_{ai-1}	=	barometric pressure change from 2 h to 1 h previous; L
Δh_{ai-n}	=	barometric pressure change from n hours to (n-1) hour previous; L
H_o	=	theoretical slug test stress level; L
H_p	=	projected or observed slug test stress level; L
I	=	hydraulic gradient; dimensionless
K	=	hydraulic conductivity; L/T
K_D	=	vertical anisotropy (K_v/K_h); dimensionless
K_h	=	hydraulic conductivity in the horizontal direction; L/T
K_{hx}/K_{hy}	=	horizontal anisotropy; dimensionless
K_{snd}	=	hydraulic conductivity of sandpack; L/T
K_v	=	hydraulic conductivity in the vertical direction; L/T
L	=	saturated thickness of test interval within well-screen section; L
M_i	=	initial tracer mass emplaced in well; M
M_r	=	tracer mass recovered during pumpback; M
M_w	=	tracer mass in well and sandpack at time of pumpback; M
$M_{50\%}$	=	50% of the tracer mass within the aquifer; M
n	=	number of hours that lagged barometric effects are apparent; dimensionless
n_e	=	effective porosity; dimensionless
Q	=	pumping rate; L^3/T
Q_{avg}	=	average pumping rate; L^3/T
Q_w	=	in-well, lateral groundwater discharge within the well test interval; L^3/T
r_c	=	well casing radius; L
r_{eq}	=	equivalent well casing radius; L
r_{obs}	=	radial distance from pumped well to monitor well location; L
r_{snd}	=	sandpack radius; L
r_t	=	equivalent radius of tracer measurement system; L
r_w	=	radius of pumping well; L
s	=	drawdown; L
S	=	storativity; dimensionless
S_s	=	specific storage; 1/L
S_y	=	specific yield; dimensionless
T	=	transmissivity; L^2/T
t	=	time; T

t_d = tracer dilution or drift time; T

t_p = pumping time required to recover 50% of the tracer; T

t_t = total elapsed tracer time, equal to $t_d + t_p$; T

V = test interval well volume; L^3

v_a = groundwater-flow velocity within aquifer; L/T

v_w = groundwater-flow velocity within well; L/T

v_{wz} = groundwater-flow velocity for individual depths within well; L/T

$X_0 \ldots X_n$ = regression coefficients corresponding to time lags of 0 to n hours; dimensionless

Y_o = slug test stress level; L

σ = dimensionless unconfined aquifer parameter, equal to S/S_y

$\propto$ = groundwater-flow distortion factor; dimensionless, common range 0.5 to 4

Contents

Figures

Tables

1.0 Introduction

Pacific Northwest National Laboratory's Hanford Groundwater Monitoring Project assesses the potential for onsite and offsite migration of contamination within the shallow, unconfined, aquifer system and the underlying, upper, basalt-confined aquifer system at the Hanford Site. As part of this activity, detailed hydrologic characterization tests are conducted within wells at selected Hanford Site locations to provide hydraulic property information and groundwater-flow characterization for the unconfined aquifer. Results obtained from these characterization tests provide hydrologic information that supports the needs of the sitewide groundwater-monitoring and -modeling programs and reduces the uncertainty of groundwater-flow conditions at selected locations on the Hanford Site.

This report is the first of a series that provides the results of detailed hydrologic characterization tests conducted within newly constructed Hanford Site wells. In this report, results conducted during fiscal year (FY) 1999 are presented. The various characterization elements employed in FY 1999, as part of the detailed hydrologic characterization program, include the following:

- groundwater-flow characterization — for quantitative determination of groundwater-flow direction and hydraulic gradient conditions

- barometric response evaluation — for determining well-response characteristics to barometric fluctuations, estimating vadose zone transmission characteristics, and removal of barometric pressure effects from hydrologic test responses

- slug testing — for evaluating well-development conditions and providing preliminary hydraulic property information (e.g., hydraulic conductivity) for design of subsequent hydrologic tests

- tracer-dilution test — for determining the vertical distribution of hydraulic conductivity and/or groundwater-flow velocity within the well-screen section and for identifying vertical flow conditions within the well column

- tracer-pumpback test — for characterizing effective porosity and average, aquifer, groundwater-flow velocity

- constant-rate pumping test — conducted in concert with tracer-pumpback phase and analysis of draw-down and recovery data provides quantitative hydraulic property information (e.g., transmissivity, hydraulic conductivity, storativity, specific yield)

- in-well vertical tracer test — for calculating in-well, vertical flow velocity within the well-screen section.

Newly constructed *Resource Conservation and Recovery Act of 1976* (RCRA) wells selected for characterization during FY 1999 include the following:

Well	RCRA Waste Management Area
299-W10-23	T
299-W10-24	T
299-W10-26	TX-TY
299-W14-13	TX-TY
299-W14-14	TX-TY
299-W15-40	TX-TY
299-W19-41	U
299-W19-42	U
299-W22-79	216-U-12 Crib
299-E33-44	B-BX-BY

The new RCRA wells are all constructed of 10.16-cm-diameter stainless-steel casing with wire-wrapped stainless-steel screens and sand pack. These wells were constructed either to replace older wells that are going dry because of the declining water table (e.g., 200-West Area) or for additional areal coverage. In most cases, the replacement wells are within 5 m of an existing well, which was used for observation well measurements during hydrologic testing. All new wells are screened across the water table and penetrate approximately the top 10 m of the aquifer. Four of the test wells (299-W10-24, -W10-26, -W14-13, and -W19-42) were selected for detailed hydrologic characterization. Figure 1.1 shows the location of the wells tested during FY 1999 in relationship to the 200-West and 200-East Areas of the Hanford Site. The boundaries of the various RCRA waste management areas are shown on site maps contained in Hartman (1999). Table 1.1 provides pertinent as-built and well-completion information for the identified new wells.

This report presents the results of various hydrologic characterization activities conducted at these well sites during FY 1999. Section 2.0 describes the hydrogeologic setting of the 200-West and 200-East Areas, where the test wells are located. Performance and methods used for analyzing the various test elements are described in Section 3.0. Section 4.0 presents results obtained from slug testing. Tracer-dilution and -pumpback results obtained for four selected test well sites are contained in Sections 5.0 and 6.0, respectively. Section 7.0 presents the results obtained from the constant-rate pumping tests. Calculations of in-well vertical flow determinations are discussed in Section 8.0. Conclusions are given in Section 9.0, followed by references cited in the text in Section 10.0. An appendix of selected barometric analysis plots is provided. Also, a list of the scientific nomenclature used throughout this report is provided on page ix.

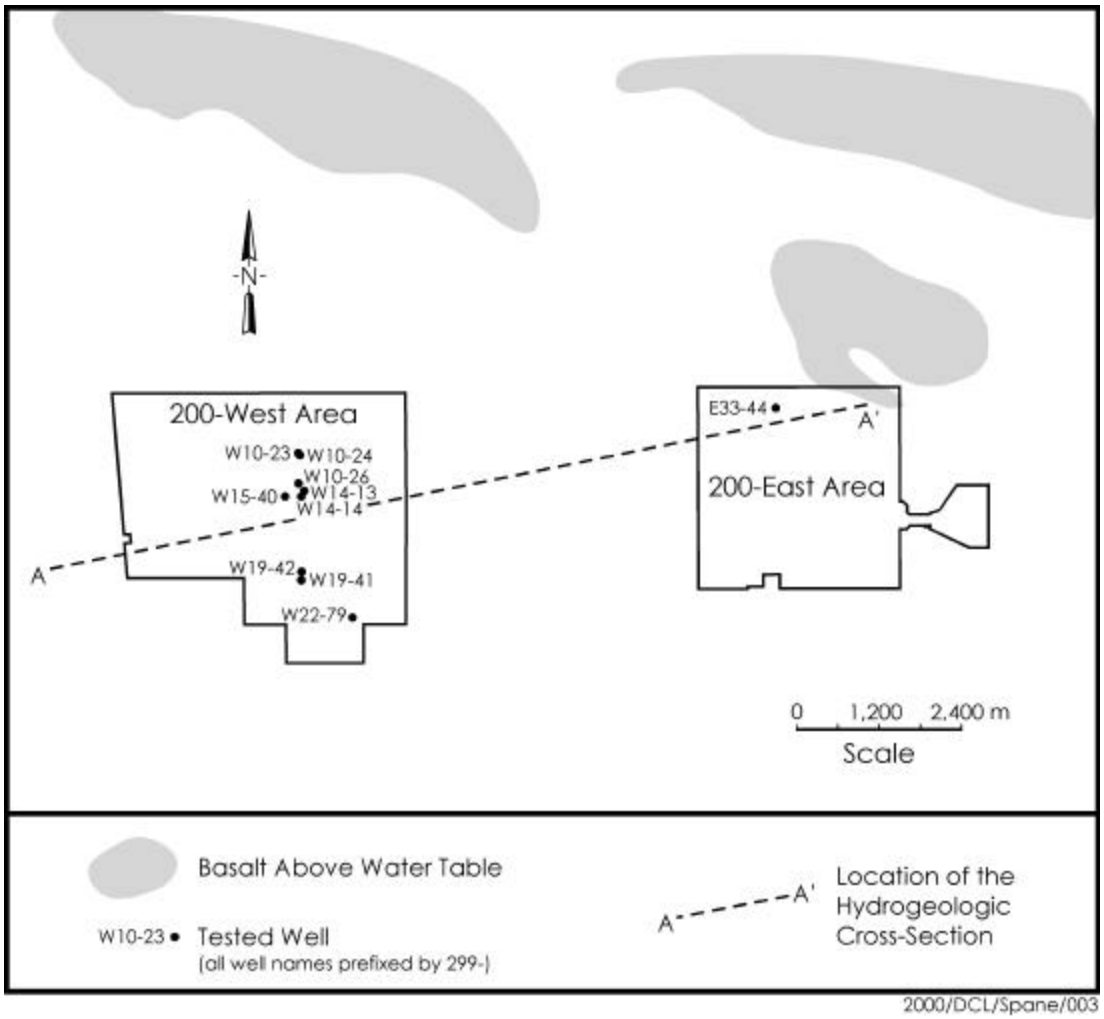

Figure 1.1. Location Map of Wells Tested During Fiscal Year 1999

Table 1.1. Pertinent As-Built Information for Wells Tested During Fiscal Year 1999

Well	Ground Surface/Brass-Cap Elevation, m, MSL (NAVD88)	Well-Screen Depth Below Ground Surface/Brass Cap, m	Saturated Well-Screen Section, m MSL (NAVD88)
299-W10-23	206.69	68.82 - 79.52	137.87 - 127.17 (10.70)[(a)]
299-W10-24	208.98	71.00 - 81.70	137.98 - 127.28 (10.70)
299-W10-26	204.67	66.15 - 76.85	138.52 - 127.82 (10.70)
299-W14-13	204.35	66.03 - 76.73	138.32 - 127.62 (10.70)
299-W14-14	204.62	66.14 - 76.81	138.48 - 127.81 (10.67)
299-W15-40	205.06	66.43 - 77.13	138.63 - 127.93 (10.70)
299-W19-41	205.78	67.07 - 77.77	138.71 - 128.01 (10.70)
299-W19-42	205.51	67.14 - 77.84	138.37 - 127.67 (10.70)
299-W22-79	210.94	73.97 - 84.67	136.97 - 126.27 (10.70)
299-E33-44	196.03	72.54 - 77.11	123.49 - 118.92 (4.57)

(a) Number in parentheses is saturated thickness.
MSL = mean sea level.
NAVD88 = North American Vertical Datum of 1988.

2.0 Hydrogeologic Setting

The hydrogeology of the 200-West and 200-East Areas is described below in terms of two classification systems used for the Hanford Site consolidated groundwater model: the first is based on hydrogeologic units (Thorne et al. 1993) and the second is based strictly on geology (Lindsey 1995). The hydrogeologic classification system subdivides units based on texture, which correlates to hydraulic properties. This geologic classification is based on the lithologic and stratigraphic relationships defined by Lindsey (1995). A comparison of the two classifications is shown in Figure 2.1. The major classification system difference in the vicinity of the 200 Areas is the grouping of the lower sand-dominated portion of Lindsey's upper Ringold with Ringold gravel units E and C to form Thorne's hydrogeologic unit 5. A general west-to-east cross section in Figure 2.2 shows the hydrogeologic units underlying the 200-West and 200-East Areas. Figure 1.1 shows the surface trace of the cross section in relationship to the test wells described in this report.

The brief hydrogeologic description for the 200-West and 200-East Areas presented below is taken primarily from the following reports: Graham et al. (1984), Lindsey et al. (1992), Connelly et al. (1992a, 1992b), Thorne et al. (1993), Lindsey (1995), and Williams et al. (2000).

2.1 Hydrogeology of the 200-West Area

The aquifer system above the basalt bedrock in the 200-West Area comprises two aquifer systems: an unconfined aquifer and an underlying, locally confined aquifer. The unconfined aquifer lies almost entirely within unit 5 of the Ringold Formation (geologic unit E) (see Figure 2.1) and is composed of fluvial, gravel-dominated sediments with a fine-sand matrix. The FY 1999 results for test wells located in the 200-West Area are reflective of this hydrogeologic unit (unit 5). Sediments within unit 5 exhibit variable degrees of cementation, ranging from partially to well developed. Cemented zones up to several meters thick and extending laterally over several hundred meters have been identified in the 200-West Area. Thin, laterally discontinuous, sand and silt beds are also intercalated in the gravelly deposits.

The lower Ringold mud (unit 8), consisting of overbank and lacustrine deposits, underlies the unconfined aquifer. This mud unit is continuous over the entire 200-West Area but is absent just north of the 200-West Area, where it pinches out. The lower mud unit generally thickens and dips to the south and southwest. The top of the mud unit, which has an irregular surface, forms the lower boundary of the unconfined aquifer in the 200-West Area.

The lower mud separates the unconfined aquifer from an underlying confined aquifer, which is composed of unit 9 (the gravel portion of geologic unit A). Unit 9 is composed of fluvial gravels with lesser amounts of intercalated sands and silts. This basal unit, which lies directly above the basalt bedrock, thickens and dips to the south and southwest. The uppermost basalt formation beneath the 200-West Area is the Saddle Mountains Basalt.

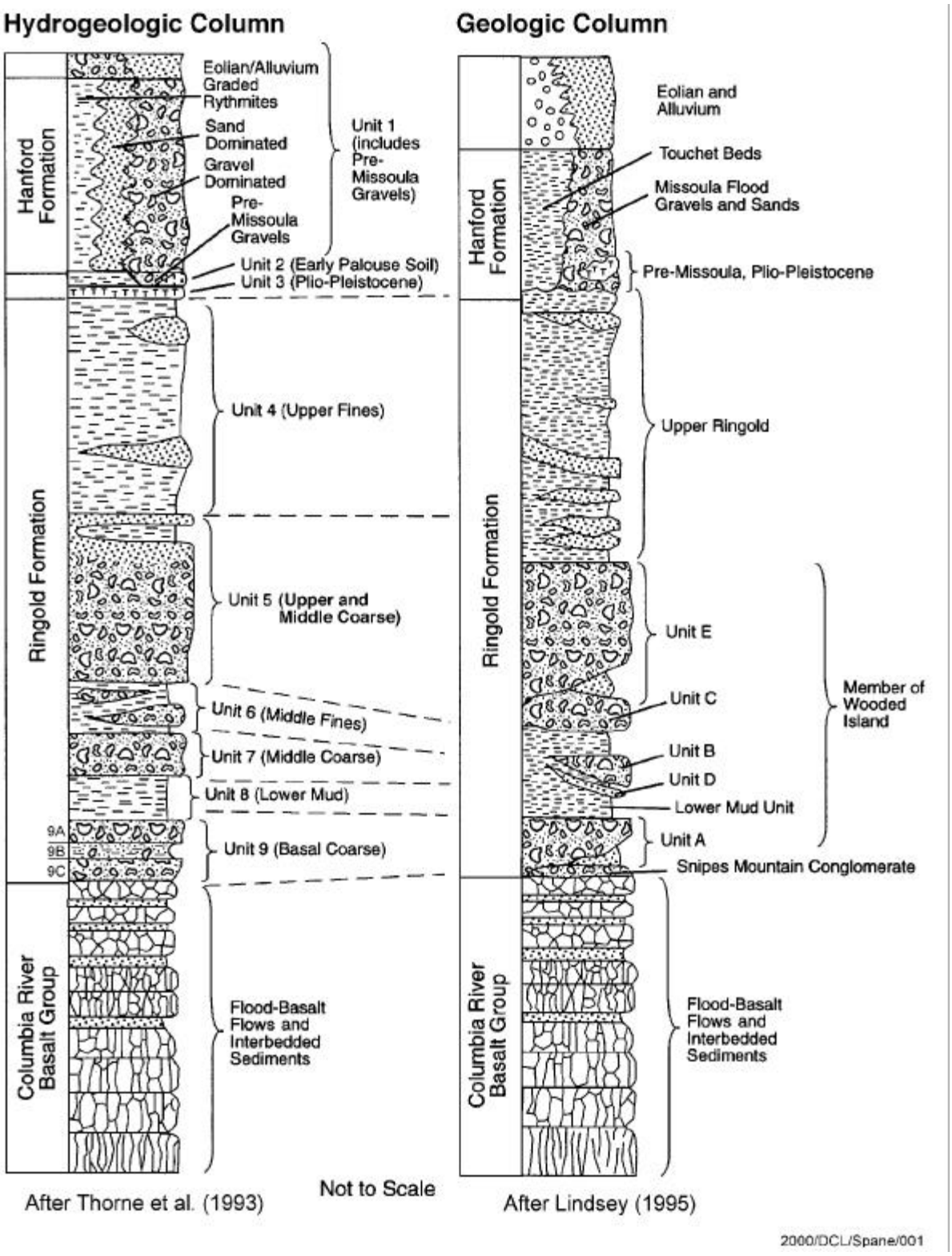

Figure 2.1. Stratigraphic Relationships of Various Hydrogeologic Units

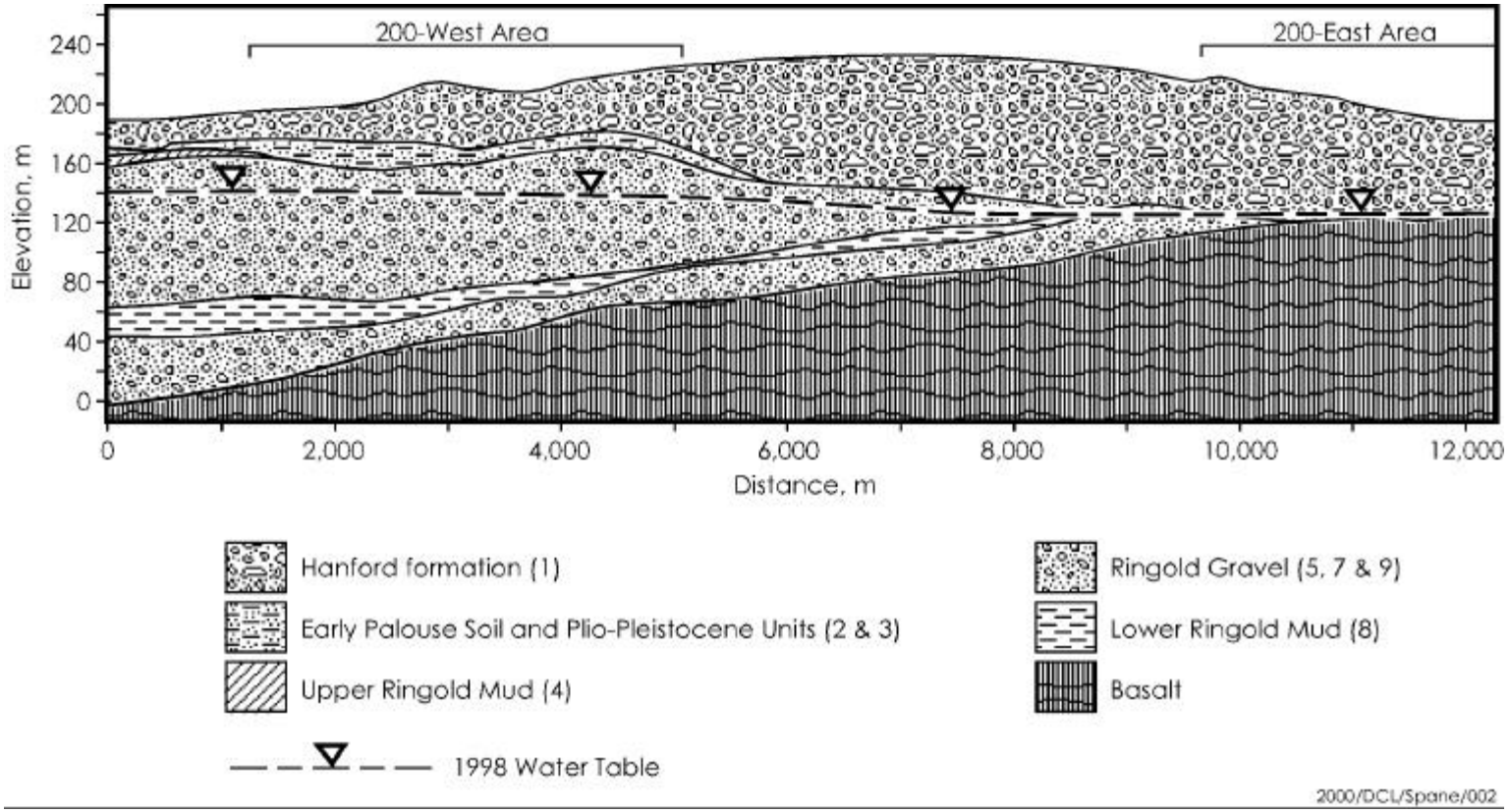

Figure 2.2. Hydrogeologic Cross Section Through 200-West and 200-East Areas

2.2 Hydrogeology of the 200-East Area

As in the 200-West Area, the aquifer system above the basalt in the 200-East Area consists of the unconfined aquifer and, in some places, a locally confined aquifer that underlies unit 8 (lower Ringold mud). The unconfined aquifer within the 200-East Area lies within the Hanford formation (unit 1) and/or Ringold Formation gravel (units 5, 7, and 9) (see Figure 2.1). In the northern part of the 200-East Area, the unconfined aquifer is thin in locations where the basalt surface forms subsurface highs. In these locations, the unconfined aquifer lies almost entirely within unit 1. This is the case at well 299-E33-44, which was tested during FY 1999. Unit 1 consists primarily of unconsolidated gravel- and sand-dominated sediments, with silt-dominated sediments becoming more common to the south. These undifferentiated sediments represent post-Ringold Formation glaciofluvial deposits from cataclysmic flooding. Because of the preponderance of unconsolidated gravel and sand-dominated deposits, unit 1 generally exhibits the highest permeabilities of the hydrogeologic units shown in Figure 2.1.

The lower boundary of the unconfined aquifer in the 200-East Area is defined by the top of unit 8, the top of unit 9B (a fine-grained subunit of unit 9), or the top of basalt. To the north of the 200-East Area, the lower Ringold Formation units and underlying upper basalt flows were extensively eroded by the Missoula floods at the time the Hanford formation was deposited. Previous reports have indicated that direct hydrogeologic communication between the unconfined and underlying, upper, basalt-confined aquifer is likely in these areas (Gephart et al. 1979; Graham et al. 1984; Spane and Webber 1995).

Ringold Formation unit 8, which represents the confining mud unit separating the overlying, unconfined aquifer from the underlying, confined, basal Ringold aquifer within unit 9, is composed primarily of low-permeability, fluvial overbank, paleosol, and lacustrine silts and clay, with minor amounts of sand and gravel. As indicated in Figure 2.1, unit 9 is composed of local subunits. Unit 9B consists of poorly characterized silt- to clay-rich zones and represents a relatively thin, low-permeability, local confining unit within the basal Ringold gravel. East of the 200-East Area near the 216-B-3 Pond facility, confining units 8 and 9B extend above the regional water table.

Subunits 9A and 9C are composed primarily of fluvial gravels, and collectively make up the Ringold confined aquifer within the southern part of the 200-East Area and near the 216-B-3 Pond facility east of the 200-East Area. The Ringold confined aquifer is defined by the lateral boundary of confining layer unit 8. Where unit 8 has been removed by erosion, the basal Ringold gravel forms part of the unconfined aquifer. The Ringold confined aquifer thickens to the south and is bounded below by the top of the Saddle Mountains Basalt.

3.0 Detailed Test Characterization Methods

This report provides the results of detailed hydrologic characterization tests conducted within newly constructed Hanford Site wells during FY 1999. Detailed characterization tests performed included groundwater-flow characterization, barometric response evaluation, slug tests, single-well tracer tests (tracer-dilution, tracer-pumpback, and in-well vertical flow tests), and constant-rate pumping tests. Table 3.1 provides a summary of the various hydrologic characterization elements. More in-depth descriptions of the methods used to analyze slug tests, various single-well tracer tests, and constant-rate pumping tests are provided below.

3.1 Slug Tests

Because of their ease of implementation and relatively short duration, slug tests are commonly used to provide initial estimates of hydraulic properties (e.g., range and spatial/vertical distribution of hydraulic conductivity, K). Because of the small displacement volumes employed during slug tests, hydraulic properties determined, using this characterization method, are representative of conditions relatively close to the well. For this reason, slug-test results are commonly used in the design of subsequent hydrologic tests having greater areas of investigation (e.g., slug interference [Novakowski 1989; Spane 1996; Spane et al. 1996], constant-rate pumping tests [Butler 1990; Spane 1993]).

Table 3.1. Detailed Hydrologic Characterization Elements

Element	Activities	Results
Groundwater-flow characterization	Trend-surface analysis of well water-level data	Quantitative determination of groundwater-flow direction and hydraulic gradient
Barometric response evaluation	Well water-level response characteristics to barometric changes	Aquifer-/well-model identification, vadose zone property characterization, correction of hydrologic test responses for barometric pressure fluctuations
Slug test	Multistress-level tests conducted at each well site	Local K_h, T of aquifer surrounding well site
Tracer-dilution test	Monitoring dilution of administered tracer at injection well site	Determination of v_w and vertical distribution of K_h
Tracer-pumpback test	Pumping/monitoring of recovered tracer and associated pressure response in monitor wells	Local- to intermediate-scale n_e and v_a
In-well vertical tracer test	Monitoring the vertical movement of tracer within the well screen	Determination of v_w within the monitor well-screen section
Constant-rate pumping test	Pumping/monitoring of pressure response in monitor wells	Intermediate to large-scale, K_h, K_v/K_h, K_{hx}/K_{hy}, T, S, S_y
Note: See Nomenclature for definitions.		

Slug tests conducted as part of the FY 1999 detailed characterization program were performed by removing a slugging rod (withdrawal test) of known displacement volume. Slug-withdrawal tests were employed rather than slug-injection tests (i.e., by rapidly immersing the slugging rod) because of their reported superior results for unconfined aquifer tests where the water table occurs within the well-screen section (e.g., Bouwer 1989). At all test sites, two different size slugging rods were used to impart varying stress levels for individual slug tests. The slug tests were repeated at each stress level to assess reproducibility of the test results. Comparison of the normalized slug-test responses is useful for assessing the effectiveness of well development and the presence of near-well heterogeneities and dynamic skin effects, as noted in Butler et al. (1996).

Based on volumetric relationships, the two different size slugging rods theoretically impart a slug-test stress level of 0.458 m (low-stress tests) and 1.117 m (high-stress tests) within a 0.051-m inside diameter well. However, for conditions where wells are screened across the water table, as for the Hanford Site wells tested in FY 1999 and where the well-screen sand pack has a relatively high permeability, the actual stress level imposed on the test formation may be lower than the theoretical stress level. This is due to the added volume of the sand pack at the time of test initiation. For these situations, the actual slug-test stress level is determined by projecting the observed early test response back to the time of test initiation. For situations where the theoretical slug-test stress level, H_o, is greater than the observed or projected stress level, H_p, an equivalent well radius, r_{eq}, must be used instead of the actual well-casing radius, r_c, in the various analytical methods. The r_{eq} can be calculated by using the following relationship presented in Butler (1998):

$$r_{eq} = r_c (H_o / H_p)^{½} \tag{3.1}$$

Two different methods were used for the slug-test analysis: the semiempirical, straight-line analysis method described in Bouwer and Rice (1976) and Bouwer (1989) and the type-curve-matching method for unconfined aquifers presented in Butler (1998). A description of the slug-test analysis methods is presented in the following sections. Analysis details and results for slug tests conducted at each of the test wells during FY 1999 are provided in Section 4.0.

3.1.1 Bouwer and Rice Method

The Bouwer and Rice method is a well-known technique and is widely applied in the analysis of slug tests. A number of analytical weaknesses, however, limit the successful application of the Bouwer and Rice method for analyzing slug-test response. These weaknesses constrain its application to slug-test responses that exhibit steady-state flow, isotropic conditions, no well-skin effects, and no elastic (storage) formation response. Unfortunately, these limitations are commonly ignored, and the Bouwer and Rice method is applied to slug-test responses that do not meet the test analysis criteria. A more detailed discussion on the analytical limitations of the Bouwer and Rice method is provided in Hyder and Butler (1995), Brown et al. (1995), and Bouwer (1996).

For slug tests exhibiting elastic storage response, it should be noted that improved estimates can be obtained if analysis criteria specified in Butler (1996, 1998) are observed. Figure 3.1 shows the predicted, normalized, slug-test response for three well/aquifer-test conditions: 1) nonelastic formation, 2) elastic

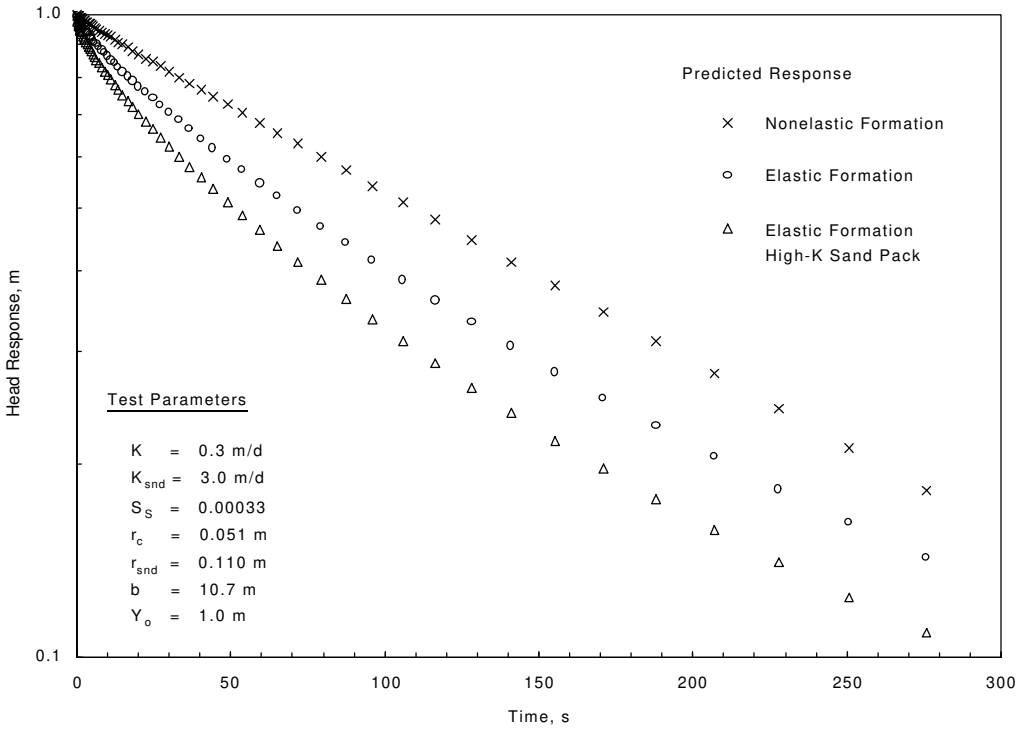

Figure 3.1. Predicted Slug-Test Response for Nonelastic Formation, Elastic Formation, and High Hydraulic Conductivity Sand-Pack Conditions

formation, and 3) elastic formation with high-K sandpack effects. The test responses were calculated using the KGS model described in Liu and Butler (1995) for the given test conditions listed in Figure 3.1. As shown, the presence of elastic aquifer storage (i.e., specific storage, S_s) and effects of a high-permeability sand pack cause curvilinear test responses (concave upward) that deviate from the predicted linear, nonelastic formation response. When this diagnostic curvilinear response is exhibited in the slug-test response, Butler (1996, 1998) recommends that the late-time test analysis be employed (i.e., the normalized head segment between 0.3 and 0.2) when using the Bouwer and Rice (1976) method. As shown in Figure 3.1, the two elastic curvilinear test responses over the specified late-time segment closely parallel the nonelastic test-formation response. This indicates that quantitative estimates for K can be obtained using the Bouwer and Rice method over a wide range of test-response conditions (nonelastic or elastic formation, high-K sandpack effects), if the proper analysis criteria are applied.

Because of its semiempirical nature, analytical results obtained using the Bouwer and Rice method (i.e., in contrast to results obtained using the type-curve-matching method) may be subject to error. Bouwer and Rice (1976) indicated that the K estimate, using their analysis method, should be accurate to within 10% to 25%. Hyder and Butler (1995) state an accuracy level for the Bouwer and Rice method within 30% of actual for homogeneous, isotropic formations, with decreasing levels of accuracy for more complex well/aquifer conditions (e.g., well-skin effects). For these reasons, greater credence is generally afforded the analytical results obtained using the type-curve-matching approach, which has a more rigorous analytical basis.

3.1.2 Type-Curve Method

Because the type-curve method can use all or any part of the slug-test response in the analysis procedure, it is particularly useful for the analysis of unconfined aquifer tests. The method also does not have any of the aforementioned analytical weaknesses of the Bouwer and Rice method. To facilitate the standardization of the slug-test type-curve analyses, a set of initial analysis parameters was assumed:

- a vertical anisotropy, K_D, value of 1.0
- a specific storage, S_s, value of 0.00001 m^{-1}
- the well-screen interval below the water table was assumed to be equivalent to the test-interval section.

To standardize the slug-test type-curve-matching analysis for all slug-test responses, a 1.0 K_D was assumed. As noted in Butler (1998), this is the recommended value to use for slug-test analysis, when setting the aquifer thickness to the well-screen length. Previous investigations by the main author have indicated that single-well slug-test responses are relatively insensitive to K_D; therefore, the use of an assumed (constant) value of 1.0 over a small well-screen section (i.e., <10 m long) is not expected to have a significant impact on the determination of hydraulic conductivity, K_h, from the type-curve-matching analysis.

To facilitate the unconfined aquifer slug-test type-curve analysis, an S_s value of 0.00001 m^{-1} was used for all initial analysis runs. After initial matches were made through adjustments of transmissivity, T, additional adjustments of S_s were then attempted to improve the overall match of the test-response pattern. In most test cases, slight modifications (i.e., increasing S_s) were made to the input S_s values to improve the final analysis type-curve matches. It should be noted, however, that other factors influence the shape of the slug-test curve (e.g., skin effects, K_D). For this reason, the S_s estimate obtained from the final slug-test analyses is considered to be of only qualitative value and should not be used (as in the case for K_h) for quantitative applications.

For the slug-test analysis, the well-screen interval below the water table (rather than the sandpack interval) was used to represent the test interval. This was based on the assumption that the formation materials within the screened interval have a higher permeability than the sandpack; therefore, test-response transmission is expected to propagate faster laterally from the well screen to the surrounding test formation than vertically within the sandpack zone. In reality, only small differences exist between individual well-screen and sandpack-interval lengths (i.e., compared to the aquifer-thickness relationship) and, subsequently, no significant differences in analysis results would be expected. This assumption is consistent with recommendations listed in Butler (1996).

The type-curves analyses presented in this report were generated using the KGS program described in Liu and Butler (1995). It should be noted that the KGS program is not strictly valid for the boundary condition, where the water table occurs within the well screen. However, a comparison of slug-test type curves generated from converted pumping test type curves (as described in Spane 1996), which accounts

for this boundary effect, indicates very little difference in predicted responses when compared to the KGS model results. Because of this close comparison and the fact that the KGS program calculates slug-test responses directly and can be applied more readily for analysis of the slug-test results, it was used as the primary type-curve-analysis method in this report.

3.2 Single-Well Tracer Tests

Single-well tracer tests can provide information on groundwater-flow characteristics (e.g., flow velocity) and aquifer properties (i.e., vertical distribution of K, effective porosity, n_e). During FY 1999, single-well tracer tests included tracer-dilution, tracer-pumpback, and in-well vertical flow tracer. Performance and analysis methods for the various single-well tracer tests are described below.

3.2.1 Tracer-Dilution Tests

For the tracer-dilution test, a bromide solution of known concentration was mixed within the well-screen section. The decline of tracer concentration (i.e., "dilution") with time within the well screen was monitored directly using a vertical array of bromide-specific ion-electrode sensors located at known depth intervals. The sensors were laboratory calibrated with standards of known bromide concentration prior to and following performance of the tracer-dilution test. Based on the dilution characteristics observed, the vertical distribution (i.e., heterogeneity) of hydraulic properties and/or in-well flow velocity can be estimated for the formation section penetrated by the well screen. The presence of vertical flow within the well screen can also be identified from the sensor/depth-dilution-response pattern. A description of the performance and analysis of tracer-dilution test characterization investigations is provided in Halevy et al. (1966), Hall et al. (1991), and Hall (1993).

Essential design elements of a tracer-dilution test include establishing a known, constant tracer concentration within the test section by mixing or circulating the tracer solution in the wellbore/test interval and monitoring the decline of tracer concentration with time within the test interval.

The decline in tracer concentration within the wellbore can be analyzed to ascertain the hydraulic gradient, I (if the formation's K is known) or the test-interval K (if the hydraulic gradient is known) using the following analytical expression:

$$\ln (C / C_o) = - (Q_w\ t) / V \qquad (3.2)$$

where C = concentration of the tracer in the test interval at time, t
C_o = initial concentration of the tracer at the start of the test
Q_w = in-well, lateral groundwater discharge within the well-test interval
V = isolated test interval well volume.

For test-analysis purposes, Equation (3.2) is commonly rewritten to calculate the groundwater-flow velocity within the well, v_w, as follows:

$$v_w = d (\ln C)/dt/(-A/V) \qquad (3.3)$$

where A = cross-sectional area within well screen; L^2
V = well volume over measurement section; L^3.

As shown by Halevy et al. (1966) to take into account the cross-sectional/well-measurement volume effects of the emplaced in-well tracer-measurement system (downhole probe, cables), Equation (3.3) can be rewritten as

$$v_w = d(\ln C)/dt/ - [2r_w / \pi(r_w^2 - r_t^2)] \quad (3.4)$$

where r_w = radius of well screen; L
r_t = equivalent radius of tracer-measurement system; L.

It should be noted that the calculated v_w is not the groundwater-flow velocity within the aquifer, v_a. The, v_w is related to actual groundwater velocity within the aquifer by the following relationship:

$$v_w = v_a \, n_e \propto \quad (3.5)$$

where n_e = effective porosity; dimensionless
$\propto$ = groundwater-flow-distortion factor; dimensionless, common range 0.5 to 4.

Various aspects of conducting tracer-dilution tests (i.e., test design, influencing factors) have been previously discussed by a number of investigators (e.g., Halevy et al. 1966; Freeze and Cherry 1979). Following completion of the tracer-dilution test, the tracer can be recovered from the formation by pumping, and the results analyzed to assess the effective porosity within the test interval. Tracer-pumpback tests are discussed in the following section.

Some investigators have noted differences in hydraulic property estimates obtained with tracer-dilution techniques and other test methods (e.g., Drost et al. 1968; Kearl et al. 1988). These differences have been attributed, in some cases, to distortions in the flow field caused by increased (or decreased) permeability near the well.

Analysis details and results for tracer-dilution tests conducted at each of the selected test wells during FY 1999 are provided in Section 5.0.

3.2.2 Tracer-Pumpback Tests

Detailed procedures for conducting standard, single-well, conservative tracer tests are provided in Pickens and Grisak (1981) and Molz et al. (1985). The tracer pumpback includes the following basic test procedure:

- emplace a conservative tracer (bromide) within the well/aquifer system
- define a prescribed residence (drift) time for the tracer to be dispersed within the aquifer

- withdraw the tracer from the well/aquifer system by pumping at a constant rate

- monitor tracer concentrations at the test well (bromide sensor/flow cell) and collect discrete groundwater samples for quantitative laboratory analysis.

It should be noted that the tracer-testing program used did not include actual "injection" of the bromide tracer into the surrounding aquifer but relied on natural groundwater flow to emplace the tracer. Because of the relatively small area represented by the well (i.e., in comparison to the aquifer) and volumes of tracer involved, the results obtained from these tracer tests may be more susceptible to wellbore effects (e.g., ∝ and possible downgradient dead zone).

For the tracer-pumpback tests, a constant-rate pumping test was initiated after the average tracer concentration had decreased (i.e., diluted) to a sufficient level within the well screen (usually a one- to two-order of magnitude reduction from the original tracer concentration). The objective of the pumpback test is to "capture" the tracer that has moved from the well into the surrounding aquifer. Tracer recovery is monitored qualitatively by measuring the tracer concentration at the surface using a bromide sensor/ flow cell installed in the discharge line. Discrete samples are collected at the surface at preselected times for quantitative laboratory tracer analysis.

The time required to recover the center of tracer mass from the aquifer provides information concerning n_e and v_a. n_e is a primary hydrologic parameter that controls contaminant transport. Analytical methods available for the analysis of single-well, tracer injection/withdrawal tests include (in addition to the previously cited references) Güven et al. (1985), Leap and Kaplan (1988), and Hall et al. (1991). The procedure to analyze the tracer-pumpback results is based on a rearrangement of the equations presented in Hall et al. (1991), which combines the basic pore velocity groundwater-flow equation (Equation [3.6]) with the regional advective flow-velocity equation (Equation [3.7]) describing tracer-drift and -pumpback tests as reported in Leap and Kaplan (1988).

$$v_a = (K\,I)/n_e \tag{3.6}$$

$$v_a = [(Q\,t_p)/\pi\,n_e\,b)]^{1/2}/t_t \tag{3.7}$$

Combining and rearranging results in

$$v_a = (Q\,t_p)/(\pi\,b\,t_t^2\,K\,I) \tag{3.8}$$

and

$$n_e = (\pi\,b\,t_t^2\,K^2\,I^2)/(Q\,t_p) \tag{3.9}$$

where v_a = advective groundwater-flow velocity within the aquifer; L/T
n_e = effective porosity; dimensionless

K = hydraulic conductivity; L/T
I = local hydraulic gradient; dimensionless
b = aquifer thickness; L
Q = tracer-pumpback rate; L^3/T
t_p = pumping time required to recover the center of mass of tracer emplaced into the aquifer
t_t = total elapsed time equal to sum of the tracer drift time, t_d, (time from tracer emplacement to start of recovery pumping) and t_p.

The K values used in Equations (3.8) and (3.9) were determined from analysis of constant-rate pumping tests for the test well (i.e., during the tracer pumpback). The I value was determined using trend-surface analysis of water-level elevation measurements from nearby wells as described in Section 3.4. The b value was calculated directly from geologic information obtained for the well or projection from known geologic relationships at nearby wells.

To calculate the time required to recover the tracer center of mass emplaced into the aquifer, several steps were required. The bromide concentration versus time profile during the pumpback test was determined by laboratory analysis of discrete samples collected closely over time. The mass of tracer recovered with time was calculated, based on integrating the product of the exhibited tracer concentration profile and observed pumping rate during the test. The t_p value, to the center of mass, was calculated by dividing the tracer mass recovered by the actual tracer mass transported into the aquifer. To calculate the actual tracer mass within the aquifer, the mass within the well-screen column and surrounding well sandpack at the start of the pumpback test was subtracted from the initial mass emplaced in the well. The mass within the well screen was determined by multiplying the known well-screen volume by the average concentration, which was calculated by the final readings of the bromide sensors used during the tracer-dilution test. The sensors were removed generally within 2 h of initiation of the tracer pumpback; therefore, their final readings are representative of initial pumpback conditions. For calculating the tracer mass within the sandpack, it was assumed that the tracer concentration was the same as observed within the well screen. Sandpack volumetric calculations were based on available as-built information, a porosity of 25%, and the assumption that 50% of the sandpack (i.e., the downgradient side) would be occupied by tracer.

The mathematical relationship for calculating half the tracer mass recovered during the pumpback, $M_{50\%}$, which is the mass used to calculate the center of mass recovery time, t_p, then can be expressed as:

$$M_{50\%} = 0.50\,(M_r - M_w)/(M_i - M_w) \qquad (3.10)$$

where M_r = mass of tracer recovered during the tracer pumpback; M
M_w = mass of tracer within well screen and well sandpack at the beginning of the tracer pumpback; M
M_i = mass of tracer initially emplaced in the well; M.

The t_p was also corrected (reduced) to account for the transit time of the pumped water from the pump intake to land surface (i.e., location where laboratory samples were collected).

Analysis details and results for tracer-pumpback tests conducted at each of the selected test wells are provided in Section 6.0.

3.2.3 In-Well, Vertical Flow Tests

As discussed in Section 3.2.1, the successful performance of tracer-dilution tests requires that lateral groundwater-flow conditions exist within the well fluid column. The presence of vertical flow is indicated during the initial phases of tracer dilution if a systematic, "stair-step," tracer-dilution pattern is exhibited for the respective depth settings of the bromide sensor. Figure 3.2 illustrates a hypothetical tracer-dilution pattern for various depths for a downward vertical flow condition within the well screen. As shown, the pattern evolves with time (after the tracer has been uniformly mixed within the well-screen section) as a result of the downward flow/mixing of nontracer groundwater. As shown in Figure 3.2, the pattern is characterized by a progressive extension of a constant tracer concentration for the sensors at greater depths, followed by a rapid decline of tracer on arrival of the downward flow mixture of tracer and nontracer groundwater. During late-test times, the various tracer versus depth profiles exhibit a parallel-linear pattern. v_w can be calculated by using the arrival time of the tracer/nontracer groundwater mixture front at the various known depth/sensor spacings.

For well sites exhibiting in-well vertical flow conditions during tracer-dilution testing, follow-up in-well vertical flow tracer tests were conducted. For indicated downward vertical flow conditions, a

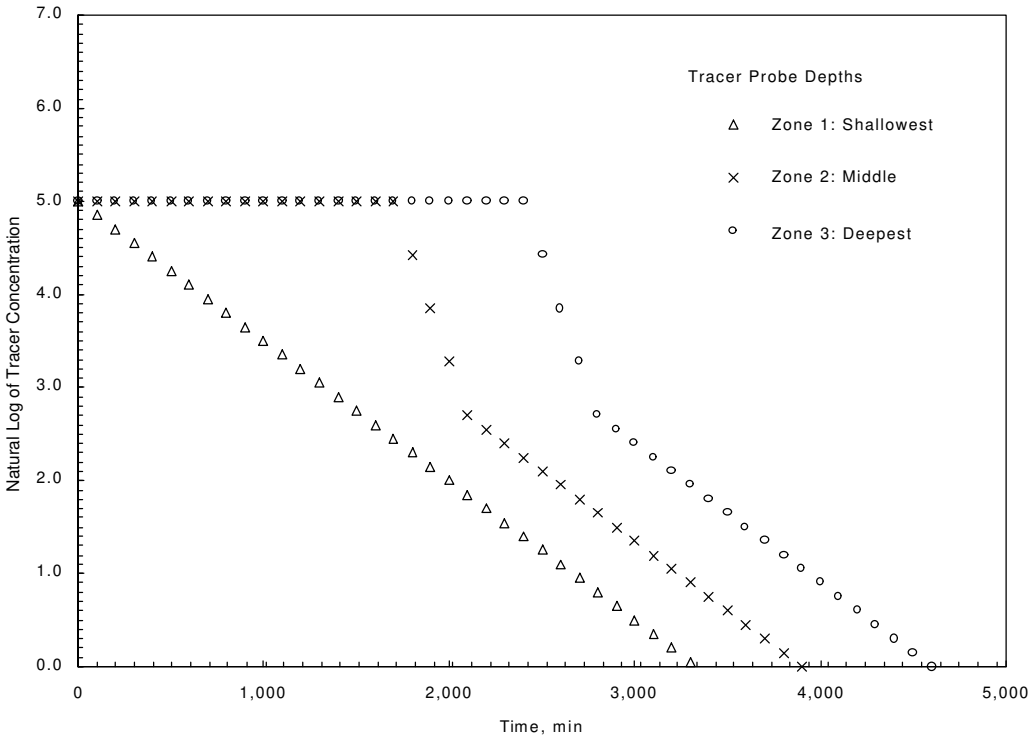

Figure 3.2. Hypothetical Tracer-Dilution Pattern Indicative of Vertical, In-Well, Downward Flow

bromide tracer solution slug was introduced within the upper 1.5 m of the well fluid column. The solution contained sufficient mass to create a concentration of ≤50 mg/L within the well column. A low concentration was employed in most tests to minimize possible tracer-density effects within the well column. A sensor array with fixed-distance spacings (i.e., 1.82 m) was then carefully installed within the well to monitor the arrival peak of the tracer solution caused by vertical flow conditions. (Note: For tests performed after FY 1999, the tracer introduction tube was fixed directly on the sensor assembly, thereby eliminating the effects of probe installation on tracer dispersal within the well.) Measurement of the arrival peaks of the tracer solution at the various known depth/distance sensor spacings provided the means of calculating the vertical downward flow velocity for individual tracer depths within the well. The tracer peak arrival method was used to provide a range of in-well vertical flow velocities. The average vertical flow velocity was calculated by determining the depth to the center of tracer mass within the well for selected test times. The slope of the linear regression of time versus the center of tracer mass provides the estimate of average in-well vertical flow. Similar in-well vertical flow tracer tests that have used the tracer peak arrival and center of mass analysis methods are presented in Michalski (1989) and Michalski and Klepp (1990).

As a third method, in-well vertical flow velocity was measured directly for the indicated well sites using an electromagnetic borehole (EM) flow meter. The EM flow-meter system is highly sensitive for measurement of low, in-well, vertical flow under either static or dynamic (pumping test) conditions. Its low-flow-detection capability is superior to commercially available mechanical and heat-pulse flow-meter systems. As described in Waldrop and Pearson (2000), the EM flow meter consists of an electromagnet and two electrodes located at 180 degrees apart and 90 degrees to the magnetic field within a hollow, flow-through cylinder. Flow measurement is based on Faraday's law of induction, which states that the voltage induced by a conductor moving at right angles through a magnetic field is directly proportional to the velocity of the conductor through the field. The flowing water within the well is the conductor, the electromagnet generates the magnetic field, and the electrodes measure the induced voltage. Subsurface electronics attached to the electrodes transmit the measured voltage to the recording system, which converts the observed voltage to a calculated vertical flow velocity. A more detailed description of the EM system and results from the in-well vertical flow surveys are presented in Waldrop and Pearson (2000). Analysis details and results for in-well vertical flow tests conducted at each of the selected test wells are provided in Section 8.0.

3.3 Constant-Rate Pumping Tests

Drawdown and recovery water levels were measured during tracer-pumpback tests at each of the four RCRA wells selected for detailed hydrologic characterization (299-W10-24, -W10-26, -W14-13, and -W19-42). Water levels were also recorded at a nearby observation well during each of these tests. Diagnostic analysis of the test responses was first conducted to determine test system characteristics and to identify test data that display infinite-acting radial flow behavior. Analysis of the drawdown and recovery phases of constant-rate discharge were then performed by type-curve fitting of log-log plots and, if appropriate, by straight-line analysis of semilogarithmic data plots of water-level change versus time. Test performance and methods used to analyze the results obtained from constant-rate testing are described in this section. Analysis details and results for each of the selected test wells are provided in Section 7.0.

3.3.1 Test Methods and Equipment

A 3-hp Grundfos® submersible pump was used to remove water during each pumping test. Flow rates were monitored with a surface turbine flow meter (insider diameter 0.025 m, Arad®, model #555061). Flow was adjusted manually using a gate valve to maintain constant-rate conditions. During the initial minutes of pumping (e.g., first 5 min), "instantaneous" flow rates were determined by measuring the time required for 19 L of flow to register on the flow-meter dials. Flow-meter totalizer readings were recorded every 5 to 20 min during pumping. Druck, Inc., 0- to 10-psig, differential pressure transducers (model # PDCR® 1830-8388) were used to monitor water levels in the pumping well and the nearby monitor wells during the test. The transducers were vented at the surface to compensate automatically for atmospheric pressure fluctuations. Pressure transducer measurements were recorded using a Campbell Scientific, Inc. model CR-10™ data logger.

Because tracer recovery was also being monitored during the tracer-pumpback test, part of the discharged groundwater was routed through a flow-through cell containing a bromide-selective ion probe, and a sampling port was used to collect water for laboratory analysis of the bromide tracer. These devices were downstream from the flow meter. The discharged water during the pumping test was collected in a tank truck for subsequent disposal at an effluent disposal facility.

3.3.2 Barometric Pressure Effects Removal

The analysis of well water-level responses during hydrologic tests provides the basis for estimating hydraulic properties that are important for evaluating groundwater-flow velocity and transport characteristics. Barometric pressure fluctuations, however, can have a discernible impact on well water-level measurements. Although the pressure transducers were vented to compensate for changes in barometric pressure, barometric pressure fluctuations can also cause changes in the water level in a well. This response effect is commonly ascribed to confined aquifers; however, wells completed within unconfined aquifers may also exhibit associated responses to barometric changes (Weeks 1979; Rasmussen and Crawford 1997). Water levels in unconfined aquifers typically exhibit variable time-lagged responses to barometric fluctuations. This time-lag response is caused by the time required for the barometric pressure change to be transmitted to the water table through the vadose zone compared to the instantaneous transmission of barometric pressure through the open well.

To determine the significance of barometric effects, water-level changes were monitored during a baseline period before or after each constant-rate discharge test and compared to the corresponding barometric pressure changes. Barometric pressures were obtained from the Hanford Meteorology Station, where they are recorded hourly. The barometric responses were then analyzed and removed from the recorded water levels using the multiple-regression deconvolution techniques described in Rasmussen and Crawford (1997) and Spane (1999). This technique relies on a least-squares fit of the water-level change to the corresponding barometric pressure change and time-lagged earlier barometric pressure changes. Because barometric changes were recorded at a constant 1-h frequency, the relationship between water-level and barometric change can be represented as follows:

$$\Delta h_w = X_0\,\Delta h_{ai} + X_1\,\Delta h_{ai-1} + X_2\,\Delta h_{ai-2} + \ldots + X_n\,\Delta h_{ai-n} \qquad (3.11)$$

where Δh_w = water-level change over the last hour
Δh_{ai} = barometric pressure change over the last hour
Δh_{ai-1} = barometric pressure change from 2 h to 1 h previous
Δh_{ai-n} = barometric pressure change from n hours to (n-1) hour previous
$X_0 \ldots X_n$ = regression coefficients corresponding to time lags of 0 to n hours
n = number of hours that lagged barometric effects are apparent.

After calculating $X_0 \ldots X_n$, simulated well water levels associated with the hourly barometric responses were calculated from the above equation for the baseline period. The results were then compared to the actual observed well water-level response for a "goodness of fit" evaluation. To remove barometric effects from water levels recorded during the constant-rate discharge test, a simulated well water-level response was calculated based on the hourly barometric changes that were observed over the test period. The predicted barometric induced response was then subtracted from the recorded pumping test water-level measurements. Analysis techniques described below were then applied to the data after removal of barometric effects.

3.3.3 Diagnostic Analysis and Derivative Plots

Log-log plots of water level versus time have traditionally been used for diagnostic purposes to examine pumping test drawdown data. More recently, the derivative of the water level or pressure has also been used (Bourdet et al. 1989; Spane 1993) as a diagnostic tool. Use of derivatives has been shown to improve significantly the diagnostic and quantitative analysis of various hydrologic test methods (Bourdet et al. 1989; Spane 1993). The improvement in test analysis is attributed to the sensitivity of pressure derivatives to various test/formation conditions. Specific applications for which derivatives are particularly useful include the following:

- determining formation-response characteristics (confined or unconfined aquifer) and boundary conditions (impermeable or constant head) that are evident within the test data

- assisting in the selection of the appropriate type-curve solution through combined type-curve/ derivative plot matching

- determining when infinite-acting, radial flow conditions are established and, therefore, when straight-line analysis methods are applicable.

Figure 3.3 shows log-log drawdown and derivative responses that are characteristic of some commonly encountered formation conditions. The early data, occurring before the straight-line approximation is valid or where wellbore storage is dominant, produce a steep, upward-trending derivative. The derivative normally decreases during transition from wellbore storage to radial flow and stabilizes at a constant value when infinite-acting, radial flow conditions are established. The stable derivative reflects the straight line on the semilog plot for infinite-acting radial flow. Unconfined and double-porosity aquifers may show two stable derivative sections at the same vertical position separated by a "valley" that represents the transition from one storage value to the other. Diagnostic derivative plots are also useful in

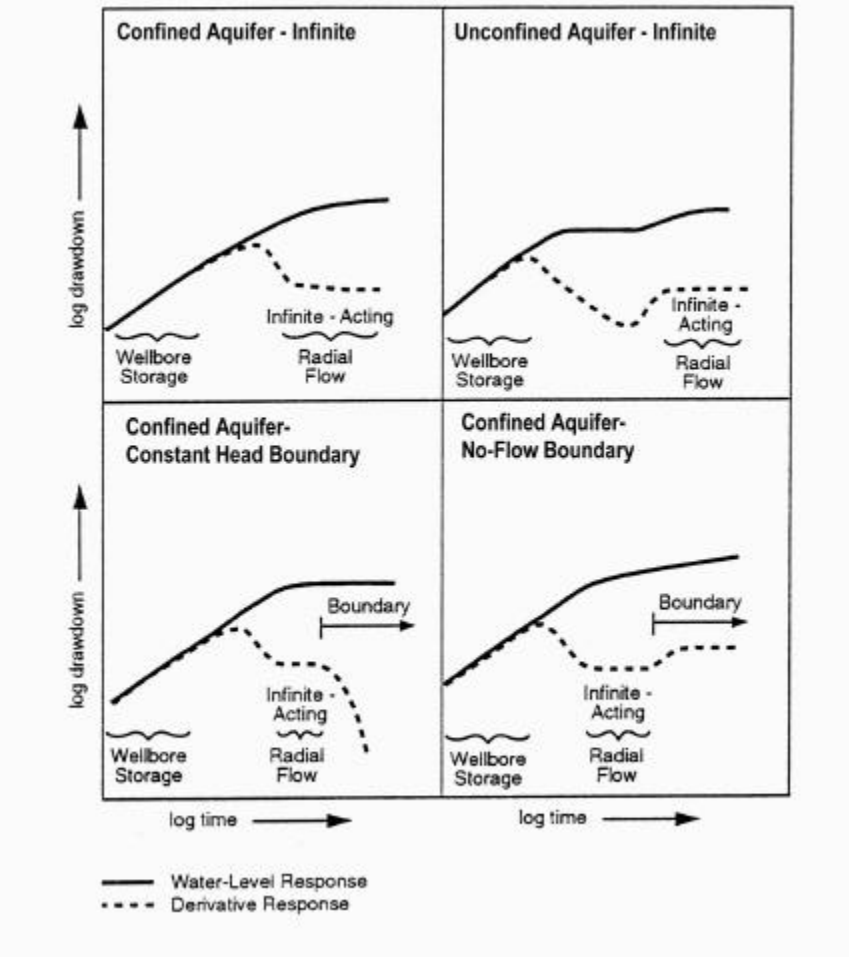

Figure 3.3. Characteristic Log-Log Drawdown and Drawdown Derivative Plots for Various Hydrogeologic Formation and Boundary Conditions

identifying boundary effects. A linear, no-flow boundary will result in a doubling of the magnitude of the derivative. If radial flow is established before the influence of the boundary is seen, a stable derivative will occur for a time followed by an upward shift to twice the original value. Constant-head boundaries display a downward trend in the derivative, which may be preceded by a stable derivative if radial flow conditions occur before the boundary effect becomes dominant. For the diagnostic and test analysis aspects of this report, derivative responses were calculated using the DERIV program described in Spane and Wurstner (1993).

For pumping tests conducted as part of the FY 1999 detailed hydrologic characterization tests, the derivative of the water level with respect to the natural logarithm of time (i.e., essentially the slope of the semilog plot) was calculated and plotted on the log-log plots of drawdown versus time. For recovery data, the "Agarwal equivalent time function" (Agarwal 1980) was used in calculating the derivative and plotting recovery data. This time function accounts for the effects of the pumping period through a superposition technique. Diagnostic and analysis results of the log-log plots of water-level and associated derivative response for each well site constant-rate pumping test is provided in Section 7.0.

3.3.4 Type-Curve-Matching Analysis Methods

Type-curve-matching methods (Theis 1935; Hantush 1964; Neuman 1972, 1974, 1975) are commonly used in the analysis of pumping test responses. For this study, unconfined aquifer pumping test type curves were generated using the WTAQ3 computer program described by Moench (1997). WTAQ3 can be used to generate type curves that represent a wide range of test and aquifer conditions, including partially penetrating wells, confined or unconfined aquifer models, well-skin effects, and wellbore storage at both the stress (pump) and observation (monitor) well locations. The type-curve-generation program also allows for noninstantaneous release (drainage-delay factor) of water from the unsaturated zone during the pumping test. However, this was found to not be a significant factor in the analysis; therefore, the type curves used in the analyses for this report all reflect an instantaneous release of water, which is the approach used by Neuman (1972, 1974, 1975).

In the type-curve-matching procedure, the log-log drawdown or recovery data and its associated derivative response for an individual well were matched simultaneously with dimensionless type-curve responses generated using WTAQ3 (Moench 1997) and the associated derivative plots obtained with the DERIV program (Spane and Wurstner 1993). The dimensionless responses depend on the assumed values of sigma, $\sigma = S/S_y$, and vertical anisotropy, $K_D = K_v/K_h$. For initial type-curve-matching runs, the values for σ and K_D were set at 0.001 and 0.10, respectively. The predicted response is also influenced by the assumed storativity, S, value because of its effect on wellbore storage. After an appropriate dimensionless match to the observed test data was obtained, dimensional curves were then generated by using the given well/test conditions (e.g., well radius, radial distance to observation well, average pumping rate) and making adjustments to aquifer properties (T, S_y) until the best match with the observed data was obtained. (Note that adjusting S_y also changes the value of S because σ was held constant.)

Type-curve-matching methods are normally applied to observation well data and not to pumping wells because of the additional head losses that commonly occur at the pumped well. However, in analyzing the test responses for the new RCRA wells in the 200-West Area, it was found that fitting of type curves to stress well responses resulted in approximately the same T as fitting type curves to the observation well data. This is probably an indication of the high efficiency of the stress well, which incorporates a screen and sand pack in a relatively low-permeability aquifer. Therefore, little head loss is associated with the movement of water into the well during pumping. Because of the lack of significant head loss, the simultaneous analysis of the observed drawdown or recovery response at the pumping well and observation well (i.e., composite plot analysis) could be demonstrated at most of the test sites for a uniform set of hydraulic properties.

3.3.5 Straight-Line Analysis Methods

For straight-line analysis methods, the rate of change of water levels within the well during drawdown and/or recovery is analyzed to estimate hydraulic properties. Because well effects are constant with time during constant-rate tests, straight-line methods can be used to analyze quantitatively the water-level response at both pumping and observation wells. The semilog, straight-line analysis techniques commonly used are based on either the Cooper and Jacob (1946) method (for drawdown analysis) or the Theis (1935) recovery method (for recovery analysis). These methods are theoretically restricted to the analysis

of test responses from wells that fully penetrate nonleaky, homogeneous, isotropic, confined aquifers. Straight-line methods, however, may be applied under nonideal well and aquifer conditions if infinite-acting, radial flow conditions exist. Infinite-acting, radial flow conditions are indicated during testing when the change in pressure, at the point of observation, increases in proportion to the logarithm of time. As discussed above, the use of diagnostic derivative methods (Bourdet et al. 1989) makes it easier to identify the portions within the test data where straight-line analysis is appropriate. As will be discussed in Section 7.0, derivative analysis of the observed test responses indicated that radial flow conditions were not established at any of the selected observation well locations. Use of straight-line analysis methods, therefore, were not appropriate. The use of straight-line analysis methods is mentioned in this report, however, because they are common in the analysis of pumping test results.

3.4 Groundwater-Flow Characterization

To support the detailed hydrologic characterization program, groundwater-flow direction and hydraulic gradient conditions were calculated at the various test sites during the period of tracer testing. Groundwater-flow direction and hydraulic gradient were determined using the commercially available WATER-VEL (In-Situ, Inc. 1991) software program. Water-level elevations from neighboring, representative wells were used as input with the WATER-VEL program to calculate groundwater-flow direction and hydraulic gradient conditions. The program uses a linear, two-dimensional trend surface (least squares) to randomly located hydrologic head or water-level elevation input data. This method is similar also to the linear approximation technique described by Abriola and Pinder (1982) and Kelly and Bogardi (1989). Reports that demonstrate the use of the WATER-VEL program for calculation of groundwater-flow velocity and direction on the Hanford Site include Gilmore et al. (1992) and Spane (1999). Details and results for groundwater-flow characterization at each of the four selected test wells are provided in Section 6.0. A summary of the groundwater-flow characterization results is presented in Section 9.0.

4.0 Slug-Test Results

Multiple slug tests were conducted at the 10 identified test wells during FY 1999. The slug tests were initiated by rapidly removing a slugging rod of known volume from the well-screen section. Two different size slugging rods were used during the testing program at each well to impose different stress levels on the test section. The stress levels for the two slugging rods are calculated to impose a slug-withdrawal test response of 0.458 m (low-stress tests) and 1.117 m (high-stress tests) within a 0.051-m inside diameter well. As noted in Butler (1996), differences exhibited between slug tests conducted at different stress levels can be used to evaluate stress-dependence effects of the well (e.g., dynamic skin, well development), which are unrelated to aquifer characteristics. Methods used to analyze the slug test results are described in Section 3.1. A summary list of the hydraulic properties determined from slug testing is provided in Table 4.1. A comparison of the average hydraulic conductivity, K, estimates obtained using the Bouwer and Rice and type-curve analysis methods is shown in Figure 4.1. As indicated, the method provided consistently lower values (generally within 35%) than the corresponding type-curve-derived estimates. This general pattern for analytical method comparison is consistent with findings reported in Hyder and Butler (1995). A description of the performance and analysis of slug tests conducted at each well site is provided below.

4.1 Well 299-W10-23

A total of four slug tests (two high and two low stress) were conducted on January 8, 1999. Selected examples of the analysis plots for this well are shown in Figure 4.2. A comparison of the normalized, high- and low-stress, slug-test responses indicates nearly identical behavior, indicating no stress dependence, which suggests that the well had been fully developed. The individual slug-test response indicates a higher permeability zone located in proximity to the well screen (as indicated by the extremely rapid recovery rate at early test times) and an elastic (concave upward) response displayed on the Bouwer and Rice analysis plot in Figure 4.2. The elastic response requires the late-time analysis to be employed (i.e., the normalized head segment between 0.3 and 0.2) when using the Bouwer and Rice (1976) method as recommended in Butler (1996, 1998). A comparison of K estimates indicates that slightly lower results (~30% lower) were obtained for the Bouwer and Rice method. For the Bouwer and Rice method, estimates for K ranged between 1.58 and 1.65 m/d (average 1.62 m/d), while the type-curve method provided an estimate of 2.35 m/d for both stress-level tests.

4.2 Well 299-W10-24

A total of four slug tests (two high and two low stress) were conducted on January 11, 1999. Selected examples of the analysis plots for this well are shown in Figure 4.3. A comparison of the normalized, high- and low-stress, slug-test responses indicates identical behavior, indicating no stress dependence, which suggests that the well had been fully developed. The individual slug-test response indicates a higher permeability zone located in proximity to the well screen (as indicated by the extremely rapid recovery rate at early test times) and an elastic (concave upward) response displayed on the Bouwer and Rice analysis plot in Figure 4.3. The elastic response requires the late-time analysis to be employed (i.e., the normalized head segment between 0.3 and 0.2) when using the Bouwer and Rice (1976) method as

Table 4.1. Slug-Test Results

Test Well	Test Parameters		Bouwer and Rice Analysis Method	Type-Curve Analysis Method	
	Aquifer Thickness, b,[(a)] m	Test Interval Saturated Thickness, L, m	Horizontal Hydraulic Conductivity, K_h,[(b)] m/d	Horizontal Hydraulic Conductivity, K_h,[(b)] m/d	Specific Storage, S_s, m^{-1}
299-W10-23	54.3	10.70	1.58 - 1.65 (1.62)	2.35	3.3E-04 - 6.6E-04
299-W10-24	54.3	10.70	1.04	1.68	3.3E-05
299-W10-26	54.9	10.42	1.25 - 1.52 (1.39)	1.74 - 2.16 (1.95)	8.3E-05 - 2.2E-04
299-W14-13	55.5	10.58	1.58 - 1.74 (1.66)	2.26 - 2.59 (2.43)	1.5E-04 - 6.6E-04
299-W14-14	56.1	10.67	1.49 - 2.44 (1.97)	2.41 - 2.87 (2.64)	6.6E-04 - 9.9E-04
299-W15-40	54.9	10.49	0.88	1.22	6.8E-04 - 8.6E-04
299-W19-41	56.4	10.27	1.07 - 1.28 (1.18)	1.52 - 1.86 (1.69)	1.6E-04 - 6.6E-04
299-W19-42	56.4	10.70	6.71 - 7.41 (7.06)	8.2 - 10.8 (9.5)	1.0E-5
299-W22-79	53.3	10.67	4.08 - 4.27 (4.18)	5.18 - 5.61 (5.4)	4.5E-04 - 6.6E-04
299-E33-44	2.23	2.23	22.0	24.2	3.3E-05

Note: For all test wells, r_c = 0.0.051 m; r_w = 0.110 m (see Nomenclature for definitions).
Number in parentheses is average.
(a) Determined, in most cases, from projection from neighboring wells.
(b) Assumed to be uniform within the well-screen test section.

recommended in Butler (1996, 1998). A comparison of K estimates indicates that slightly lower results (~30% lower) were obtained for the Bouwer and Rice method. An estimate of 1.04 m/d was obtained from the Bouwer and Rice method, while the type-curve method provided an estimate of 1.68 m/d for both stress-level tests.

4.3 Well 299-W10-26

A total of four slug tests (two high and two low stress) were conducted on October 15, 1998. Selected examples of the analysis plots for this well are shown in Figure 4.4. A comparison of the normalized, high- and low-stress, slug-test responses indicates a small stress dependence, which suggests that the well had not been fully developed. Examination of individual responses also indicates a higher permeability zone located in proximity to the well screen (as indicated by the extremely rapid recovery rate at early test times) and an elastic (concave upward) response displayed on the Bouwer and Rice

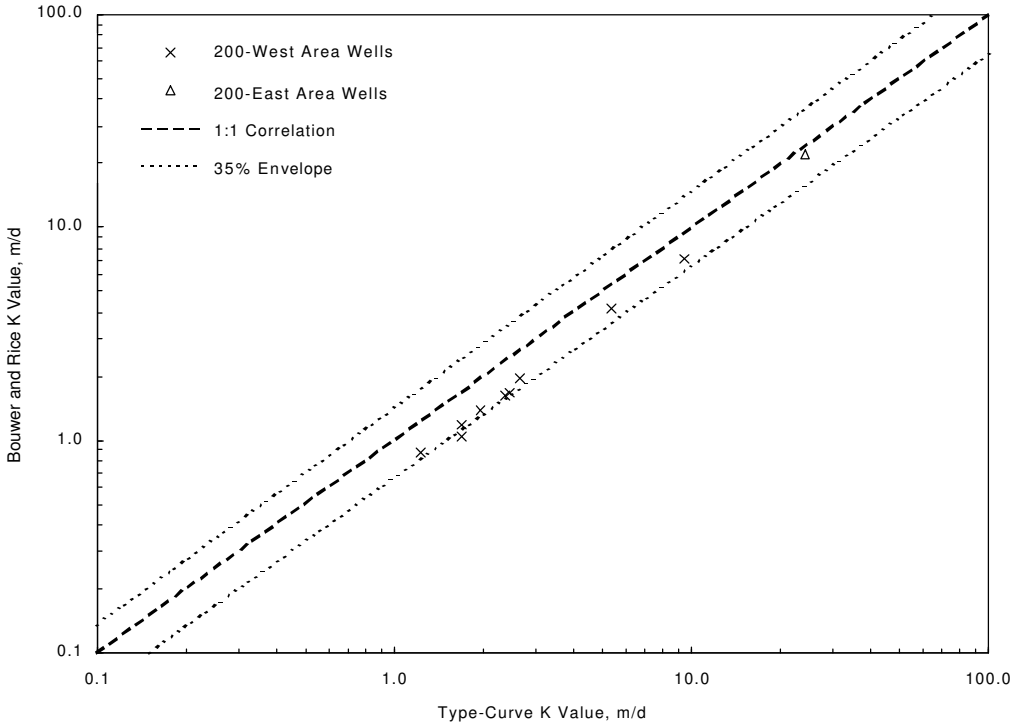

Figure 4.1. Comparison of Hydraulic Conductivity Estimates Obtained Using Bouwer and Rice and Type-Curve Analysis Methods

analysis plot in Figure 4.4. The elastic response requires the late-time analysis to be employed (i.e., the normalized head segment between 0.3 and 0.2) when using the Bouwer and Rice (1976) method as recommended in Butler (1996, 1998). A comparison of K estimates indicates that slightly lower results (~40% lower) were obtained for the Bouwer and Rice method. For the Bouwer and Rice method, estimates for K ranged between 1.25 and 1.52 m/d (average 1.39 m/d), while the type-curve method provided estimates between 1.74 and 2.16 m/d (average 1.95 m/d) for both stress-level tests.

4.4 Well 299-W14-13

A total of four slug tests (two high and two low stress) were conducted on October 14, 1998. Selected examples of the analysis plots for this well are shown in Figure 4.5. A comparison of the normalized, high- and low-stress, slug-test responses indicates similar early and late-time test responses, with only a slight divergence during intermediate test times. The cause of the slight divergence during intermediate test times is not known. Examination of individual slug-test responses also indicates a higher permeability zone located in proximity to the well screen (as indicated by the extremely rapid recovery rate at early test times) and an elastic (concave upward) response displayed on the Bouwer and Rice analysis plot in Figure 4.5. The elastic response requires the late-time analysis to be employed (i.e., the normalized head segment between 0.3 and 0.2) when using the Bouwer and Rice (1976) method as recommended in Butler (1996, 1998). A comparison of K estimates indicates that slightly lower results (~30% lower) were obtained for the Bouwer and Rice method. For the Bouwer and Rice method, estimates for K ranged between 1.58 and 1.74 m/d (average 1.66 m/d), while the type-curve method provided estimates between 2.26 and 2.59 m/d (average 2.43 m/d) for both stress-level tests.

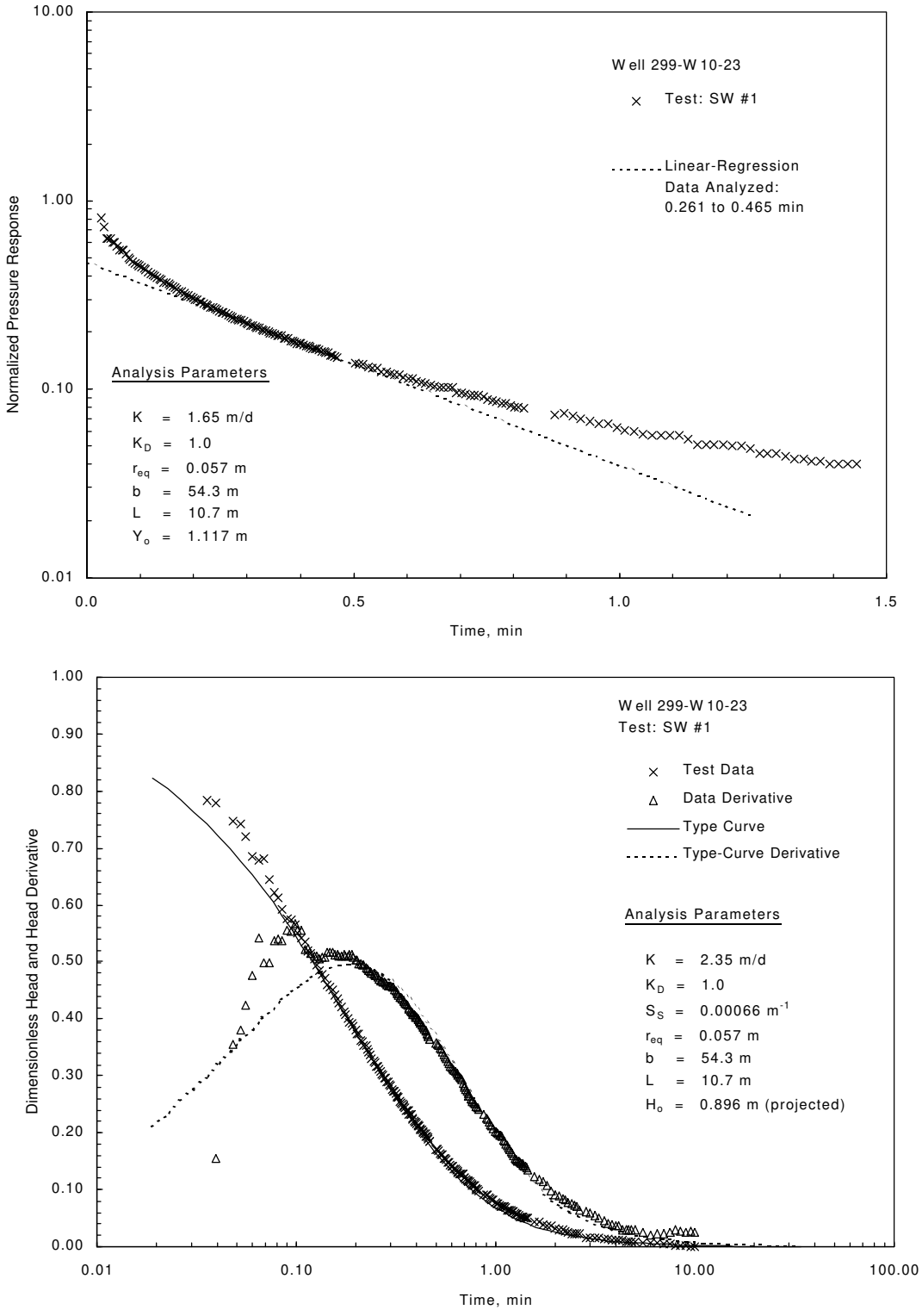

Figure 4.2. Selected Slug-Test Analysis Plots for Well 299-W10-23 (Bouwer and Rice method [top] and type-curve method [bottom])

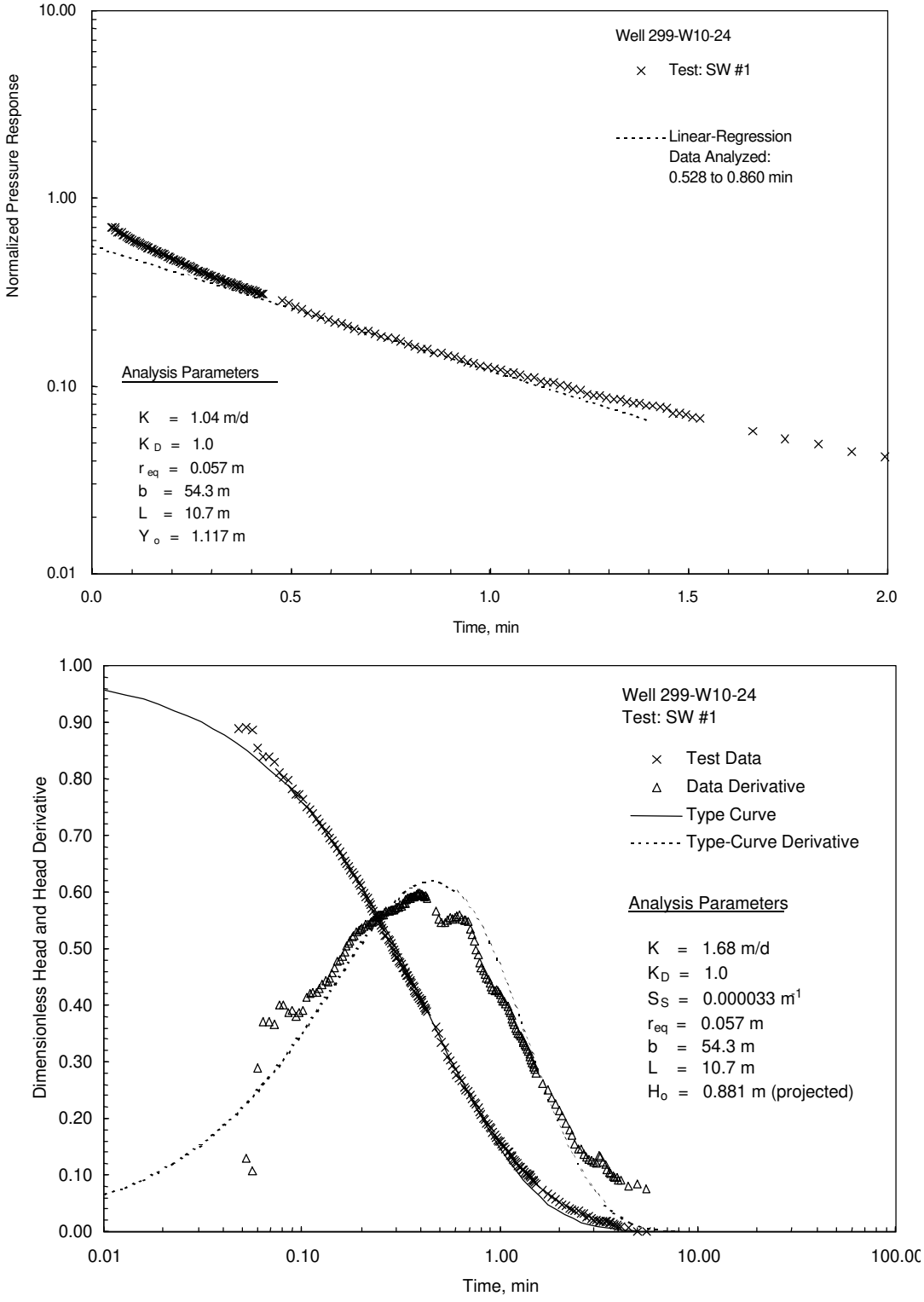

Figure 4.3. Selected Slug-Test Analysis Plots for Well 299-W10-24 (Bouwer and Rice method [top] and type-curve method [bottom])

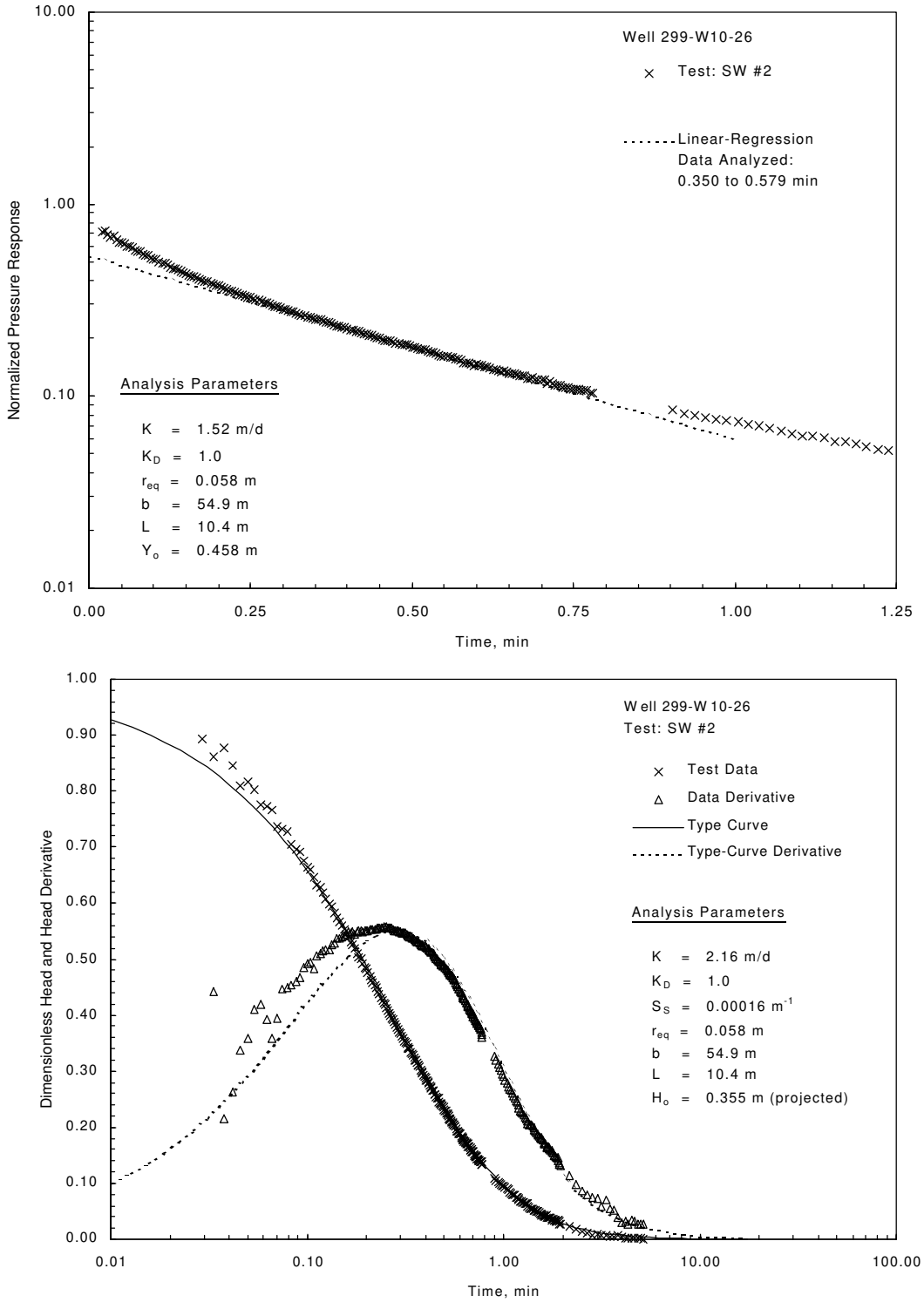

Figure 4.4. Selected Slug-Test Analysis Plots for Well 299-W10-26 (Bouwer and Rice method [top] and Type-Curve Method [Bottom])

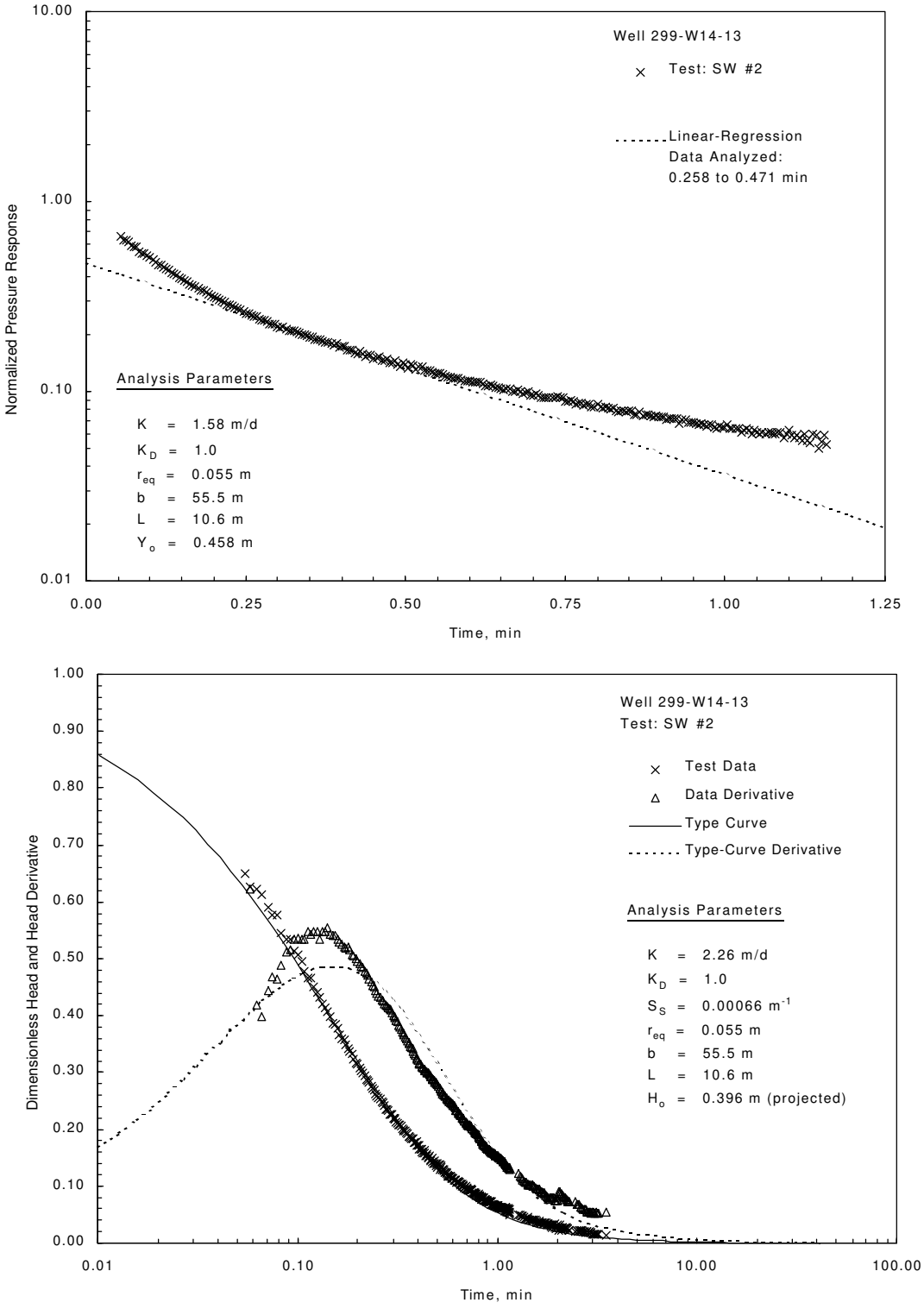

Figure 4.5. Selected Slug-Test Analysis Plots for Well 299-W14-13 (Bouwer and Rice method [top] and type-curve method [bottom])

4.5 Well 299-W14-14

A total of four slug tests (two high and two low stress) were conducted on January 11, 1999. Selected examples of the analysis plots for this well are shown in Figure 4.6. A comparison of the normalized, high- and low-stress, slug-test responses indicates a stress dependence, which suggests that the well had not been fully developed. Examination of individual slug-test responses also indicates a higher permeability zone located in proximity to the well screen (as indicated by the extremely rapid recovery rate at early test times) and an elastic (concave upward) response displayed on the Bouwer and Rice analysis plot in Figure 4.6. The elastic response requires the late-time analysis to be employed (i.e., the normalized head segment between 0.3 and 0.2) when using the Bouwer and Rice (1976) method as recommended in Butler (1996, 1998). A comparison of K estimates indicates that slightly lower results (~40% lower) were obtained for the Bouwer and Rice method. For the Bouwer and Rice method, estimates for K ranged between 1.49 and 2.44 m/d (average 1.97 m/d), while the type-curve method provided estimates between 2.41 and 2.87 m/d (average 2.64 m/d) for both stress-level tests.

4.6 Well 299-W15-40

A total of four slug tests (two high and two low stress) were conducted on October 14, 1998. Selected examples of the analysis plots for this well are shown in Figure 4.7. A comparison of the normalized, high- and low-stress, slug-test responses indicates a small stress dependence, which suggests that the well had not been fully developed. Examination of individual slug-test responses also indicates a higher permeability zone located in proximity to the well screen (as indicated by the extremely rapid recovery rate at early test times) and an elastic (concave upward) response displayed on the Bouwer and Rice analysis plot in Figure 4.7. The elastic response requires the late-time analysis to be employed (i.e., the normalized head segment between 0.3 and 0.2) when using the Bouwer and Rice (1976) method as recommended in Butler (1996, 1998). A comparison of K estimates indicates that slightly lower results (~30% lower) were obtained for the Bouwer and Rice method. For the Bouwer and Rice method, an identical K estimate of 0.88 m/d was obtained; while for the type-curve method, an identical K estimate of 1.22 m/d was calculated for both stress-level tests.

4.7 Well 299-W19-41

A total of four slug tests (two high and two low stress) were conducted on October 19, 1998. Selected examples of the analysis plots for this well are shown in Figure 4.8. A comparison of the normalized, high- and low-stress, slug-test responses indicates a stress dependence, which suggests that the well had not been fully developed. Examination of individual slug-test responses also indicates a higher permeability zone located in proximity to the well screen (as indicated by the extremely rapid recovery rate at early test times) and an elastic (concave upward) response displayed on the Bouwer and Rice analysis plot in Figure 4.8. The elastic response requires the late-time analysis to be employed (i.e., the normalized head segment between 0.3 and 0.2) when using the Bouwer and Rice (1976) method as recommended in Butler (1996, 1998). A comparison of K estimates indicates that slightly lower results (~30% lower) were obtained for the Bouwer and Rice method. For the Bouwer and Rice method, estimates for K ranged between 1.07 and 1.28 m/d (average 1.18 m/d), while the type-curve method provided estimates between 1.52 and 1.86 m/d (average 1.69 m/d) for both stress-level tests.

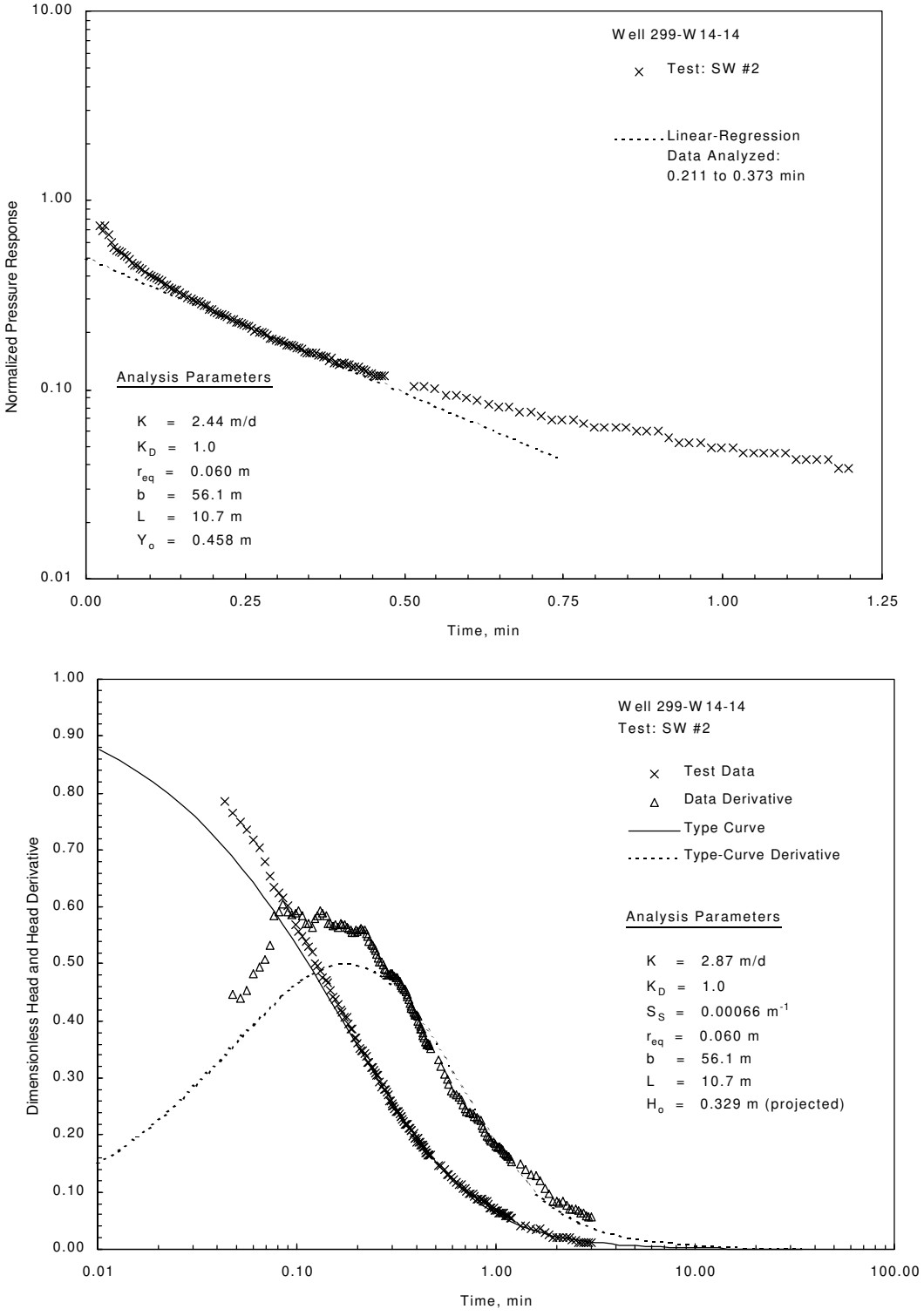

Figure 4.6. Selected Slug-Test Analysis Plots for Well 299-W14-14 (Bouwer and Rice method [top] and type-curve method [bottom])

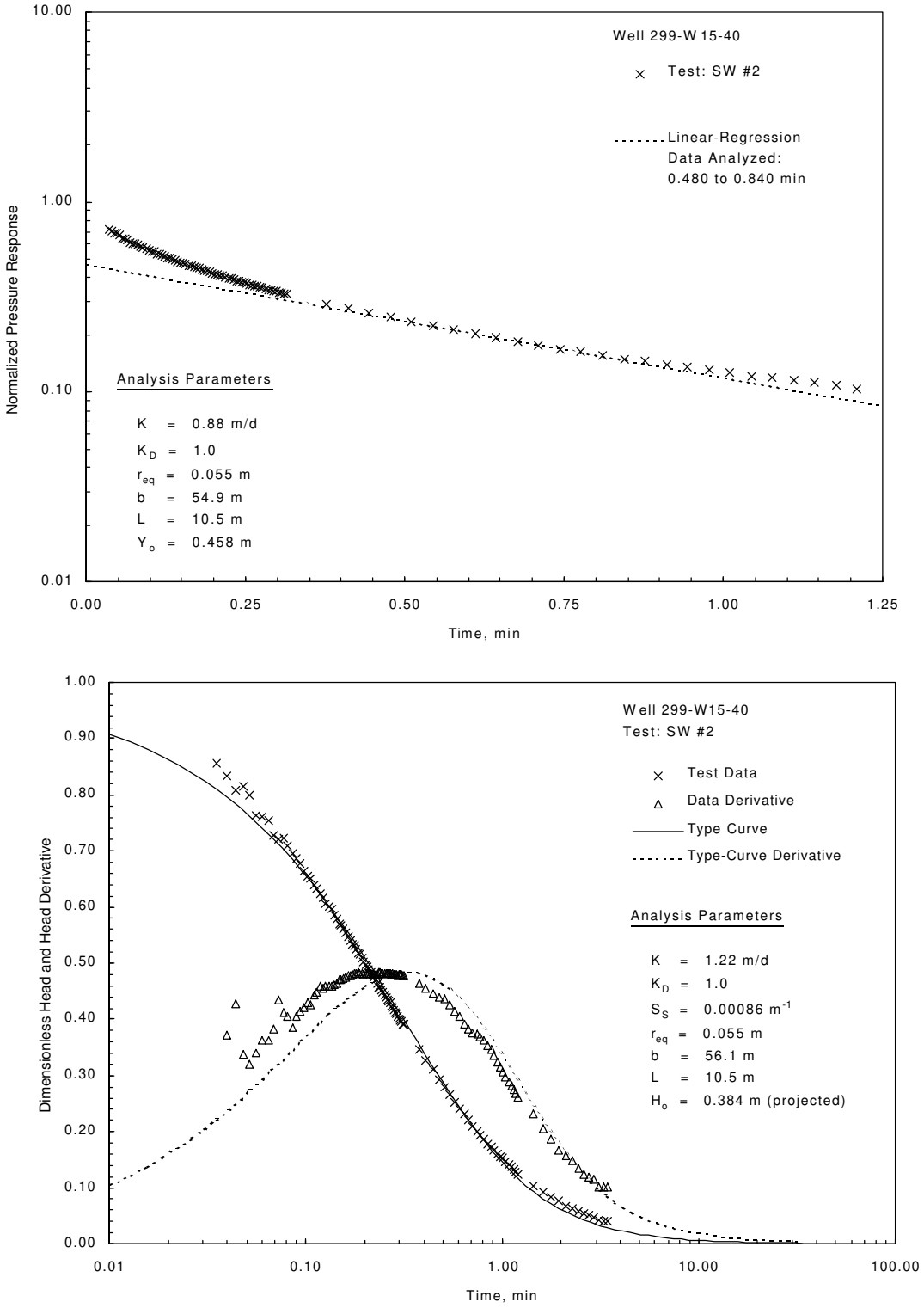

Figure 4.7. Selected Slug-Test Analysis Plots for Well 299-W15-40 (Bouwer and Rice method [top] and type-curve method [bottom])

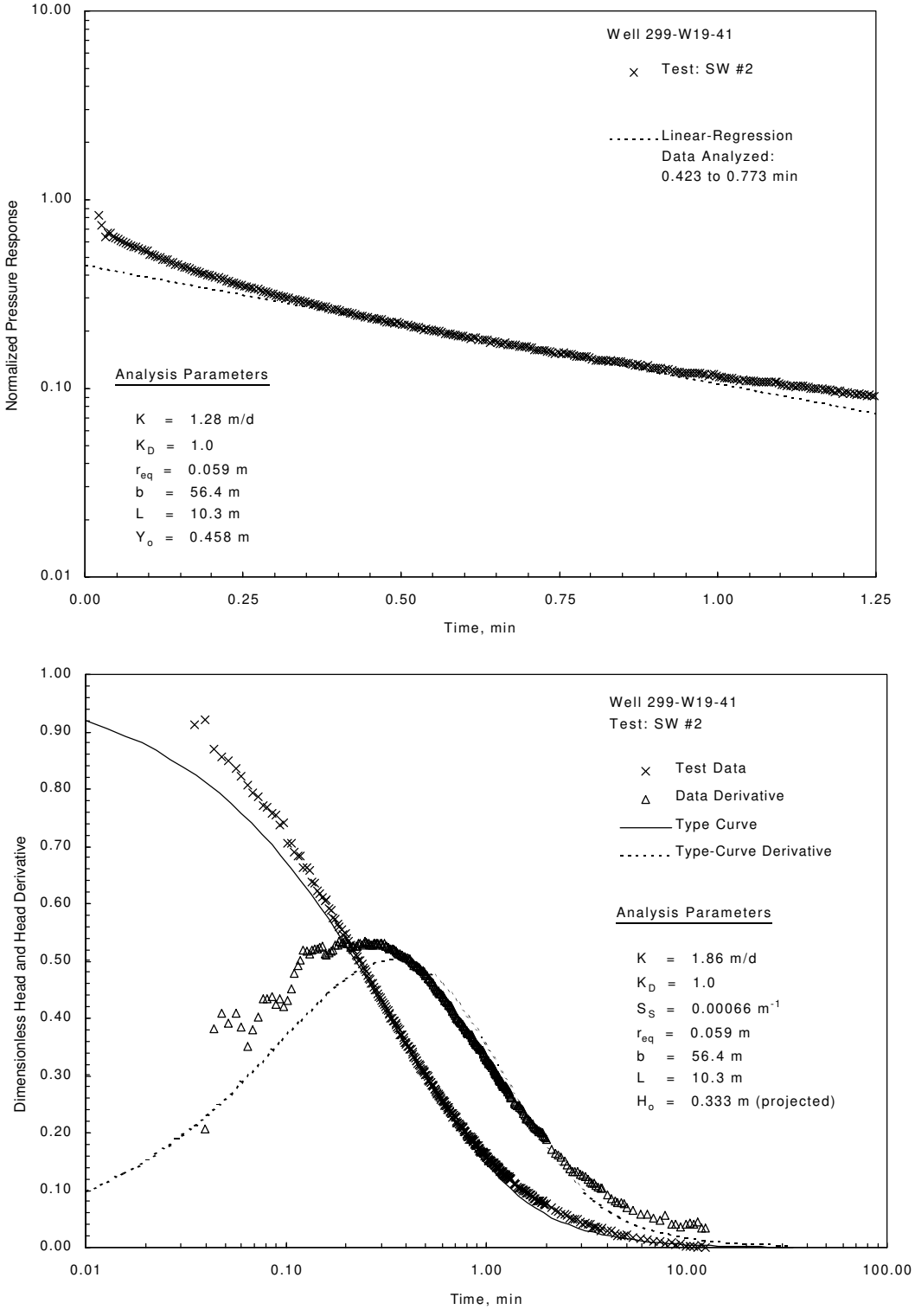

Figure 4.8. Selected Slug-Test Analysis Plots for Well 299-W19-41 (Bouwer and Rice method [top] and type-curve method [bottom])

4.8 Well 299-W19-42

A total of four slug tests (two high and two low stress) were conducted on October 15, 1998. Selected examples of the analysis plots for this well are shown in Figure 4.9 A comparison of the normalized, high- and low-stress, slug-test responses indicates a stress dependence, which suggests that the well had not been fully developed. Examination of individual slug-test responses also indicates a higher permeability zone located in proximity to the well screen (as indicated by the extremely rapid recovery rate at early test times) and an elastic (concave upward) response displayed on the Bouwer and Rice analysis plot in Figure 4.9. The elastic response requires the late-time analysis to be employed (i.e., the normalized head segment between 0.3 and 0.2) when using the Bouwer and Rice (1976) method as recommended in Butler (1996, 1998). A comparison of K estimates indicates that slightly lower results (~30% lower) were obtained for the Bouwer and Rice method. For the Bouwer and Rice method, estimates for K ranged between 6.71 and 7.41 m/d (average 7.06 m/d), while the type-curve method provided estimates between 8.2 and 10.8 m/d (average 9.50 m/d) for both stress-level tests.

4.9 Well 299-W22-79

A total of four slug tests (two high and two low stress) were conducted on October 19, 1998. Selected examples of the analysis plots for this well are shown in Figure 4.10. A comparison of the normalized, high- and low-stress, slug-test responses indicates nearly identical behavior, indicating no stress dependence, which suggests that the well had been fully developed. The individual slug-test response indicates a higher permeability zone located in proximity to the well screen (as indicated by the extremely rapid recovery rate at early test times) and an elastic (concave upward) response displayed on the Bouwer and Rice analysis plot in Figure 4.10. The elastic response requires the late-time analysis to be employed (i.e., the normalized head segment between 0.3 and 0.2) when using the Bouwer and Rice (1976) method as recommended in Butler (1996, 1998). A comparison of K estimates indicates that slightly lower results (~25% lower) were obtained for the Bouwer and Rice method. For the Bouwer and Rice method, estimates for K ranged between 4.08 and 4.27 m/d (average 4.18 m/d), while the type-curve method provided estimates between 5.18 and 5.61 m/d (average 5.40 m/d) for both stress-level tests.

4.10 Well 299-E33-44

A total of four slug tests (two high and two low stress) were conducted on October 13, 1998. Both stress-level slug-test responses indicate a high test formation permeability (i.e., test recovery within 20 s). The high-stress slug tests, however, exhibited turbulent flow conditions (i.e., Reynolds number >2,000) and an excessive stress level to well-screen length dimension relationship (i.e., stress level ~50% of well-screen length). For these reasons, only the low-stress results are analyzable. A comparison of K estimates for the low-stress tests indicates that slightly lower results (~10% lower) were obtained for the Bouwer and Rice method. For the Bouwer and Rice method, a K value of 22.0 m/d was obtained, while the type-curve method provided an estimate of 24.2 m/d. Selected examples of the slug-test analysis plots for this well are shown in Figure 4.11.

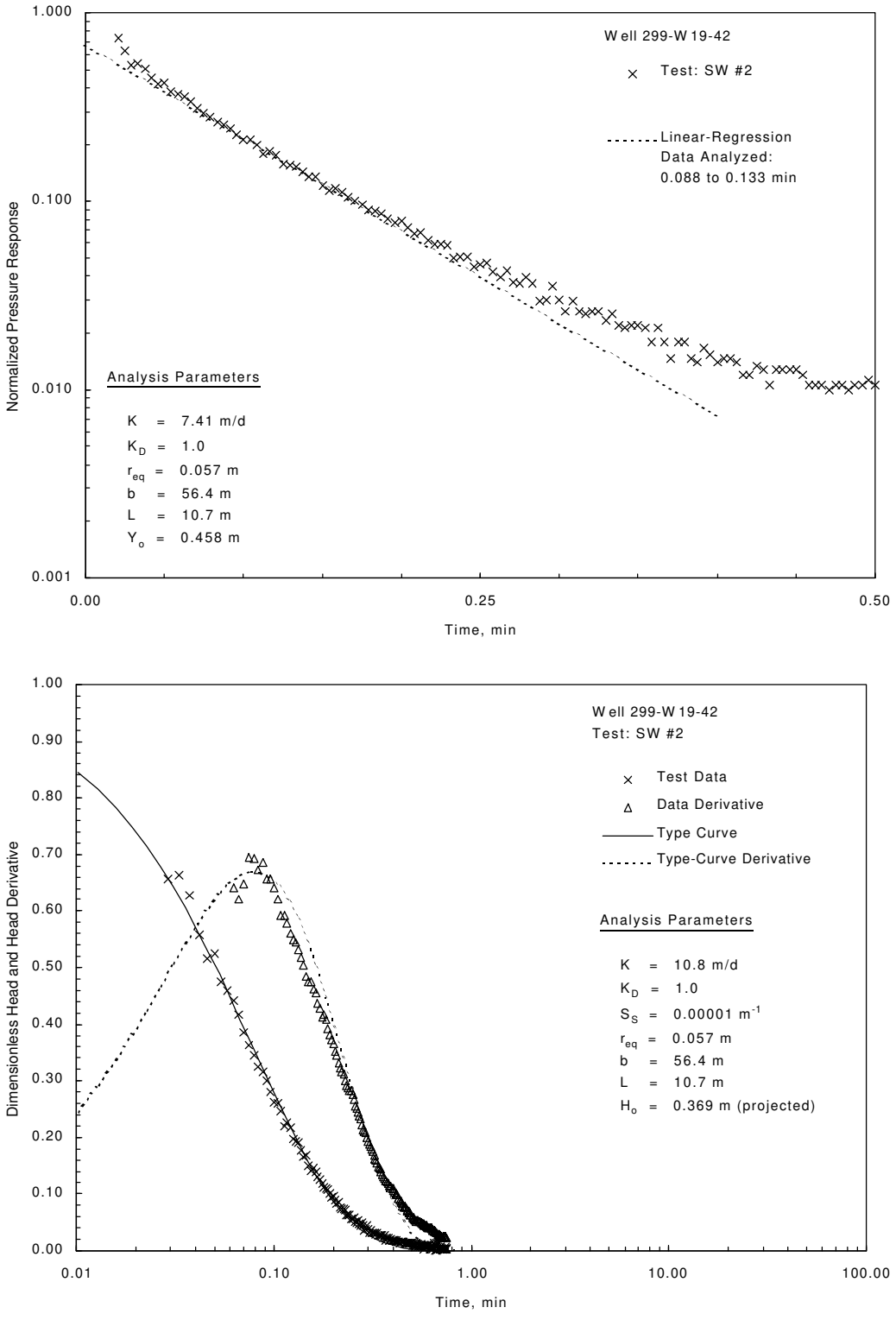

Figure 4.9. Selected Slug-Test Analysis Plots for Well 299-W19-42 (Bouwer and Rice method [top] and type-curve method [bottom])

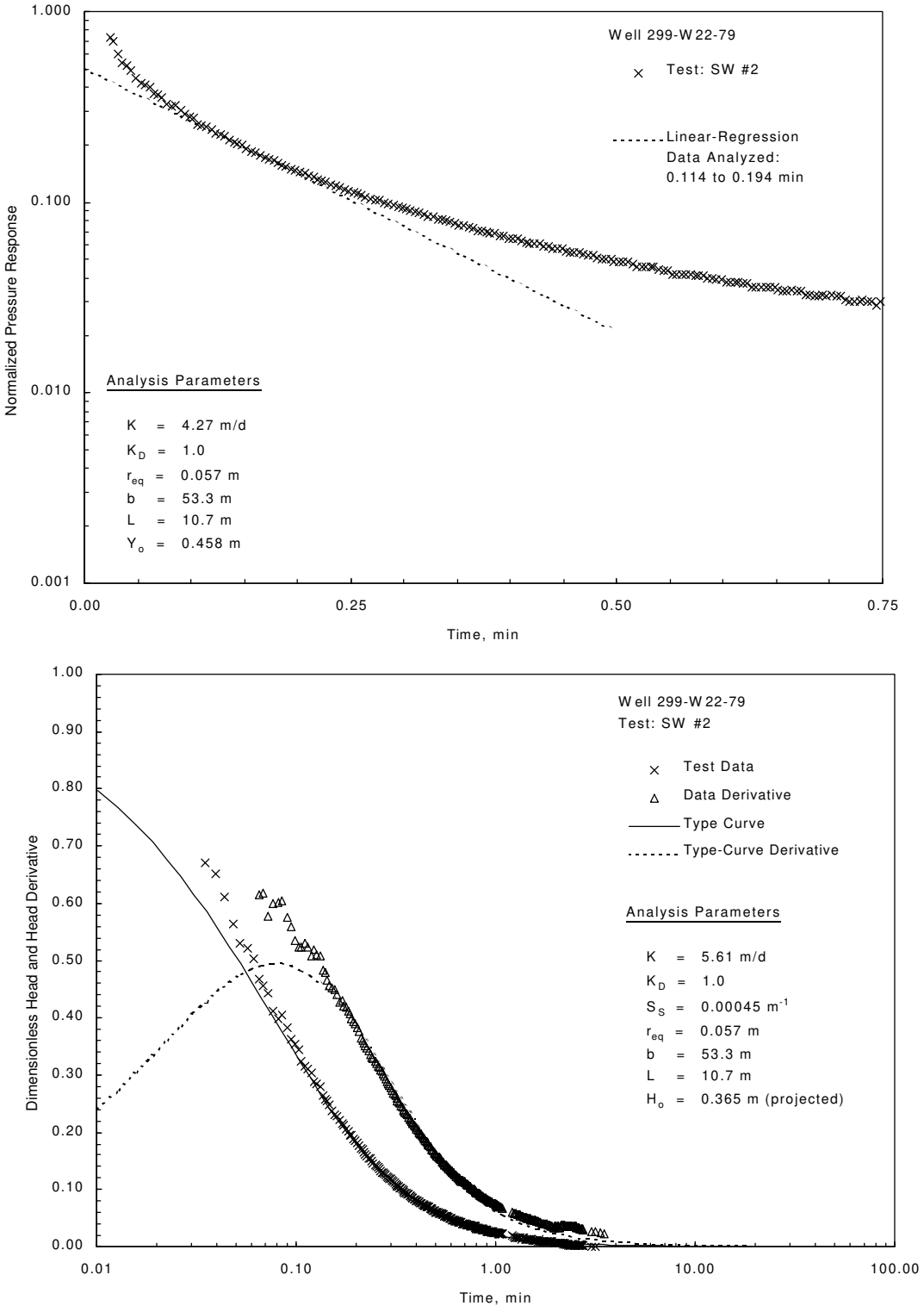

Figure 4.10. Selected Slug-Test Analysis Plots for Well 299-W22-79 (Bouwer and Rice method [top] and type-curve method [bottom])

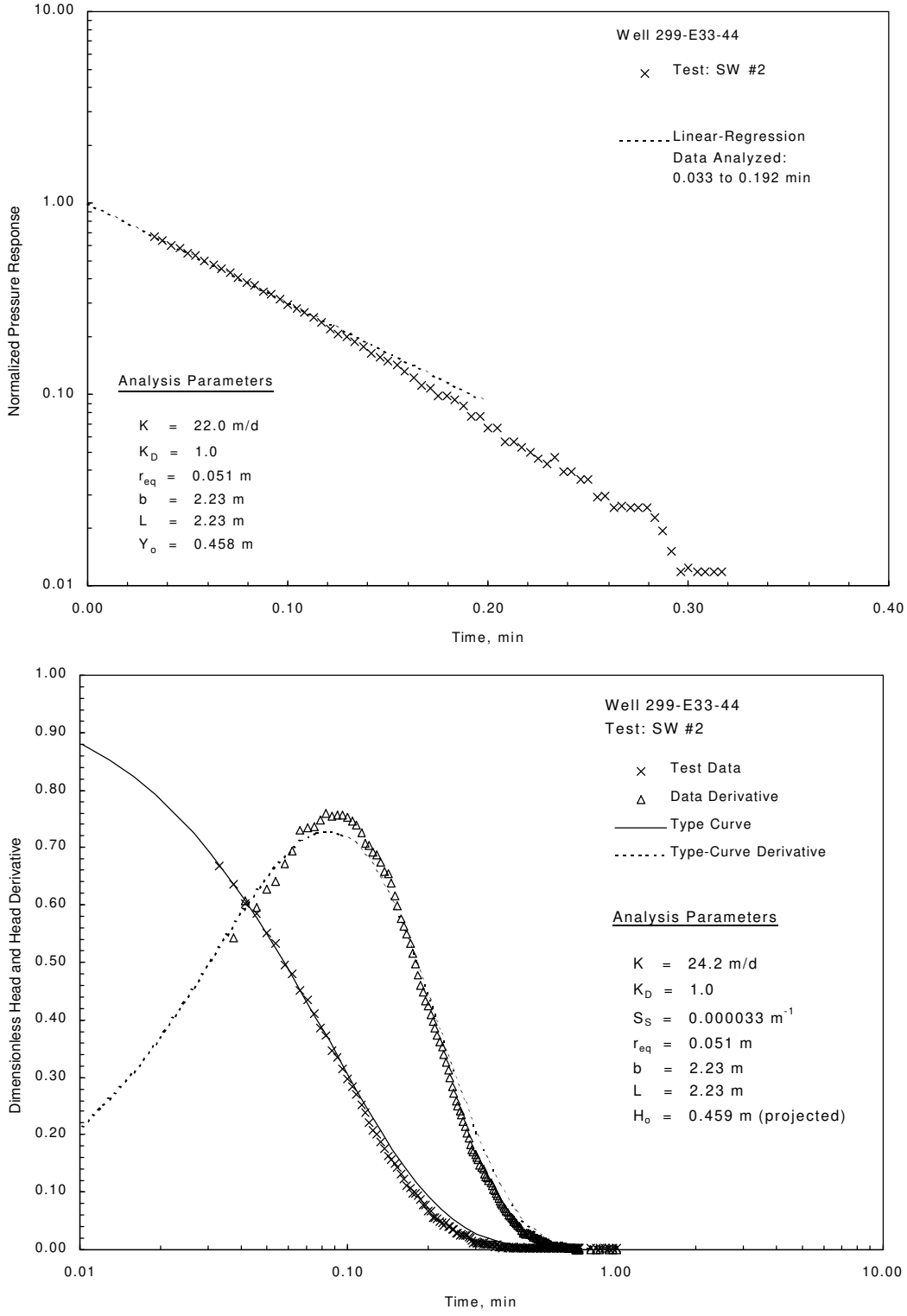

Figure 4.11. Selected Slug-Test Analysis Plots for Well 299-E33-44 (Bouwer and Rice method [top] and type-curve method [bottom])

5.0 Tracer-Dilution Test Results

Results from the tracer-dilution phase of the single-well tracer testing were analyzed using the methods described in Section 3.2.1. As noted previously, to be strictly valid, the analytical assumptions require that the dilution occurs only as the result of lateral groundwater inflow (i.e., no vertical groundwater flow). As will be discussed, tracer-dilution tests conducted at wells 299-W10-26 and -W14-13 exhibited evidence of vertical flow conditions within the well-screen section. For well 299-W14-13, which exhibited significant, downward, in-well, flow conditions, no estimation of average in-well (lateral) groundwater-flow velocity, v_w, or distribution of relative permeability (permeability profile) within the well-screen section was possible. For well 299-W10-26, which exhibited a small, downward, in-well, flow condition, only a calculation of the average v_w was attempted. It should be noted, however, that the results for well 299-W10-26 are highly suspect and should only be used for qualitative comparison purposes. A description of the performance and analysis of the tracer-dilution tests conducted in four of the test wells is provided below.

5.1 Well 299-W10-24

A single-well tracer-dilution test was initiated on April 9, 1999 (0905 Pacific daylight time) by introducing 5.26 L of tracer solution (containing 16.82 g of bromide) within the 10.27-m well-screen section (72.37 to 82.64 m below top of casing). The tracer was introduced into the well using a 0.025-m polypropylene tube that was open at a depth setting of 82.2 m below top of casing. Following tracer introduction, an equilibration time of ~15 min was observed to allow for dissipation of the displaced water from the tube into the surrounding well-screen column. After the equilibration period, the tube was slowly raised out of the well-water column, causing emplacement of the 5.26 L of prepared tracer. The tube was then slowly lowered and raised four times within the water column over a 10-min period to mix the tracer within the well-screen section. To facilitate mixing of the tracer, a bottom-line static mixer was attached to the bottom of the tube. The designed concentration within the well screen following mixing of the added tracer was ~200 mg/L.

Following mixing of the tracer solution, an assembly of six bromide probe sensors, spaced uniformly at a separation distance of 1.83 m, was slowly lowered into the well. Final depth settings for the six sensors were 72.8, 74.7, 76.5, 78.3, 80.2, and 82.0 m below top of casing. Installation of the assembly was completed in ~30 min, following the mixing of the tracer within the well-screen section. The concentration within the borehole following emplacement and equilibration of the sensors (i.e., after 70 min following initial mixing) was ~133 mg/L, ranging between 98 and 170 mg/L for the various sensor-depth settings. The projected, average, initial concentration within the well screen, C_o, based on back-projection of the fitted linear-regression concentration response to time = 0 min, was 148 mg/L. The uneven dilution pattern within the test interval is believed to be attributed to a too rapid mixing procedure and use of the bottom-line static mixer, which may have caused movement of “fresh” groundwater from the aquifer into the well-screen section. The dilution and dissipation within the well screen were observed for a period of 17,455 min (12.12 d). At the end of the test, the average concentration was <20 mg/L.

Visual examination of the dilution patterns for the various sensor-depth settings indicates no significant vertical flow conditions within the well-screen section. The natural log of concentration versus time depth-setting plots exhibits linear relationships over the period of observation for the upper five sensor locations. Readings for the lowest sensor-depth setting (82.0 m below top of casing) were aberrant and could not be used in the tracer-dilution analysis. The reason for the aberrant readings is unknown.

The observed dilution pattern versus time can be analyzed to calculate v_w, using Equation (3.3). Linear-regression analysis of the average dilution response (shown in Figure 5.1) for the upper five sensor-depth settings within the well screen ($r^2 = 0.99$) indicates a slope on the natural log of concentration versus time of -0.000113 min^{-1}. The calculated average A/V relationship for the test interval, taking into account the presence of sensor instrumentation/cable test system cross-sectional area, is 13.577 m^{-1}. Based on these observed and measured parameters, an average calculated v_w is 0.012 m/d.

If lateral groundwater-flow conditions occur throughout the entire well, then a comparison of the calculated well velocities at the various sensor-depth settings can provide an assessment of the vertical permeability profile within the well-screen section. A comparison of the average well-flow velocities at the upper five individual sensor-depth settings indicates the lowest in-well flow velocities for the upper two sensor-depth settings. If it can be assumed that a direct correlation between well-flow velocity and aquifer permeability exists for the well/aquifer site, then the highest permeability occurs within the lower half of the well-screen section, with the highest permeability occurring for the fourth sensor-depth setting (78.3 m below top of casing). Table 5.1 summarizes results from the tracer-dilution test at well 299-W10-24.

5.2 Well 299-W10-26

A single-well tracer-dilution test was initiated on April 23, 1999 (0910 Pacific daylight time) by introducing 5.28 L of tracer solution (containing 16.89 g of bromide) within the 10.42-m well-screen section (67.39 to 77.81 m below top of casing). The tracer was introduced into the well using a 0.025-m polypropylene tube that was open at a depth setting of 77.5 m below top of casing. Following tracer introduction, an equilibration time of ~15 min was observed to allow for dissipation of the displaced water from the tube into the surrounding well-screen column. After the equilibration period, the tube was slowly raised out of the well-water column, causing emplacement of the 5.28 L of prepared tracer. The tube was then slowly lowered and raised eight times within the water column over a 15-min period to mix the tracer within the well-screen section. To facilitate mixing of the tracer, a bottom-line static mixer was attached to the tube. The designed concentration within the well screen following mixing of the added tracer was ~200 mg/L.

Following mixing of the tracer solution, an assembly of six bromide probe sensors, using separation distances ranging between 1.4 to 2.5 m, was lowered into the well. Final depth settings for the six sensors were 67.8, 69.2, 71.0, 73.5, 75.0, and 77.1 m below top of casing. Variable sensor separations were used to coincide with response characteristics evident from a gamma-log survey for the well-screen section (not given in this report). Each sensor had an attached plastic centralizer to keep the sensor approximately centered within the well-screen section. Installation of the assembly was completed in ~25 min, following the mixing of the tracer within the well screen. The concentration within the borehole

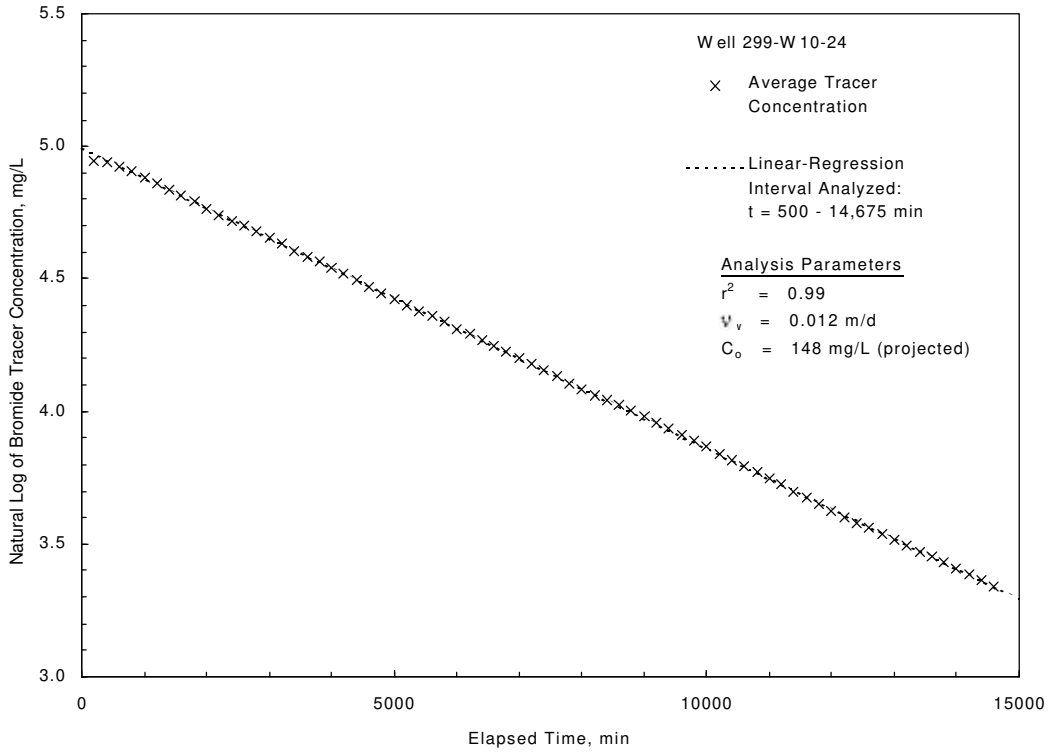

Figure 5.1. Average Tracer-Dilution Test Results Within Well 299-W10-24

Table 5.1. Tracer-Dilution Test Results for Well 299-W10-24

Well Sensor/ Depth Setting, m, below top of casing	Tracer Concentration/ Dilution Slope, d (ln C) dt min^{-1}	Linear-Regression Correlation Coefficient, r^2	Projected Initial Tracer Concentration, C_o, mg/L	Well Measurement Area/Volume Ratio, A/V, m^{-1}	Calculated Well-Screen Flow Velocity, v_w, m/d
72.8	-0.000087	0.99	117	13.723	0.009
74.7	-0.000084	0.99	126	13.650	0.009
76.5	-0.000122	0.99	178	13.577	0.013
78.3	-0.000158	0.99	164	13.505	0.017
80.2	-0.000125	0.99	165	13.435	0.013
82.0	(a)	(a)	(a)	(a)	(a)
Average	-0.000113	0.99	148	13.577	0.012
(a) No tracer-dilution analysis possible because of aberrant sensor readings.					

following emplacement and equilibration of the sensors (i.e., after 40 min following initial mixing) ranged between 138 and 182 mg/L for the various sensor-depth settings. The projected, average, initial C_o within the well screen, based on back-projection of the fitted linear-regression concentration response to time = 0 min for the upper five sensors, was 219 mg/L. The bottom sensor readings were not used because of erratic behavior. The reason for the erratic readings is not known. The dilution and dissipation within the well screen were observed for a period of 7,259 min (5.04 d). At the end of the test, the average concentration was 2 mg/L.

Visual examination of the dilution patterns for the various sensor-depth settings indicates a small, vertical, downward, flow condition within the well-screen section. Downward, in-well, flow velocities, ranging between 0.002 and 0.004 m/min, were calculated by using the arrival times of recognizable signatures between the lower three sensors (see Section 8.1). The measured downward flow velocities are comparable with those reported for well 299-W10-26 by Waldrop and Pearson (2000) (0.006 m/min detected with a vertical EM flow meter).

As previously discussed, to be strictly valid, tracer-dilution tests require that no vertical flow conditions exist within the well and that the tracer is continually mixed within the test section. To "simulate" a continuously mixed condition, an average well-screen tracer concentration was calculated, based on averaging the upper five sensor-depth readings recorded with time. It is not known whether the vertical flow conditions observed within the well are significant enough to affect adversely the results of the tracer-dilution test. The analysis results, therefore, should be viewed as being qualitative estimates.

The observed, average dilution pattern versus time can be analyzed to calculate v_w, using Equation (3.3). Linear-regression analysis of the average dilution response (shown in Figure 5.2) within the well screen ($r^2 = 0.99$) indicates a slope on the natural log of concentration versus time of -0.000815 min^{-1}. The calculated average A/V relationship for the test interval, taking into account the presence of sensor instrumentation/cable test system cross-sectional area, is 13.577 m^{-1}. Based on these observed and measured parameters, an average calculated v_w is 0.086 m/d.

Because lateral groundwater-flow conditions do not occur throughout the entire test interval, an assessment of the vertical permeability profile within the well-screen section (using calculated sensor-depth well-flow velocities) could not be estimated. However because of the observed, linear, tracer-dilution behavior, in-well flow-velocity measurements for the upper three individual sensor-depth settings were calculated. Results for these three depth settings should also be considered questionable, given the observed vertical flow conditions existing within the well. Table 5.2 summarizes the results from the tracer-dilution test at well 299-W10-26.

5.3 Well 299-W14-13

Two single-well tracer-dilution tests were conducted at the well site. The first was initiated on March 26, 1999 (1025 Pacific standard time) by introducing 1.36 L of tracer solution (containing 12.80 g of bromide) within the 10.65-m well-screen section (67.12 to 77.77 m below top of casing). The tracer was introduced into the well using a 0.025-m polypropylene tube that was open at a depth setting of 77.5 m below top of casing. Following tracer introduction, an equilibration time of ~5 min was observed

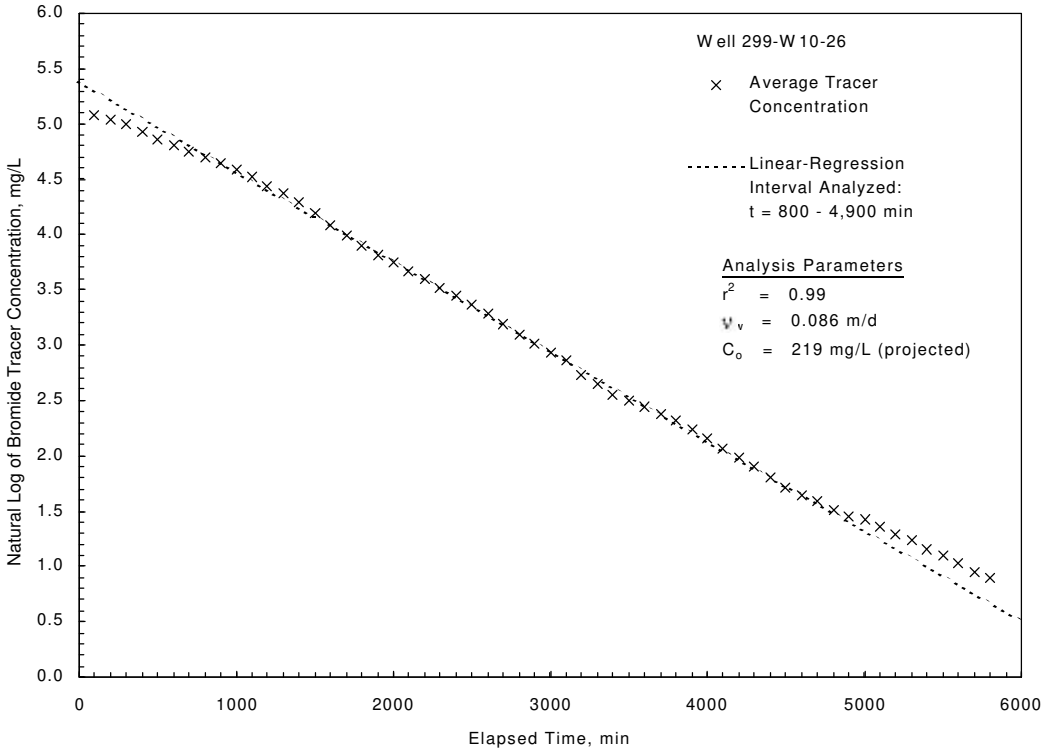

Figure 5.2. Average Tracer-Dilution Test Results Within Well 299-W10-26

Table 5.2. Tracer-Dilution Test Results for Well 299-W10-26

Well Sensor/ Depth Setting m, below top of casing	Tracer Concentration/ Dilution Slope, d (ln C) dt min^{-1}	Linear-Regression Correlation Coefficient, r^2	Projected Initial Tracer Concentration, C_o, mg/L	Well Measurement Area/Volume Ratio, A/V m^{-1}	Calculated Well-Screen Flow Velocity, v_w, m/d
67.8	-0.000874	0.99	160	13.723	0.092
69.2	-0.000856	0.99	174	13.650	0.090
71.0	-0.000859	0.99	173	13.577	0.091
73.5	(a)	(a)	(a)	13.505	(a)
75.0	(a)	(a)	(a)	13.435	(a)
77.1	(a)	(a)	(a)	13.364	(a)
Average(b)	-0.000815	0.99	219	13.577	0.086

(a) Not applicable because of nonlinear tracer-dilution pattern or erratic sensor readings.
(b) Linear-regression analysis of average concentration response for upper five sensor-depth settings.

to allow for dissipation of the displaced water from the tube into the surrounding well-screen column. After the equilibration period, the tube was slowly raised out of the well-water column, causing emplacement of the 1.36 L of prepared tracer. The tube was then slowly lowered and raised five times within the water column over a 10-min period to mix the tracer within the well-screen section. To facilitate mixing of the tracer, a bottom-line static mixer was attached to the tube. The designed concentration within the well screen following mixing of the added tracer was ~150 mg/L.

Following mixing of the tracer solution, an assembly of six bromide probe sensors, uniformly spaced at a separation distance of 1.83 m, was lowered into the well. The sensors performed erratically after installation. Repeated efforts to rectify the performance were not completely successful during the course of the test. The cause of the erratic behavior is believed to be associated with interference effects of the sensor surface and proximity to the metal well-screen surface. The individual sensors were subsequently replated, and plastic centralizers were used to eliminate direct contact with the well-screen metal surface for subsequent tracer-dilution tests. A tracer-pumpback test was initiated on April 1, 1999 (0930 Pacific standard time) to remove the introduced tracer from the well and surrounding aquifer.

The second test was initiated on April 30, 1999 (0935 Pacific daylight time) by introducing 5.41 L of tracer solution (containing 17.32 g of bromide) within the 10.68-m well-screen section (67.09 to 77.77 m below top of casing). The tracer was introduced into the well using a 0.025-m polypropylene tube that was open at a depth setting of 77.5 m below top of casing. Following tracer introduction, an equilibration time of ~10 min was observed to allow for dissipation of the displaced water from the tube into the surrounding well-screen column. After the equilibration period, the tube was slowly raised out of the well-water column, causing emplacement of the 5.41 L of prepared tracer into the water column. The tube was then slowly lowered and raised seven times within the water column over a 7-min period to mix the tracer within the well-screen section. To facilitate mixing of the tracer within the well screen, a bottom-line static mixer was attached to the bottom of the tube. The designed concentration within the well screen following mixing of the added tracer was ~200 mg/L.

Following mixing of the tracer solution, an assembly of six bromide probe sensors, uniformly spaced at a separation distance of 1.83 m, was lowered into the well. Final depth settings for the six sensors was 68.0, 69.8, 71.6, 73.5, 75.3, and 77.1 m below top of casing. Each sensor had an attached plastic centralizer to keep the probe approximately centered within the well-screen section. Installation of the assembly was completed in ~30 min, following the mixing of the tracer within the well-screen section. The concentration within the borehole following emplacement and equilibration of the sensors (i.e., after 70 min following initial mixing) ranged between 91 (bottom sensor) to 168 mg/L for the other sensor-depth settings. The uneven dilution pattern within the test interval is believed to be attributed to the too rapid mixing procedure and use of the bottom-line static mixer, which may have caused movement of "fresh" water from the aquifer into the well-screen section. The dilution and dissipation within the well screen were observed for a period of 5,738 min (3.98 d). At the end of the test, the concentration was <1.1 mg/L within the well-screen section.

Visual examination of the dilution patterns for the various sensor-depth settings indicates a significant, vertical, downward-flow condition within the well-screen section (see Section 8.2). Downward, in-well, flow velocities, ranging between 0.008 and 0.015 m/min, were calculated by using the arrival

times of recognizable signatures between the lower three sensors. The measured velocities are comparable with those reported for well 299-W14-13 by Waldrop and Pearson (2000) (0.012 - 0.013 m/min detected with a vertical EM flow meter).

To be strictly valid, tracer-dilution tests require that no vertical flow conditions exist within the well and that the tracer is continually mixed within the test section. Because of the significant vertical flow conditions within the well screen, no v_w or vertical permeability profile within the well-screen section could be estimated based on the dilution pattern. A tracer-pumpback test was initiated on May 4, 1999 (0930 Pacific daylight time) to remove the introduced tracer from the well and surrounding aquifer.

5.4 Well 299-W19-42

Two single-well tracer tests (including tracer dilution and pumpback) were conducted at the well site. The first was initiated on March 9, 1999 (1153 Pacific standard time) by introducing 5.32 L of tracer solution (containing 8.57 g of bromide) within the 10.5-m well-screen section. The tracer was introduced into the well using a 0.025-m galvanized pipe, onto which six bromide sensor probes were attached. Following tracer introduction, an equilibration time of ~5 min was observed to allow for dissipation of the displaced water from the pipe into the surrounding well-screen column. After the equilibration period, the pipe was slowly raised and lowered repeatedly within the water column to mix the tracer within the well-screen section. It was recognized early in the test that the sensors were performing erratically. The cause of the erratic behavior was found to be associated with interference effects of the sensor surface and proximity to the pipe, onto which the sensors were attached. Because of the interference effects, the tracer-dilution test could not be monitored. Subsequently, a tracer-pumpback test was initiated on March 16, 1999 (0853 Pacific standard time) to remove the introduced tracer from the well and surrounding aquifer.

The second test was initiated on May 17, 1999 (0938 Pacific standard time) by introducing 5.32 L of tracer solution (containing 17.13 g of bromide) within the 10.5-m well-screen section. The tracer was introduced into the well using a 0.025-m polypropylene tube that was open at a depth setting of 78.5 m below top of casing. Following tracer introduction, an equilibration time of ~12 min was observed to allow for dissipation of the displaced water from the tube into the surrounding well-screen column. After the equilibration period, the tube was slowly raised out of the well-water column, causing emplacement of the 5.32 L of prepared tracer. The tube was then slowly lowered and raised six times within the water column over a 9-min period to mix the tracer within the well-screen section. To facilitate mixing of the tracer, a bottom-line static mixer was attached to the bottom of the tube. The designed concentration within the well screen following mixing of the added tracer was ~200 mg/L.

Following mixing of the tracer solution, an assembly of six bromide probe sensors, spaced uniformly at a separation distance of 1.83 m, was lowered into the well. Final depth settings for the six sensors were 68.9, 70.7, 72.5, 74.4, 76.2, and 78.0 m below top of casing. Installation of the assembly was completed in ~15 min, following the mixing of the tracer within the well-screen section. The concentration within the borehole following emplacement and equilibration of the sensors (i.e., after 60 min following initial mixing) was ~159 mg/L and ranged between 137 and 183 mg/L for the various sensor-depth settings. The projected, average, initial C_o, based on back-projection of the fitted linear-regression concentration

response to time = 0 min, was 221 mg/L. The uneven dilution pattern within the test interval is believed to be attributed to a too rapid mixing procedure and use of the bottom-line static mixer, which may have caused movement of "fresh" groundwater from the aquifer into the well-screen section. The dilution and dissipation within the well screen were observed for a period of 4,240 min (2.94 d). At the end of the test, the average concentration was <1 mg/L.

Visual examination of the dilution patterns for the various sensor-depth settings indicates no significant vertical flow conditions within the well-screen section. The natural log of concentration versus time depth-setting plots exhibit linear relationships over the period of observation for all sensor locations. The observed dilution pattern versus time can be analyzed to calculate v_w, using Equation (3.3). Linear-regression analysis of the average dilution response (shown in Figure 5.3) for the six sensor-depth settings within the well screen ($r^2 = 0.99$) indicates a slope on the natural log of concentration versus time of $-0.001601\ min^{-1}$. The calculated average A/V relationship for the test interval, taking into account the presence of sensor instrumentation/cable test system cross-sectional area, is $13.541\ m^{-1}$. Based on these observed and measured parameters, an average calculated v_w is 0.170 m/d.

If lateral groundwater-flow conditions occur throughout the entire well, then a comparison of the calculated velocities at the various sensor-depth settings can provide an assessment of the vertical permeability profile within the well-screen section. A comparison of the calculated velocities at the six

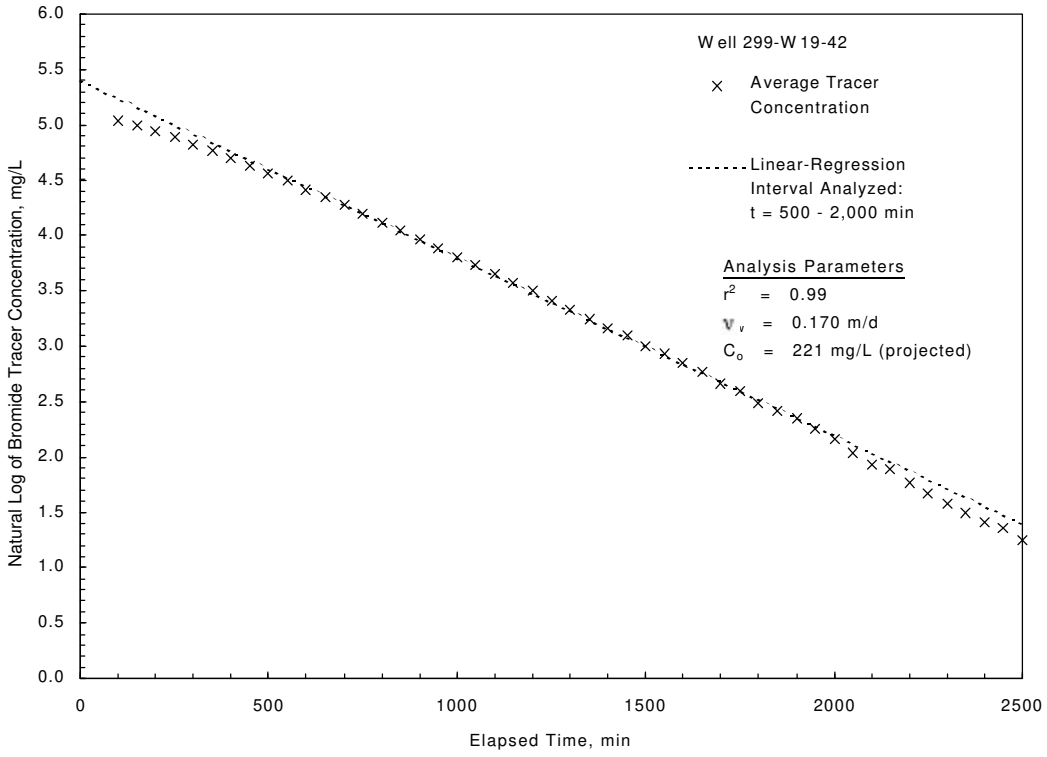

Figure 5.3. Average Tracer-Dilution Test Results Within Well 299-W19-42

sensor-depth settings at well 299-W19-42, however, indicates rather uniform velocities across the well-screen section (i.e., 0.149 to 0.181 m/d). This small range in calculated velocities suggests that no significant variations in permeability exist within the well-screen interval. Table 5.3 summarizes the results from the tracer-dilution test at well 299-W19-42.

Table 5.3. Tracer-Dilution Test Results for Well 299-W19-42

Well Sensor/ Depth Setting m, below top of casing	Tracer Concentration/ Dilution Slope, d (ln C) dt min^{-1}	Linear-Regression Correlation Coefficient, r^2	Projected Initial Tracer Concentration, C_o, mg/L	Well Measurement Area/Volume Ratio, A/V, m^{-1}	Calculated Well-Screen Flow Velocity, v_w, m/d
68.9	-0.001613	0.99	187	13.723	0.169
70.7	-0.001531	0.99	252	13.650	0.161
72.5	-0.001707	0.99	225	13.577	0.181
74.4	-0.001613	0.99	213	13.505	0.172
76.2	-0.001524	0.99	210	13.434	0.163
78.0	-0.001386	0.99	193	13.364	0.149
Average	-0.001601	0.99	221	13.541	0.170

6.0 Tracer-Pumpback Test Results

Results from the bromide tracer-pumpback phase of the single-well tracer testing were analyzed using the methods described in Section 3.2.2. As noted previously, the analytical assumptions of full aquifer penetration and rapid pulse injection into the aquifer were not met with the given field test conditions. Because of these test deficiencies, the estimates derived from the pumpback test for effective porosity, n_e, and average groundwater-flow velocity within the aquifer, v_a, should be used qualitatively only. Future efforts will be directed to improve the estimates for n_e and v_a by accounting for these effects. A description of the information pertinent to the tracer-pumpback test performed in four wells is provided below.

6.1 Well 299-W10-24

After a 17,455-min (12.12-d) tracer-drift period, t_d, recovery of the tracer from well 299-W10-24 and the surrounding aquifer was initiated with a constant-rate pumping test beginning on April 21, 1999 (1225 Pacific daylight time). Tracer recovery was terminated after 235 min. The average tracer concentration within the well was 26.0 mg/L at the beginning of pumpback. Given the calculated well screen and sandpack volumes of 84.07 and 71.12 L, respectively, 13.71 g of the 16.82 g of tracer initially emplaced in the well are estimated to have been transported within the aquifer. After minor flow adjustments were completed during the first 2 min of the test, pumping rates remained relatively constant during tracer pumpback, ranging between 37.8 and 41.7 L/min (average 41.2 L/min) for the entire test. An estimated 12.81 g of the total 16.82 g of tracer (i.e., 76 %) emplaced in the well were recovered during the constant-rate pumping test. The pumping time, t_p, to recover 50% of the tracer emplaced within the aquifer (accounting for transit time during pumping from the well screen to land surface) is estimated at 37.1 min. The time required to recover the center of the tracer mass that was transported within the aquifer was used in Equations (3.8) and (3.9) to calculate n_e and v_a. As indicated in the equations, information pertaining to hydraulic conductivity, K, hydraulic gradient, I, aquifer thickness, b, and pumping rate, Q, must also be known for the test well site.

A K value of 1.22 m/d was used, which is based on results from the constant-rate pumping test for the test well (i.e., during tracer pumpback). The calculated local I value of 0.00172 m/m and flow direction of 5 degrees (0 degrees East; 90 degrees North) were determined using trend-surface analysis for water-level elevation measurement periods from well 299-W10-24 and five nearby monitor wells (299-W10-8, -W10-12, -W10-22, -W11-23, and -W11-27) immediately prior to initiating tracer-pumpback testing on April 21, 1999. The I value is consistent with other trend-surface analysis results for 1998 water-level measurements for monitor wells analyzed. The b value of 54 m was calculated directly from projection of known geologic relationships at nearby wells.

Based on these input parameters and tracer-pumpback results, n_e and v_a are estimated to be 0.072 and 0.029 m/d, respectively. Based on the observed tracer-pumpback profile (Figure 6.1) and calculated radial distance traveled within the aquifer by the tracer's center of mass (i.e., product of v_a and t_d = 0.35 m), the results of pumpback are reflective of local, near-well, aquifer conditions and may be susceptible to the adverse wellbore effects discussed in Section 3.2.2.

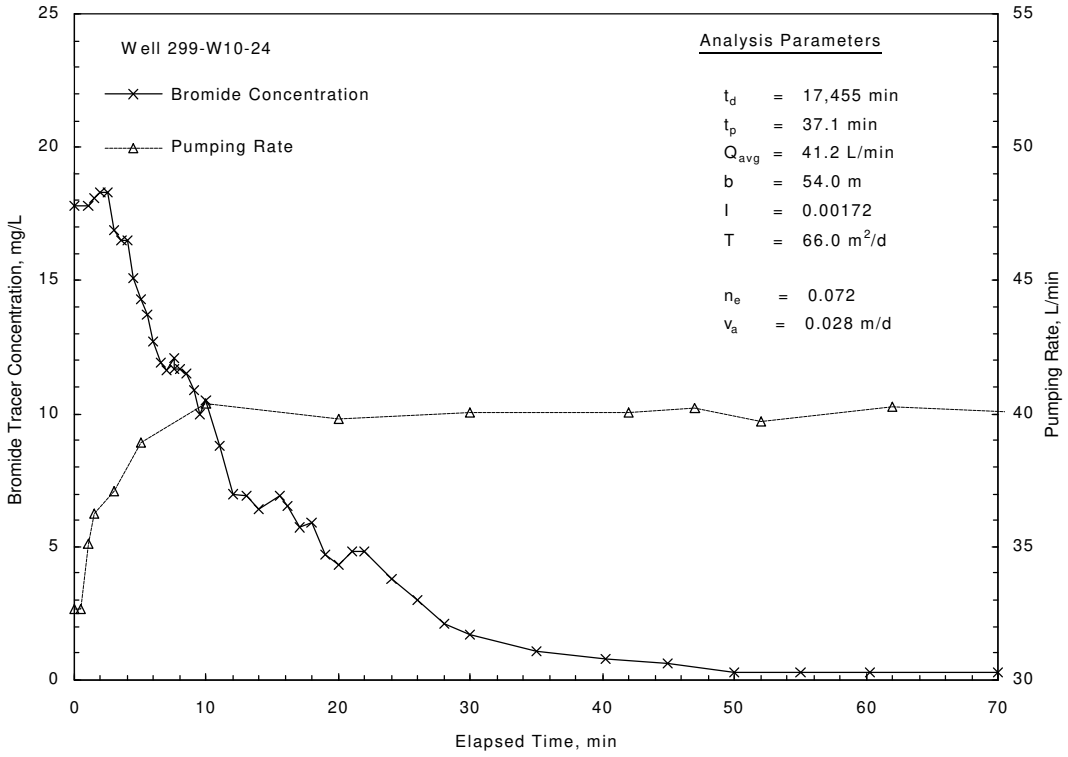

Figure 6.1. Tracer-Pumpback Test Results for Well 299-W10-24

Table 6.1 summarizes the pertinent information associated with the tracer-pumpback results for well 299-W10-24. The hydraulic property estimates obtained for the tracer-pumpback results fall slightly below the reported range (n_e = 0.1 to 0.3; v_a = 0.047 to 0.14 m/d) for these parameters in Table 3.3-1 of Hartman (1999) for Waste Management Area T. It should be noted, however, that the property ranges listed by Hartman (1999) are not based on direct field test results and are either assumed values (i.e., for n_e) or calculated, based on the Darcy groundwater-flow equation relationship (i.e., to estimate v_a).

6.2 Well 299-W10-26

After a 7,259-min (5.04-d) t_d, recovery of the tracer from well 299-W10-26 and the surrounding aquifer was initiated with a constant-rate pumping test beginning on April 28, 1999 (1039 Pacific daylight time). Tracer recovery was terminated after 213 min. The average tracer concentration within the well was <1.0 mg/L at the beginning of pumpback. Because of the extremely small in-well concentrations, ~16.79 g of the 16.89 g of tracer initially emplaced in the well are estimated to have been transported within the aquifer. After minor flow adjustments were completed during the first 5 min of the test, pumping rates remained relatively constant during tracer pumpback, ranging between 38.7 and 44.7 L/min (average 39.5 L/min) for the entire test. An estimated 12.82 g of the total 16.89 g of tracer (i.e., 76%) emplaced in the well were recovered during the constant-rate pumping test. The t_p to recover 50% of the tracer emplaced within the aquifer (accounting for transit time during pumping from the well

Table 6.1. Tracer-Pumpback Test Summary

Waste Management Area	Well	Hydrologic Characterization Data				Tracer-Pumpback Test			
		Aquifer Thickness, b, m	Pumping Rate, Q, L/min	Hydraulic Gradient, I, m/m	Transmissivity, T, m^2/d	Tracer Drift Time, t_d, min	Tracer Recovery Time, t_p, min	Effective Porosity, n_e	Groundwater-Flow Velocity, v_a, m/d
T	299-W10-24	54.0	41.2	0.00172	66	17,455	37.3	0.072	0.029
TX-TY	299-W10-26[(a)]	55.0	39.5	0.00073	82	7,259	16.0	vf[(b)] (0.010)	vf[(b)] (0.124)
	299-W14-13[(a)]	55.0	48.9	0.00073	135	8,575	43.3	VF[(c)] (0.009)	VF[(c)] (0.191)
U	299-W19-42	56.4	62.4	0.00184	345	4,240	123.2	0.027	0.419

(a) Tracer-pumpback test results are highly questionable and are provided for information only.
(b) Slight vertical flow conditions detected in well tracer test estimates for n_e and v_a are questionable.
(c) Significant vertical flow conditions detected in well tracer test estimates for n_e and v_a are highly questionable.

screen to land surface) is estimated at 16.0 min. The time required to recover the center of the tracer mass that was transported within the aquifer was used in Equations (3.8) and (3.9) to calculate n_e and v_a. As indicated in the equations, information pertaining to K, I, b, and Q must also be known for the test well site.

A K value of 1.49 m/d was used, which is based on results from the constant-rate pumping test for the test well (i.e., during tracer pumpback). The local calculated I value of 0.00073 m/m and flow direction of 288 degrees (0 degrees East; 90 degrees North) were determined using trend-surface analysis for water-level elevation measurement periods from five nearby monitor wells (299-W10-17, -W10-18, -W14-12, -W15-12, and -W15-22) ~5 d after termination of tracer pumpback. The I value is consistent with that listed in Table 3.3-1 of Hartman (1999) (0.00079 for Waste Management Area TX-TY). The b value of 55 m was calculated directly from projection from known geologic relationships at nearby wells.

Based on these input parameters and tracer-pumpback results, n_e and v_a are estimated to be 0.010 and 0.124 m/d, respectively (Figure 6.2). Because of the vertical flow conditions that were observed during the tracer-dilution test, the estimated values from the tracer-pumpback test are questionable also. The effects of vertical flow likely induce a significant underestimate for n_e. This is attributed to the fact that the part of the aquifer within the well-screen section receiving the tracer during dilution/injection is significantly smaller than the part of the aquifer providing groundwater during pumpback. There is no correction method available for modifying Q in Equation (3.8) to account for the testing differences.

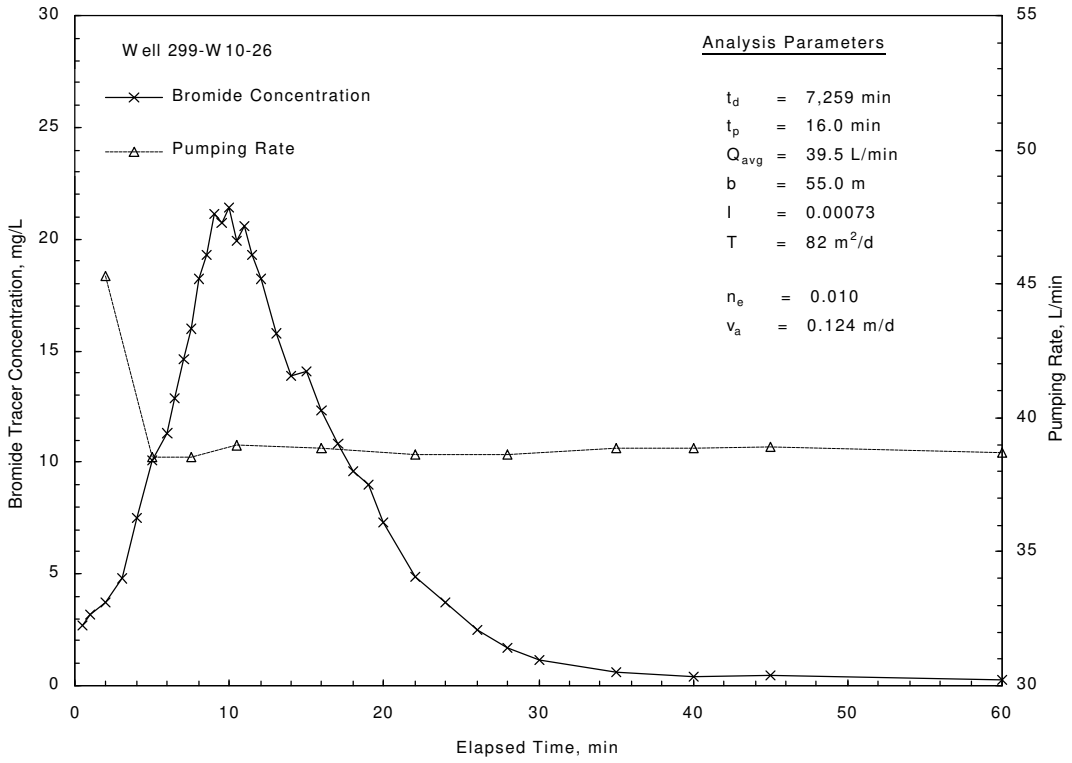

Figure 6.2. Tracer-Pumpback Test Results for Well 299-W10-26

Although the estimate for v_a falls within the range listed in Table 3.3-1 of Hartman (1999) for Waste Management Area TX-TY (i.e., v_a = 0.04 to 0.43 m/d), it is also likely influenced by the effects of vertical flow during the tracer-dilution test and should be considered highly questionable. The pumpback results for well 299-W10-26 are included in Table 6.1 for comparison purposes only.

6.3 Well 299-W14-13

After a 8,575-min (5.95-d) t_d, recovery of the tracer from well 299-W14-13 and the surrounding aquifer was initiated with a constant-rate pumping test beginning on April 1, 1999 (0930 Pacific standard time). Tracer recovery was terminated after 270 min. The average tracer concentration within the well was <1.0 mg/L at the beginning of pumpback. Because of the extremely small in-well concentration, 12.7 g of the 12.8 g of tracer initially emplaced in the well are estimated to have been transported within the aquifer. After minor flow adjustments were completed during the first 5 min of the test, pumping rates remained relatively constant during tracer pumpback, ranging between 48.2 and 49.1 L/min (average 48.9 L/min) for the entire test. An estimated 10.83 g of the total 12.8 g of tracer (i.e., 85%) emplaced in the well were recovered during the constant-rate pumping test. The t_p to recover 50% of the tracer emplaced within the aquifer (accounting for transit time during pumping from the well screen to land surface) is estimated at 43.3 min. The time required to recover the center of the tracer mass that was transported within the aquifer was used in Equations (3.8) and (3.9) to calculate n_e and v_a. As indicated in the equations, information pertaining to K, I, b, and Q must also be known for the test well site.

A K value of 2.45 m/d was used, which is based on results from the constant-rate pumping test for the test well (i.e., during tracer pumpback). The local calculated I value of 0.00073 m/m and flow direction of 288 degrees (0 degrees East; 90 degrees North) were determined using trend-surface analysis for water-level elevation measurement periods from five nearby monitor wells (299-W10-17, -W10-18, -W14-12, -W15-12, and -W15-22) ~30 d after termination of tracer pumpback. The I value is consistent with Table 3.3-1 of Hartman (1999) (0.00079) for Waste Management Area TX-TY. The b value of 55 m was calculated directly from projection from known geologic relationships at nearby wells.

Based on these input parameters and tracer-pumpback results, n_e and v_a are estimated to be 0.009 and 0.191 m/d, respectively (Figure 6.3). Because of the vertical flow conditions that were observed during the tracer-dilution test, the estimated values from the tracer-pumpback test are highly questionable also. The effects of vertical flow likely induce a significant underestimate for n_e. This is attributed to the fact that the part of the aquifer within the well-screen section receiving the tracer during dilution/injection is significantly smaller than the part of the aquifer providing groundwater during pumpback. There is no correction method available for modifying Q in Equation (3.8) to account for the testing differences.

Although the estimate for v_a falls within the range listed in Table 3.3-1 of Hartman (1999) for Waste Management Area TX-TY (i.e., v_a = 0.04 to 0.43 m/d), it is also likely influenced by the effects of vertical flow during the tracer-dilution test and should be considered highly questionable. The pumpback results for well 299-W14-13 are included in Table 6.1 for comparison purposes only.

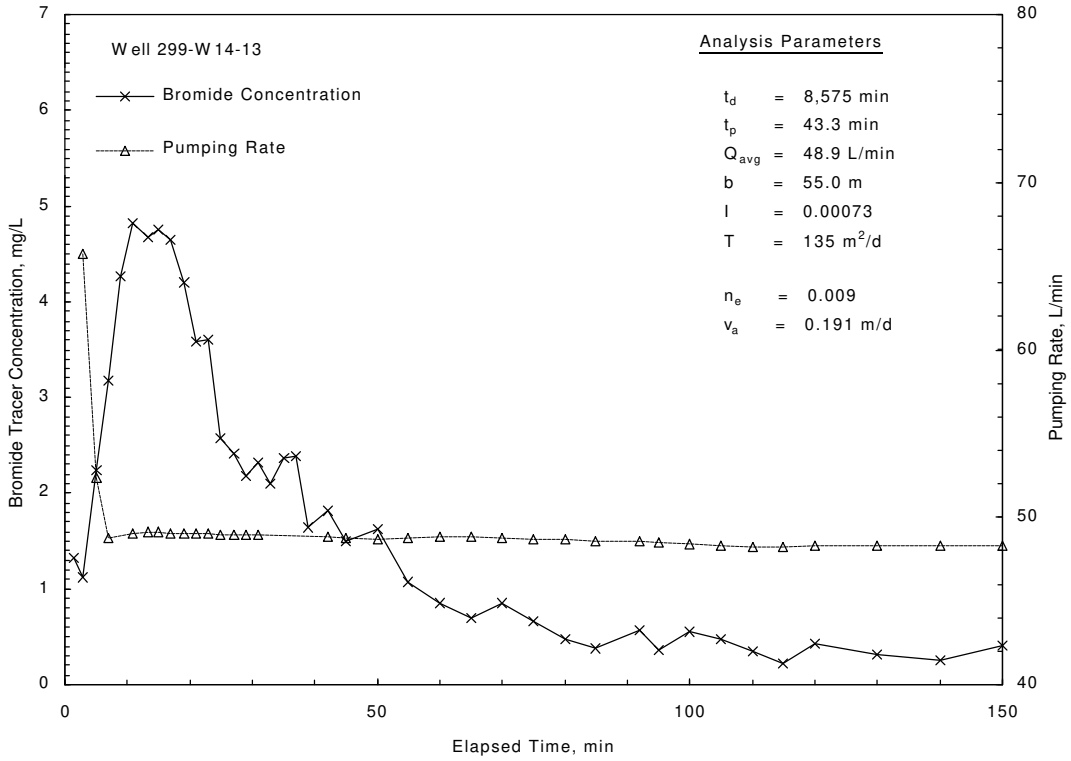

Figure 6.3. Tracer-Pumpback Test Results for Well 299-W14-13

6.4 Well 299-W19-42

After a 4,240-min (2.94-d) t_d, recovery of the tracer from well 299-W19-42 and the surrounding aquifer was initiated with a constant-rate pumping test beginning on May 20, 1999 (0835 Pacific standard time). Tracer recovery was terminated after 265 min. The average tracer concentration within the well-screen section was <1.0 mg/L at the beginning of pumpback, indicating that ≤0.1 g of the 17.13 g was not emplaced within the aquifer. After minor flow adjustments were completed during the first 2 min of the test, pumping rates remained relatively constant during tracer pumpback, ranging between 61.5 and 63.0 L/min (average 62.4 L/min) for the entire test. An estimated 12.62 g of the total 17.13 g of tracer (i.e., 74 %) emplaced in the well were recovered during the constant-rate pumping test. The t_p to recover 50% of the tracer emplaced within the aquifer (accounting for transit time during pumping from the well screen to land surface) is estimated at 123.2 min. The time required to recover the center of the tracer mass that was transported within the aquifer was used in Equations (3.8) and (3.9) to calculate n_e and v_a. As indicated in the equations, information pertaining to K, I, b, and Q must also be known for the test well site.

A K value of 6.12 m/d was used, which is based on results from the constant-rate pumping test for the test well (i.e., during tracer pumpback). The calculated local I value of 0.00184 m/m and flow direction of 284 degrees (0 degrees East; 90 degrees North) were determined using trend-surface analysis for water-level elevation measurement periods from well 299-W19-42 and six nearby monitor wells

(299-W18-25, -W18-30, -W18-31, -W19-12, -W19-31, and -W19-32) during the tracer-dilution test. The I value is slightly higher than that listed in Table 3.3-1 of Hartman (1999) (0.0014 m/m) for Waste Management Area U. The b value of 56.4 m was calculated directly from projection from known geologic relationships at nearby wells.

Based on these input parameters and tracer-pumpback results, n_e and v_a are estimated to be 0.027 and 0.419 m/d, respectively (Figure 6.4). Based on the observed tracer-pumpback profile and calculated radial distance traveled within the aquifer by the tracer's center of mass (i.e., product of v_a and t_d = 1.23 m), the results of the tracer pumpback are reflective of local, near-well, aquifer conditions and may be susceptible to the adverse wellbore effects discussed in Section 3.2.2.

Table 6.1 summarizes the pertinent information associated with the tracer-pumpback results for well 299-W19-42. The hydraulic property estimates obtained fall slightly below the reported range (n_e = 0.1 to 0.3; v_a = 0.028 to 0.52 m/d) for the parameters listed in Table 3.3-1 of Hartman (1999) for Waste Management Area U. It should be noted, however, that the property ranges listed by Hartman (1999) are not based on direct field test results and are either assumed values (i.e., for n_e) or calculated, based on the Darcy groundwater-flow equation relationship (i.e., to estimate v_a).

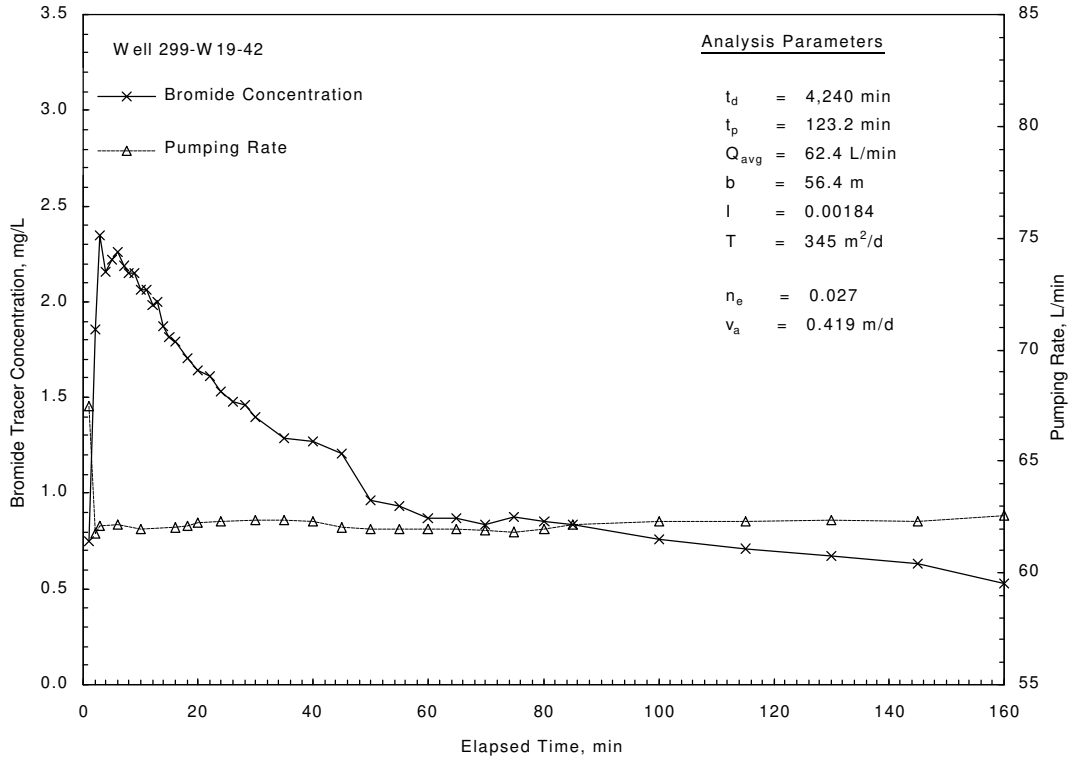

Figure 6.4. Tracer-Pumpback Test Results for Well 299-W19-42

7.0 Constant-Rate Pumping Test Results

Constant-rate pumping tests were conducted in concert with the tracer-pumpback tests at the four well sites selected for detailed hydrologic characterization. Analysis of the drawdown and recovery test data at the pumped well and neighboring observation well provides large-scale hydraulic property estimates (i.e., transmissivity, T; hydraulic conductivity, K; vertical anisotropy, K_D; storativity, S; and specific yield, S_y). Analysis of the constant-rate pumping-test data included barometric response analysis for removing the effects of barometric pressure fluctuations from well water-level test responses, diagnostic derivative analysis for model identification and selection of the appropriate analysis method, and combined type-curve and derivative plot analysis for hydraulic property determination. A detailed description of the various components of the constant-rate pumping-test analysis is provided in Section 3.3. A description of the performance and analysis of the constant-rate pumping tests conducted at each of the four well sites is provided below. A summary of the constant-rate pumping results is presented in Table 7.1. As shown, good correspondence for T and K estimates obtained from pumping well and observation well test analysis were exhibited for most test sites. K estimates were calculated by dividing T by the total aquifer thickness, b, rather than the length of the well-screen section at the pumping well. This is appropriate because the analysis type curves account for partial penetration of the aquifer and K_D.

Table 7.1. Constant-Rate Pumping Test Summary

Pumping Well	Well Analyzed	Transmissivity, T, m^2/d	Horizontal Hydraulic Conductivity, K_h, m/d	Vertical Anisotropy, K_D	Storativity, S	Specific Yield, S_y
299-W10-24	299-W10-24	66	1.22	0.001	0.00011	0.11
	299-W11-27[(a)]	66	1.22	0.001	0.0065	>1.0[(b)]
	Best estimate	66	1.22	0.001	0.00011	0.11
299-W10-26	299-W10-26	82	1.49	0.1	0.0014	0.14
	299-W10-18[(a)]	75	1.36	0.1	0.0048	0.48[a]
	Best estimate	82	1.49	0.1	0.0014	0.14
299-W14-13	299-W14-13	135	2.45	0.005	0.0012	0.12
	299-W14-12[(a)]	135	2.45	0.005	0.0025	0.25
	Best estimate	135	2.45	0.005	0.0012	0.12
299-W19-42	299-W19-42	345	6.12	0.1	0.00017	0.17
	299-W19-31[(a)]	345	6.12	0.1	0.0024	>1.0[(a)]
	Best estimate	345	6.12	0.1	0.00017	0.17

(a) Observation well.
(b) The unrealistically high value is attributed to capillary/drainage effects associated with the shallow observation well screen completion across the water table.

Test analyses of observation well responses indicated a delay that could not be entirely accounted for by well-storage effects. Type-curve analyses of the observation well data, therefore, produced reasonable T and K estimates but unrealistically high S and S_y estimates. This additional delay is probably caused by the relatively small penetration of the aquifer by the observation well screen and its location at the water table, where capillary forces are significant.

7.1 Well 299-W10-24

Well 299-W10-24 penetrates the upper 10.7 m of the unconfined aquifer. An observation well, 299-W11-27, is located at a radial distance of 2.27 m from well 299-W10-24 and penetrates only 0.43 m below the water table. The aquifer thickness at the test site is estimated at 54 m. The constant-rate discharge test was conducted from 1125 to 1520 Pacific standard time on April 21, 1999. The average flow rate was 41.2 L/min over the 235-min pumping period.

Prior to the constant-rate test, barometric response characteristics were monitored for a 10-d period at observation well 299-W11-27. Well 299-W10-24 was not monitored during most of this period because the tracer-dilution test was being performed. Following the constant-rate test, barometric response characteristics at well 299-W10-24 were evaluated over a 5-d period. The multiple-regression deconvolution technique (Rasmussen and Crawford 1997; Spane 1999) was used to remove barometric pressure effects from the measured water levels. A total lag time of 21 h provided the best match of barometric responses for both wells. Appendix Figure A.1 (top) shows both the original data and the data corrected for barometric effects for observation well 299-W11-27. The barometric pressure record, shifted by a constant, is also shown. Appendix Figure A.1 (bottom) shows a similar comparison for pumping well 299-W10-24.

Figure 7.1 shows the diagnostic log-log plot and type-curve match of the barometric corrected recovery data and derivative for pumping well 299-W10-24. Drawdown data were not selected for analysis because of the detrimental effects caused by small variations in discharge rate (not shown). The declining derivative pattern exhibited in Figure 7.1 (as a result of partial penetration effects) indicates there is no portion of the data where infinite-acting radial flow conditions are established. Therefore, straight-line analysis techniques cannot be used to analyze the test data.

The type-curve displayed is based on an assumed K_D of 0.001. Less extreme anisotropy values (e.g., 0.01, 0.10) did not provide a good fit of the test data. As discussed in Section 3.3, the type curve also accounts for partial penetration of the aquifer thickness and well-bore storage. The type-curve fit shown in Figure 7.1 provided the following results: T = 66 m^2/d, S = 1.1E-04, and S_y = 0.11. (Note: S is assumed, based on the calculated value for S_y and a fixed σ value of 0.001.) As discussed in Section 3.3, the pumping well did not display significant head losses at the pumping rates used in these tests. This is apparent because type-curve fitting of the pumping and observation well data yielded similar values for T. Therefore, results of the type-curve-fitting analysis for pumping well 299-W10-24 are considered to provide representative estimates of aquifer hydraulic properties.

Drawdown and recovery data for observation well 299-W11-27 are shown in Figure 7.2, along with the derivative of the recovery data. The recovery data for this observation well are smoother than the drawdown data but are steeper and do not fit the predicted type curve as well. The recovery data may be

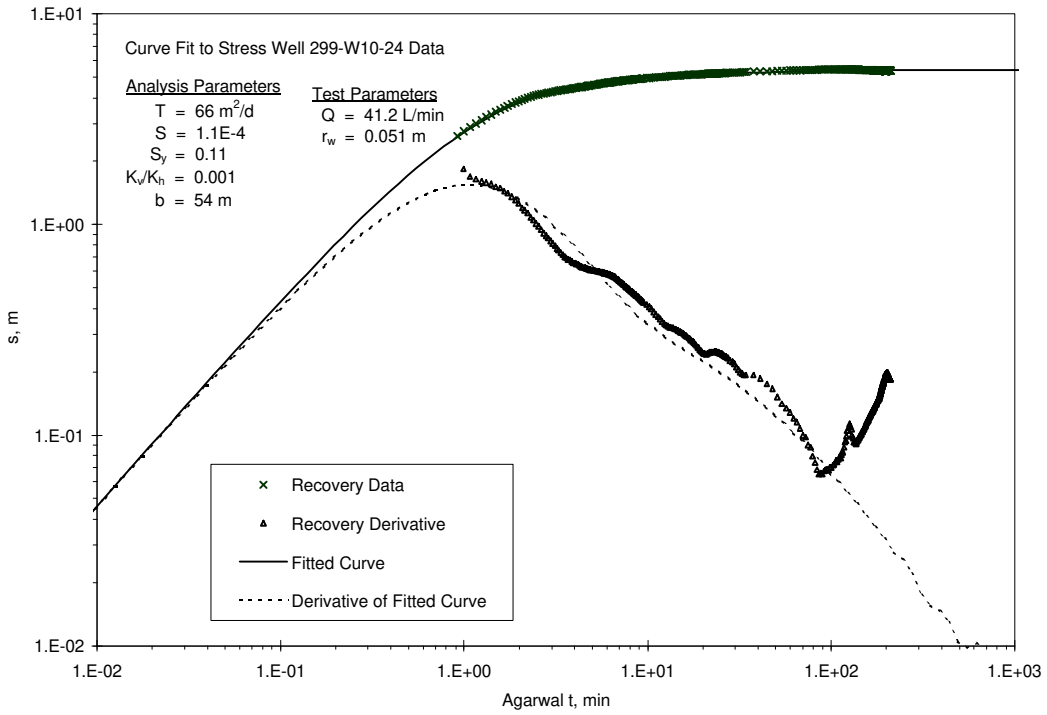

Figure 7.1. Type-Curve and Derivative Plot Analysis of Recovery Test Data for Pumping Well 299-W10-24

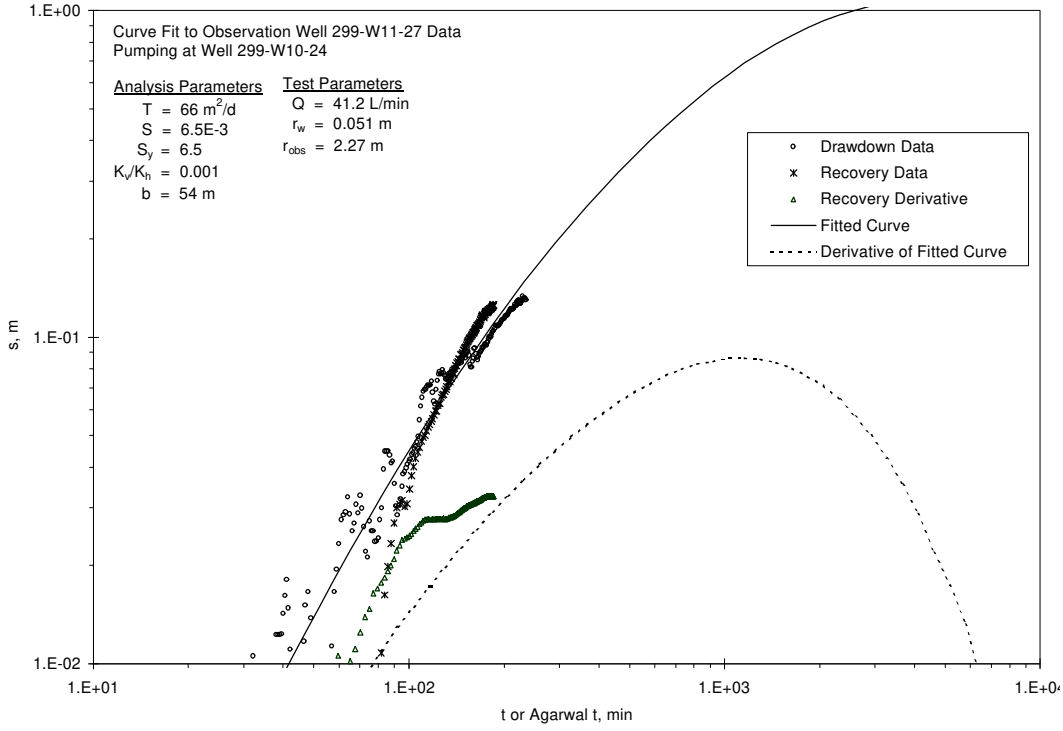

Figure 7.2. Type-Curve and Derivative Plot Analysis of Drawdown and Recovery Test Data for Observation Well 299-W11-27

affected by some residual barometric effects, which are more pronounced at the observation well because of the low magnitude of the water-level changes. As was the case for the pumping well test analysis, the type curve displayed in Figure 7.2 is also based on an assumed K_D of 0.001 and accounts for partial penetration and wellbore storage at the observation well. The type-curve fit produced the following analysis results: T = 66 m^2/d, S = 6.5E-03, and S_y >1.0. Although the T values from type-curve matches of the observation well and recovery data are identical, the calculated S value is unrealistically high, and the estimate for S_y is >1. The unrealistic values estimated for S and S_y are believed to be attributed to an additional delayed response at the observation well that is probably caused by the small penetration of the observation well below the water table. Capillary forces that are significant at the aquifer/vadose zone interface, and which are not accounted for in the analysis method, may explain the delayed response. (Note: The type curve plotted in Figure 7.2 only accounts for the delayed response at the observation well caused by wellbore storage.)

The additional delayed response in the observation well data is readily apparent in the composite analysis plot of well 299-W10-24 (recovery data) and well 299-W11-27 (drawdown data) shown in Figure 7.3. Shown also are the predicted test responses for the pumping and observations wells, based on analysis results obtained solely from well 299-W10-24. As shown, the additional delay of the observation well response is apparent by its shift to the right of the predicted response. Best estimates of hydraulic properties for the test site are based on the recovery analysis for pumping well 299-W10-24. These best estimate values are T = 66 m^2/d, S = 1.1E-04, S_y = 0.11, and K = 1.22 m/d (K is calculated by dividing T by b).

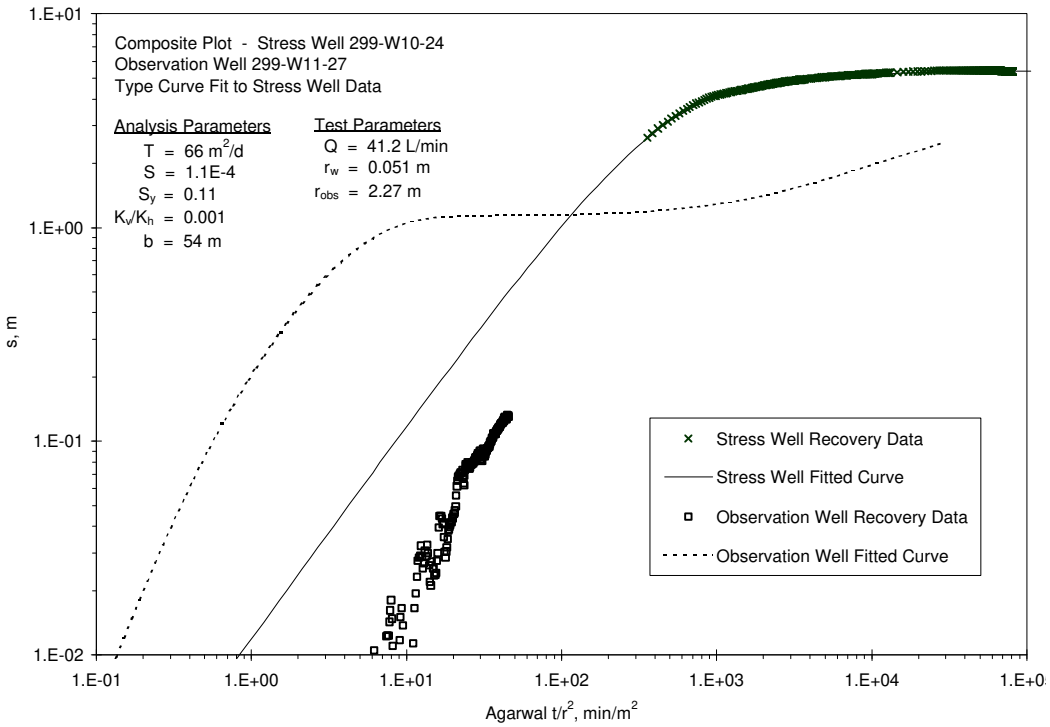

Figure 7.3. Composite Type-Curve and Derivative Plot Analysis for Pumping Well 299-W10-24 and Observation Well 299-W11-27

7.2 Well 299-W10-26

Well 299-W10-26 penetrates the upper 10.4 m of the unconfined aquifer. An observation well, 299-W10-18, is located at a radial distance of 5.53 m from well 299-W10-26 and penetrates only 0.8 m below the water table. The aquifer thickness at the test site is estimated at 55 m. The constant-rate discharge test was conducted from 0913 to 1312 Pacific standard time on April 24, 1999. The average flow rate was 39.5 L/min over the 213-min pumping period.

During a 10-d period in January 2000, barometric response characteristics were monitored at observation well 299-W10-26. The multiple-regression deconvolution technique (Rasmussen and Crawford 1997; Spane 1999) was used to remove barometric pressure effects from the measured water-levels. Total lag times of 20 and 21 h provided the best match of barometric responses for pumping and observation wells, respectively. Appendix Figure A.2 (top) shows both the original data and the data corrected for barometric effects for observation well 299-W10-18. The barometric pressure record, shifted by a constant, is also shown. Appendix Figure A.2 (bottom) shows a similar comparison for pumping well 299-W10-26.

Figure 7.4 shows the diagnostic log-log plot and type-curve match of the barometric corrected recovery data and derivative for pumping well 299-W10-26. Drawdown data were not selected for analysis because of the detrimental effects caused by small variations in discharge rate (not shown) during the early part of the test. The drawdown response, however, is identical to the recovery data after ~10 min

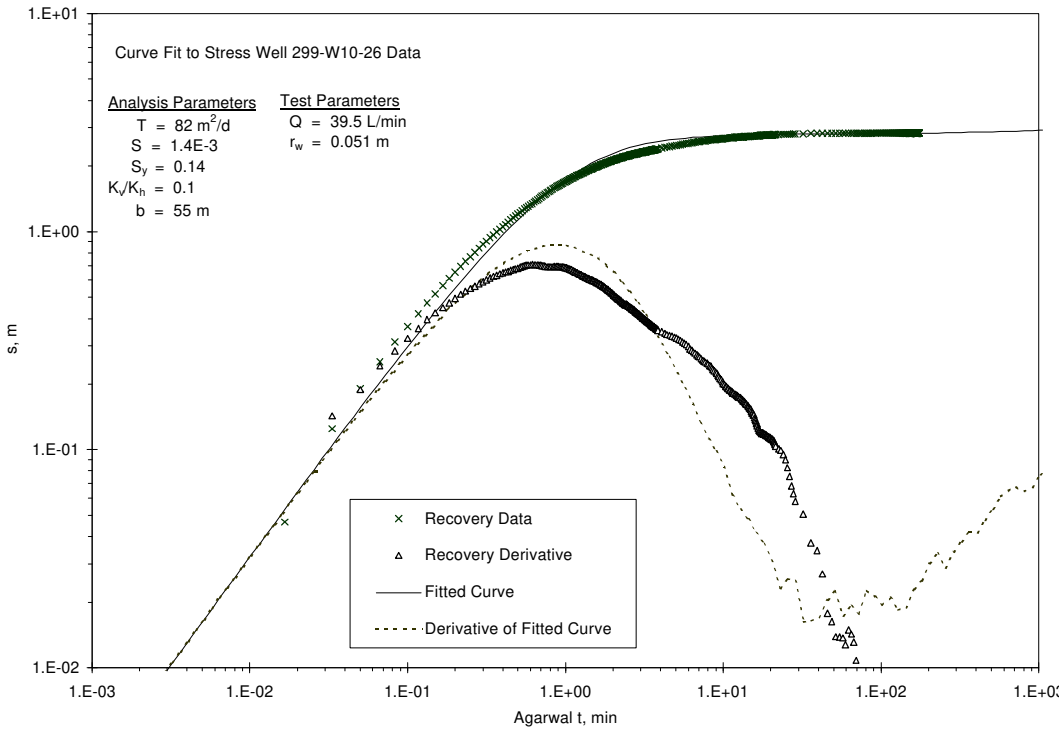

Figure 7.4. Type-Curve and Derivative Plot Analysis of Recovery Test Data for Pumping Well 299-W10-26

into the test. The declining derivative pattern exhibited in Figure 7.4 (as a result of partial penetration effects) indicates there is no portion of the data where infinite-acting radial flow conditions are established. Therefore, straight-line analysis techniques cannot be used to analyze the test data.

The type-curve displayed is based on an assumed K_D of 0.1. As discussed in Section 3.3, the type curve also accounts for well partial penetration of the aquifer thickness and wellbore storage. The type-curve fit shown in Figure 7.4 provided the following analysis results: T = 82 m^2/d, S = 1.4E-03, and S_y = 0.14. (Note: S is assumed, based on the calculated value for S_y and a fixed σ value of 0.001.) As discussed in Section 3.3, the pumping well did not display significant head losses at the pumping rates used in these tests. This is apparent because type-curve fitting of the pumping and observation well data yielded similar values for T. Therefore, results of the type-curve-fitting analysis for pumping well 299-W10-26 are considered to provide representative estimates of aquifer hydraulic properties.

Drawdown and recovery data for observation well 299-W10-18 are shown in Figure 7.5, along with the derivative of the recovery data. The drawdown data fit the predicted type curve better than the recovery data that may have been affected by some residual barometric effects, which are more pronounced at the observation well because of the low magnitude of the water-level changes. As was the case for the pumping well test analysis, the type curve displayed in Figure 7.5 is also based on an assumed K_D of 0.1 and accounts for partial penetration and wellbore storage at the observation well. The type-curve fit produced the following analysis results: T = 75 m^2/d, S = 4.8E-03, and S_y = 0.48. Although the T values from type-curve matches of the observation well and recovery data are identical, the calculated S and S_y values are higher than expected for the Ringold Formation. The higher-than-expected estimated S and S_y values are believed to be attributable to an additional delayed response at the observation well that is probably caused by the small penetration of the observation well below the water table. Capillary forces that are significant at the aquifer/vadose zone interface, and which are not accounted for in the analysis method, may explain the delayed response. It should be noted that there is a smaller difference between the storage values calculated for the pumping and observation wells for this test site than for the test conducted at well 299-W10-24, where the observation well penetration was even smaller, 0.43 m compared to 0.80 m.

The additional delayed response in the observation well data is readily apparent in the composite analysis plot of well 299-W10-26 (recovery data) and well 299-W10-18 (drawdown data) shown in Figure 7.6. Shown also are the predicted test responses for the pumping and observations wells, based on analysis results obtained solely from well 299-W10-26. As shown, the additional delay of the observation well response is apparent by its shift to the right of the predicted response. Best estimates of hydraulic properties for the test site are based on the recovery analysis for pumping well 299-W10-24. These best estimate values are T = 82 m^2/d, S = 1.43E-04, S_y = 0.14, and K = 1.49 m/d (K is calculated by dividing T by b).

7.3 Well 299-W14-13

Well 299-W14-13 penetrates the upper 10.6 m of the unconfined aquifer. An observation well, 299-W14-12, is located at a radial distance of 4.36 m from well 299-W14-13 and penetrates only 0.6 m

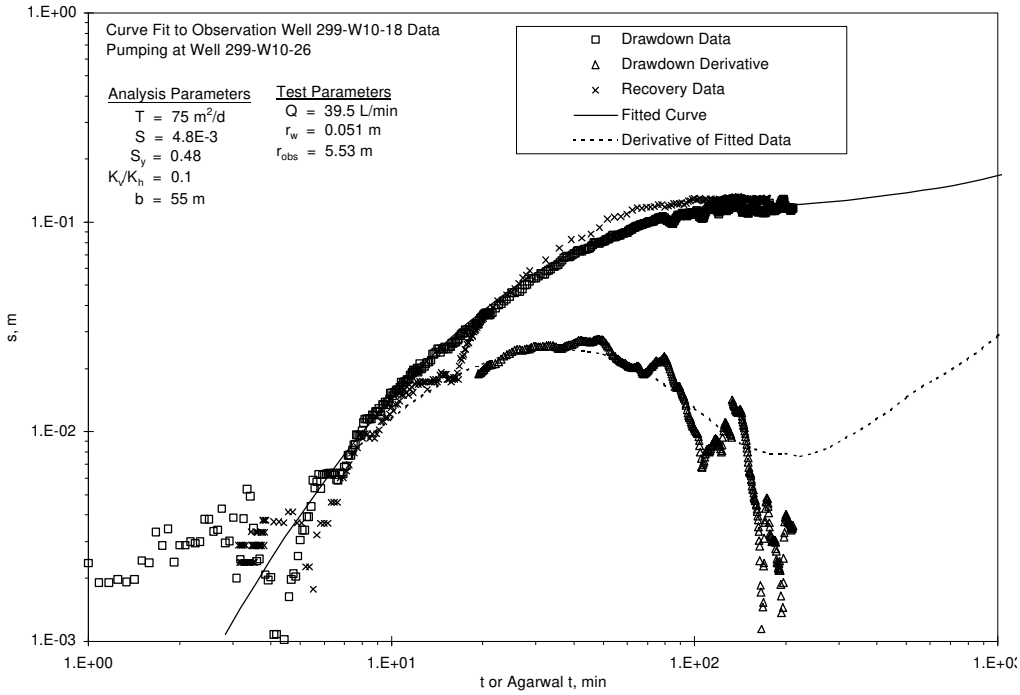

Figure 7.5. Type-Curve and Derivative Plot Analysis of Drawdown and Recovery Test Data for Observation Well 299-W10-18

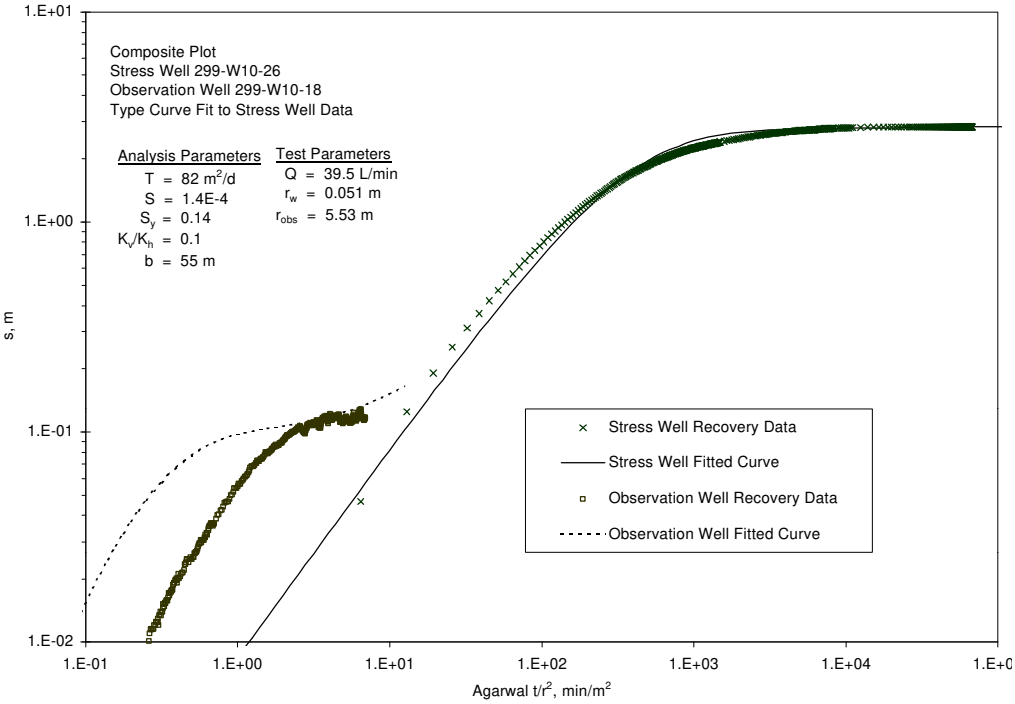

Figure 7.6. Composite Type-Curve and Derivative Plot Analysis for Pumping Well 299-W10-26 and Observation Well 299-W10-18

below the water table. The aquifer thickness at the test site is estimated at 55 m. The constant-rate discharge test was conducted from 0930 to 1430 Pacific standard time on April 1, 1999. The average flow rate was 48.9 L/min over the 270-min pumping period.

Directly following the test, barometric response characteristics were monitored for 3 d at both the pumping and observation wells (299-W14-13 and -W14-12). The multiple-regression deconvolution technique (Rasmussen and Crawford 1997; Spane 1999) was used to remove barometric pressure effects from the measured water levels. A total lag time of 15 h provided the best match of barometric responses for both well sites. Appendix Figure A.3 (top) shows both the original data and the data corrected for barometric effects for observation well 299-W14-12. The barometric pressure record, shifted by a constant, is also shown. Appendix Figure A.3 (bottom) shows a similar comparison for pumping well 299-W14-13.

Figure 7.7 shows the diagnostic log-log plot and type-curve match of the barometric corrected recovery data and derivative for pumping well 299-W14-13. Drawdown data were not selected for analysis because of the detrimental effects caused by small variations in discharge rate (not shown) during the test. The declining derivative pattern exhibited in Figure 7.7 (as a result of partial penetration effects) indicates there is no portion of the data where infinite-acting radial flow conditions are established. Therefore, straight-line analysis techniques cannot be used to analyze the test data.

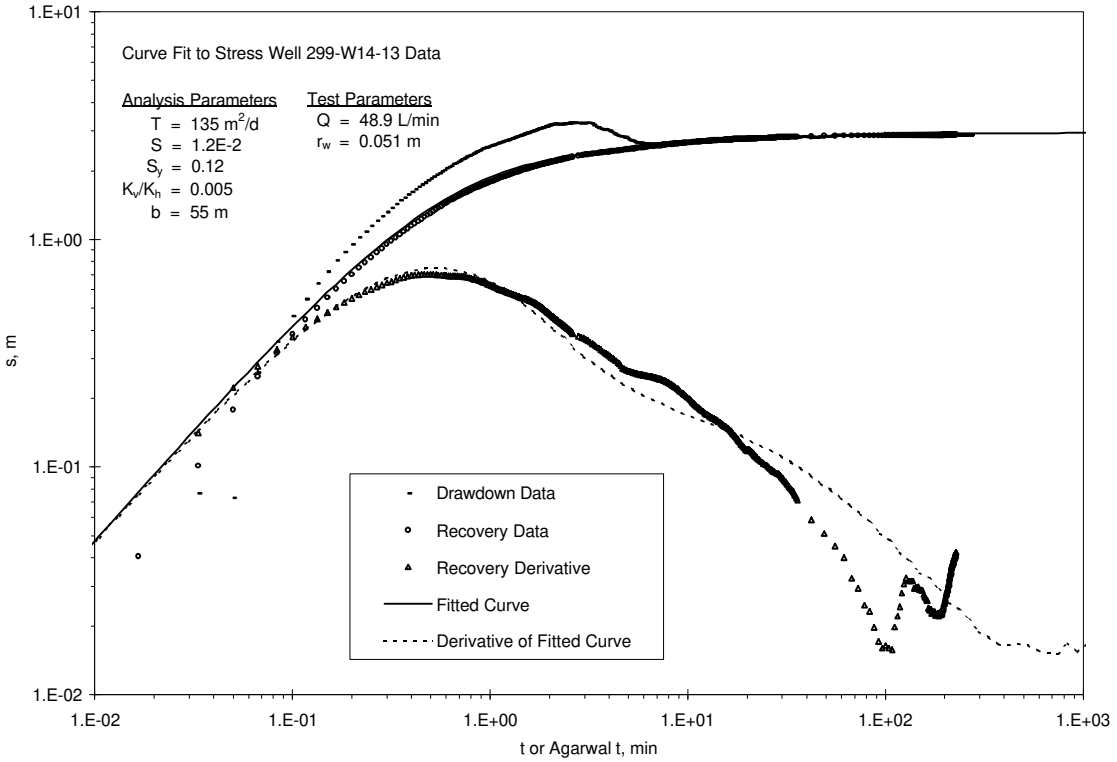

Figure 7.7. Type-Curve and Derivative Plot Analysis of Recovery Test Data for Pumping Well 299-W14-13

The type-curve displayed is based on an assumed K_D of 0.005. As discussed in Section 3.3, the type curve also accounts for well partial penetration of the aquifer thickness and wellbore storage. The type-curve fit shown in Figure 7.7 provided the following analysis results: T = 135 m^2/d, S = 1.2E-03, and S_y = 0.12. (Note: S is assumed, based on the calculated value for S_y and a fixed σ value of 0.001.) As discussed in Section 3.3, the pumping well did not display significant head losses at the pumping rates used in these tests. This is apparent because type-curve fitting of the pumping and observation well data yielded similar values for T. Therefore, results of the type-curve-fitting analysis for pumping well 299-W14-13 are considered to provide representative estimates of aquifer hydraulic properties.

Drawdown and recovery data for observation well 299-W14-12 are shown in Figure 7.8, along with the derivative of the recovery data. The drawdown data fit the predicted type curve better than the recovery data that may have been affected by some residual barometric effects, which are more pronounced at the observation well because of the low magnitude of the water-level changes. As was the case for the pumping well test analysis, the type curve displayed in Figure 7.8 is also based on an assumed K_D of 0.005 and accounts for partial penetration and wellbore storage at the observation well. The type-curve fit produced the following analysis results: T = 135 m^2/d, S = 2.5E-03, and S_y = 0.25. Although the T values from type-curve matches of the observation well and recovery data are identical, the calculated S and S_y values are approximately double for the observation well. Although these storage values are more reasonable than those determined from observation well data from the two previously discussed sites, Figure 7.8 shows that the early-time data do not match the predicted response and are shifted to the right, suggesting an additional delay mechanism. As at the other observation well sites, this additional delay response is also believed to be attributed to the small penetration of the observation well below the water table and the effect of capillary forces that are significant at the aquifer/vadose zone interface.

The additional delayed response in the observation well data is readily apparent in the composite analysis plot of well 299-W14-13 (recovery data) and well 299-W14-12 (drawdown data) shown in Figure 7.9. Shown also are the predicted test responses for the pumping and observations wells, based on analysis results obtained solely from well 299-W14-13. As shown, the additional delay of the observation well response is apparent by its shift to the right of the predicted response. Best estimates of hydraulic properties for the test site are based on the recovery analysis for pumping well 299-W14-13. These best estimate values are T = 135 m^2/d, S = 1.2E-04, S_y = 0.12, and K = 2.45 m/d (K is calculated by dividing T by b).

7.4 Well 299-W19-42

Well 299-W19-42 penetrates the upper 10.7 m of the unconfined aquifer. An observation well, 299-W19-31, is located at a radial distance of 4.59 m from well 299-W19-42 and penetrates only 0.7 m below the water table. The aquifer thickness at the test site is estimated at 56 m. The constant-rate discharge test was conducted from 0753 to 1300 Pacific standard time on March 26, 1999. The average flow rate was 56.8 L/min over the 307-min pumping period.

Approximately 14 d later, barometric response characteristics were monitored for 5 d at both the pumping and observation wells (299-W19-42 and -W19-31). The multiple-regression deconvolution

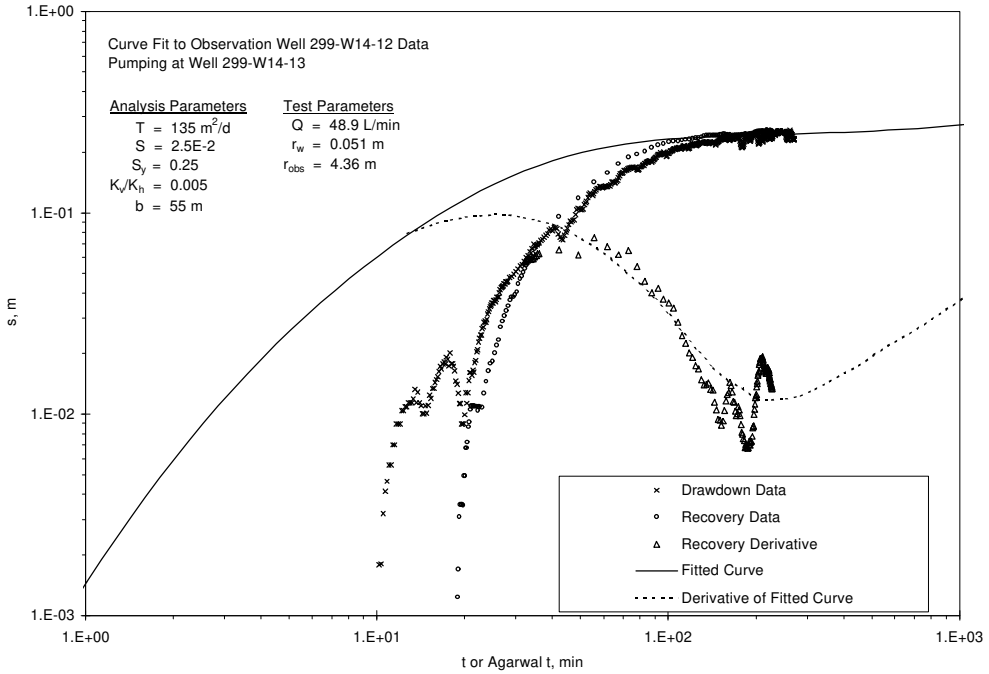

Figure 7.8. Type-Curve and Derivative Plot Analysis of Drawdown and Recovery Test Data for Observation Well 299-W14-12

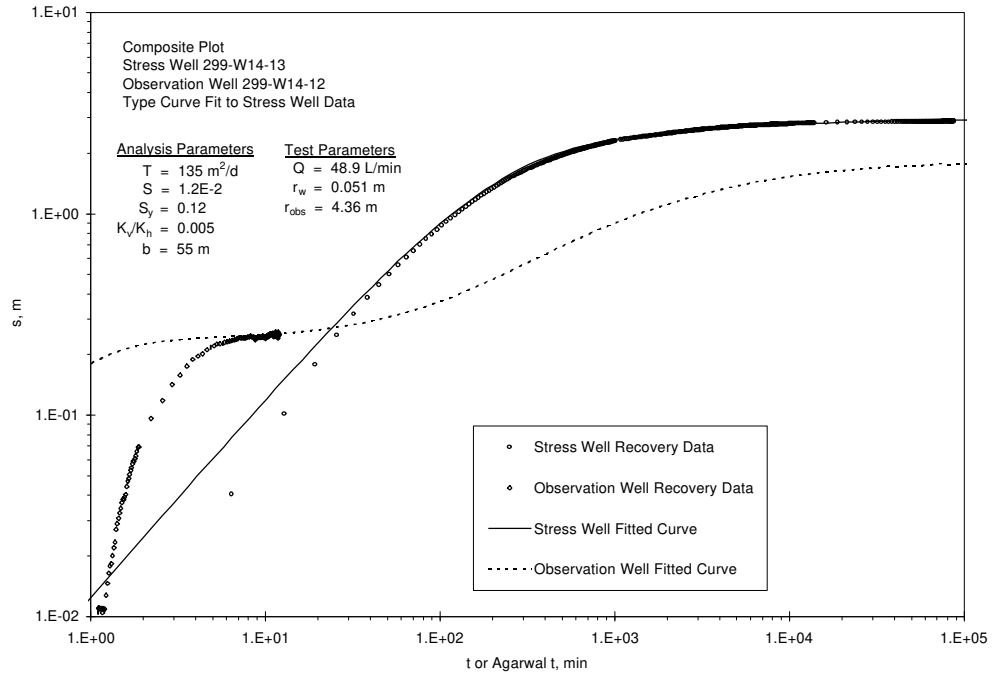

Figure 7.9. Composite Type-Curve and Derivative Plot Analysis for Pumping Well 299-W14-13 and Observation Well 299-W14-12

technique (Rasmussen and Crawford 1997; Spane 1999) was used to remove barometric pressure effects from the measured water levels. A total lag time of 15 h provided the best match of barometric responses for both well sites. Appendix Figure A.4 (top) shows both the original data and the data corrected for barometric effects for observation well 299-W19-31. The barometric pressure record, shifted by a constant, is also shown. Appendix Figure A.4 (bottom) shows a similar comparison for pumping well 299-W19-42.

Figure 7.10 shows the diagnostic log-log plot and type-curve match of the barometric corrected recovery data and derivative for pumping well 299-W19-42. Drawdown data were not selected for analysis because of the detrimental effects caused by small variations in discharge rate (not shown) during the test. The declining derivative pattern exhibited in Figure 7.10 (as a result of partial penetration effects) indicates there is no portion of the data where infinite-acting radial flow conditions are established. Therefore, straight-line analysis techniques cannot be used to analyze the test data.

The type-curve displayed is based on an assumed K_D of 0.10. As discussed in Section 3.3, the type curve also accounts for well partial penetration of the aquifer thickness and wellbore storage. The type-curve fit shown in Figure 7.10 provided the following analysis results: T = 345 m^2/d, S = 1.7E-04, and S_y = 0.17. (Note: S is assumed, based on the calculated value for S_y and a fixed σ value of 0.001.) As discussed in Section 3.3, the pumping well did not display significant head losses at the pumping rates used in these tests. This is apparent because type-curve fitting of the pumping and observation well data yielded similar values for T. Therefore, results of the type-curve-fitting analysis for pumping well 299-W19-42 are considered to provide representative estimates of aquifer hydraulic properties.

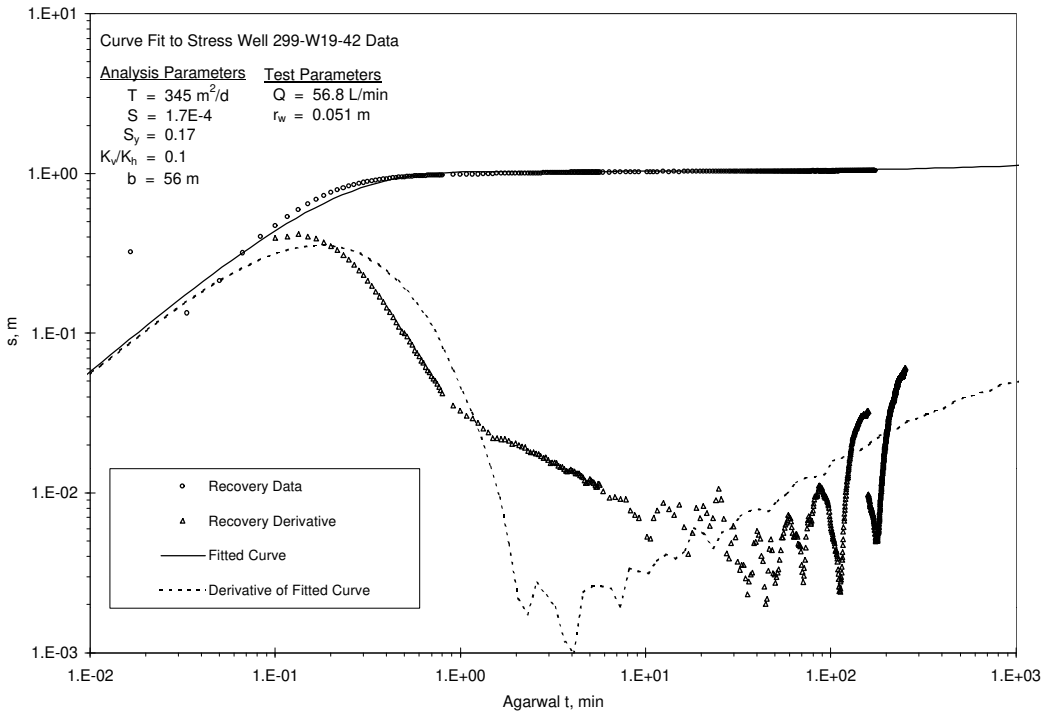

Figure 7.10. Type-Curve and Derivative Plot Analysis of Recovery Test Data for Pumping Well 299-W19-42

Drawdown and recovery data for observation well 299-W19-31 are shown in Figure 7.11, along with the derivative of the recovery data. The drawdown data fit the predicted type curve better than the recovery data that may have been affected by some residual barometric effects, which are more pronounced at the observation well because of the low magnitude of the water-level changes. As was the case for the pumping well test analysis, the type curve displayed in Figure 7.11 is also based on an assumed K_D of 0.10 and accounts for partial penetration and wellbore storage at the observation well. The type-curve fit produced the following analysis results: T = 345 m^2/d, S = 2.4E-03, and S_y >1.0. Although the T values from type-curve matches of the observation well and recovery data are identical, the calculated S and S_y values are higher than expected for the Ringold Formation. The higher-than-expected estimated values for S and S_y are believed to be attributed to an additional delayed response at the observation well that is probably caused by the small penetration of the observation well below the water table. Capillary forces that are significant at the aquifer/vadose zone interface, and which are not accounted for in the analysis method, may explain the delayed response.

The additional delayed response in the observation well data is readily apparent in the composite analysis plot of well 299-W19-42 (recovery data) and well 299-W19-31 (drawdown data) shown in Figure 7.12. Shown also are the predicted test responses for the pumping and observations wells, based on analysis results obtained solely from well 299-W19-42. As shown, the additional delay of the observation well response is apparent by its shift to the right of the predicted response. Best estimates of hydraulic properties for the test site are based on the recovery analysis for pumping well 299-W19-42. These best estimate values are T = 345 m^2/d, S = 1.7E-04, S_y = 0.17, and K = 6.12 m/d (K is calculated by dividing T by b).

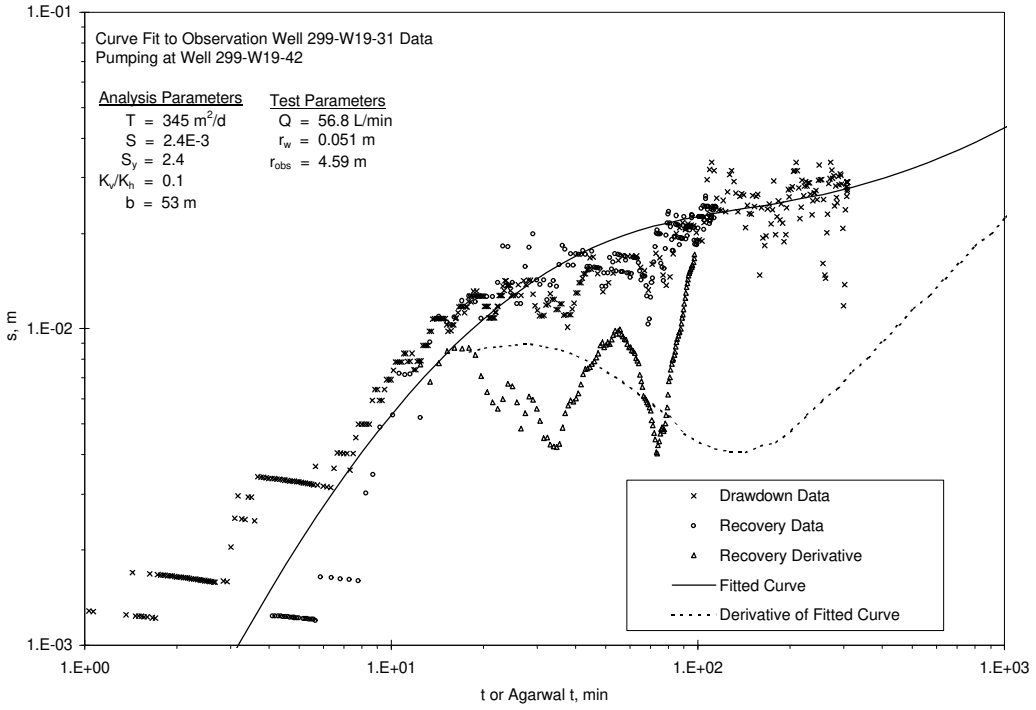

Figure 7.11. Type-Curve and Derivative Plot Analysis of Drawdown and Recovery Test Data for Observation Well 299-W19-31

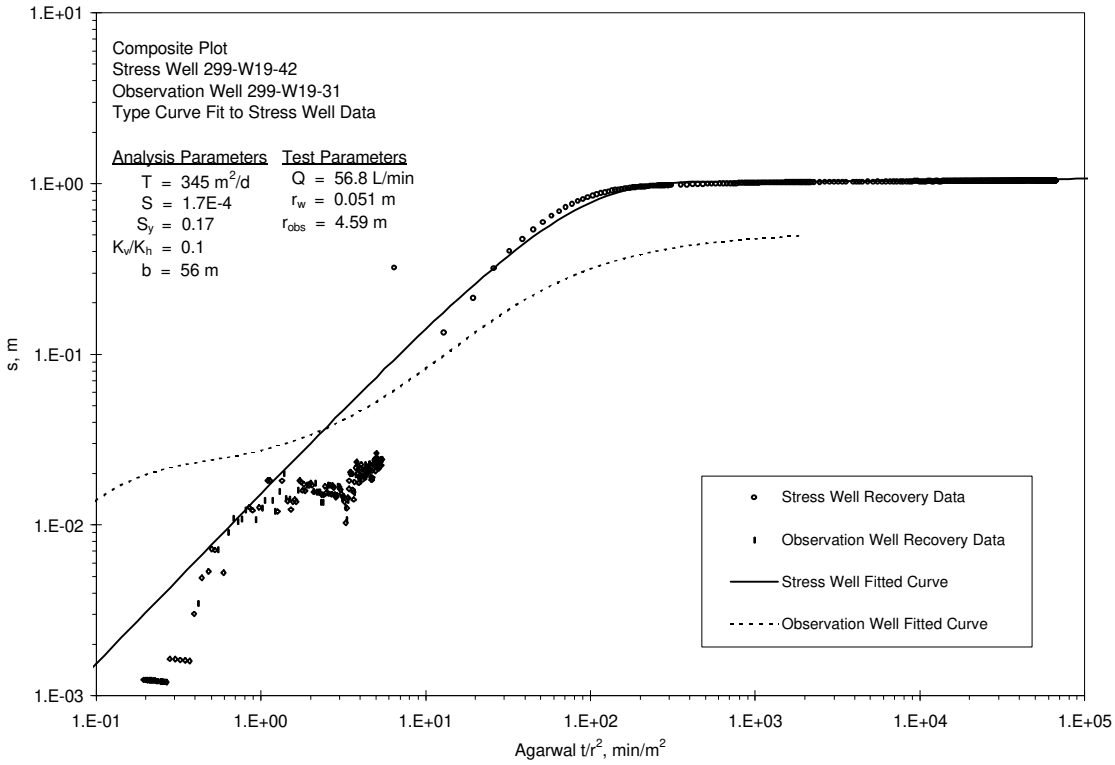

Figure 7.12. Composite Type-Curve and Derivative Plot Analysis for Pumping Well 299-W19-42 and Observation Well 299-W19-31

8.0 In-Well, Vertical Flow Test Results

As will be discussed in this section, the tracer concentration versus depth-response patterns exhibited during the tracer-dilution tests conducted at wells 299-W10-26 and 299-W14-13 exhibited evidence of vertical flow conditions within the well-screen section. The cause of the induced vertical flow conditions is not known, but may be the result of either 1) proximity to local recharge areas, 2) use of relatively long well screens (i.e., 10 m) that intersect a heterogeneous formation, or 3) effects from neighboring well-pumping/-sampling activities. The existence of vertical flow is not necessarily reflective of actual groundwater-flow conditions within the surrounding aquifer, but its presence implies a vertical flow gradient and has implications pertaining to the representativeness of groundwater samples collected from such monitor well facilities. An instructive numerical model study that examines the effects of vertical flow imposed by well-screen completions, in the presence of extremely low hydraulic gradients, is presented in Reilly et al. (1989).

To corroborate the downward vertical flow conditions calculated during the tracer-dilution tests, a follow-up, vertical, flow-tracer test and an EM vertical flow-meter survey were conducted at both well sites. Results determined from the three methods are discussed below for each well site and are summarized in Table 8.1. As indicated in Table 8.1, consistent and comparable vertical flow estimates were obtained using all three methods.

8.1 Well 299-W10-26

Visual examination of the tracer concentration versus depth-response patterns shown in Figure 8.1 for the tracer-dilution test conducted on April 23, 1999 (discussed in Section 5.2) indicates a small, vertical, downward-flow condition within the lower half of the well-screen section. (Note: Zones 2 and 3 provide

Table 8.1. In-Well, Vertical, Flow-Velocity Calculation Summary for Wells 299-W10-26 and 299-W14-13

Test Well	Tracer-Dilution Profile		Vertical Tracer Test[(a)]		Electromagnetic Flow-Meter Survey	
	Range, m/min	Average, m/min	Range, m/min	Average, m/min	Range, m/min	Average, m/min
299-W10-26	0.002 - 0.004 ↓	0.003 ↓	0.004 - 0.008 ↓	0.005 ↓	0.003 - 0.006 ↓	0.004 ↓
299-W14-13	0.008 - 0.015 ↓	0.011 ↓	0.013 - 0.014 ↓	0.012 ↓	0.012 - 0.013 ↓	0.012 ↓

Note: Directional symbol (↓) indicative of vertical flow direction.
(a) In-well, vertical, flow-velocity range calculated using tracer peak arrival method for selected sensor depths, while the average was determined using the center-of-mass technique.

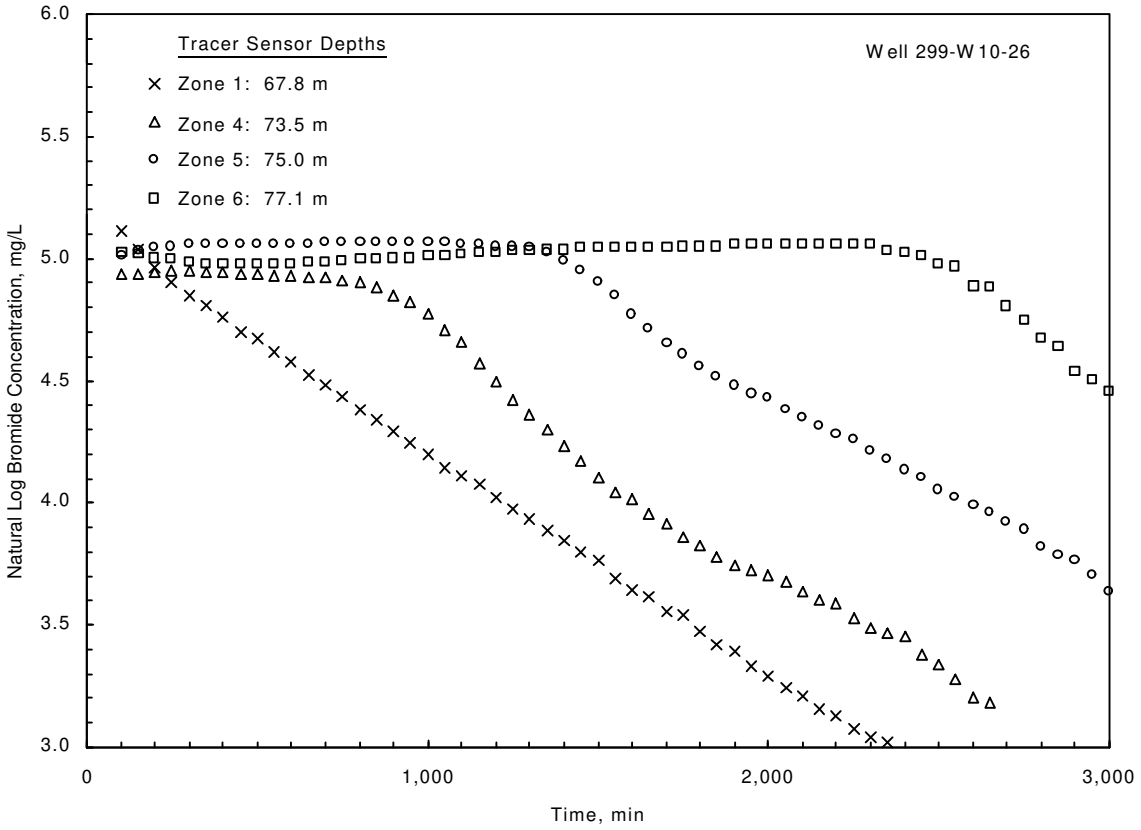

Figure 8.1. Tracer Concentration Versus Depth-Response Patterns Within Well 299-W10-26 During Tracer-Dilution Testing

response patterns nearly identical to Zone 1 and are omitted from the figure.) Downward-flow velocities, ranging between 0.002 to 0.004 m/min, were calculated, based on arrival times of recognizable signatures between the lower three bromide probe sensors.

To corroborate vertical flow conditions within the well-screen section, a vertical flow-tracer test was conducted on May 10, 1999 (1105 Pacific daylight time) by introducing 0.766 L of tracer solution (containing 0.613 g of bromide) within the upper 1.5-m well-screen section. The tracer was introduced into the well using a 0.025-m polypropylene tube that was open at a depth of 65.9 m below top of casing. Efforts were made to maintain the tracer at the expected fluid-column temperature of ~17°C prior to its introduction. An electronic water-level sounder was attached to the tube for locating the depth of tracer introduction below the water level. A bottom-line static mixer was attached to the tube to enhance mixing when removing the tracer-delivery system from the well-water column.

Following tracer introduction, an equilibration time of 5 min was observed to allow for dissipation of the displaced water from the tube into the surrounding well-screen column. After the equilibration period, the tube was slowly raised out of the water column, causing emplacement and mixing of the 0.766 L of prepared tracer. The designed concentration within the well screen following mixing was ~50 mg/L.

Following mixing, an assembly of six bromide probe sensors, spaced at a uniform 1.83-m separation, was lowered into the well. Final depth settings for the sensors were 68.0, 69.8, 71.6, 73.5, 75.3, and 77.1 m below top of casing. The sensor at the bottom depth setting malfunctioned during the test and did not provide analyzable data. Each sensor had an attached plastic centralizer to keep it approximately centered within the well-screen section. Installation of the assembly was completed in ~30 min, following the mixing of the tracer within the well screen. The concentration measured within the top sensor depth following emplacement and equilibration (i.e., after ~35 min following initial mixing) was 28 mg/L.

Figure 8.2 shows the tracer versus time profiles for the various depth locations. Readings for the lowest depth setting (Zone 6, 77.1 m) were aberrant and could not be used in the vertical tracer analysis. The reason for the aberrant readings is unknown. Vertical flow velocities were calculated for the individual depths within the well screen, based on the tracer peak arrival times between sensor-depth locations, divided by the distance spacing of 1.83 m. To aid in the identification of the tracer peak arrival times, linear-regression analysis of the tracer buildup and recovery limbs were employed for each sensor-depth location. The intersection of the buildup and recovery limb linear-regression lines provided the basis for the tracer peak arrival time determination. Linear-regression analysis was particularly useful for the lower sensor-depth settings, where tracer profiles were broad and arrival peak discernment less visually obvious. Calculated flow velocities within well 299-W10-26 decreased vertically downward within the well-screen section and ranged between 0.004 m/min (between the two lowest functioning sensor-depth settings (i.e., 73.5 to 75.3 m below top of casing) and 0.008 m/min (between the top two sensor-depth settings).

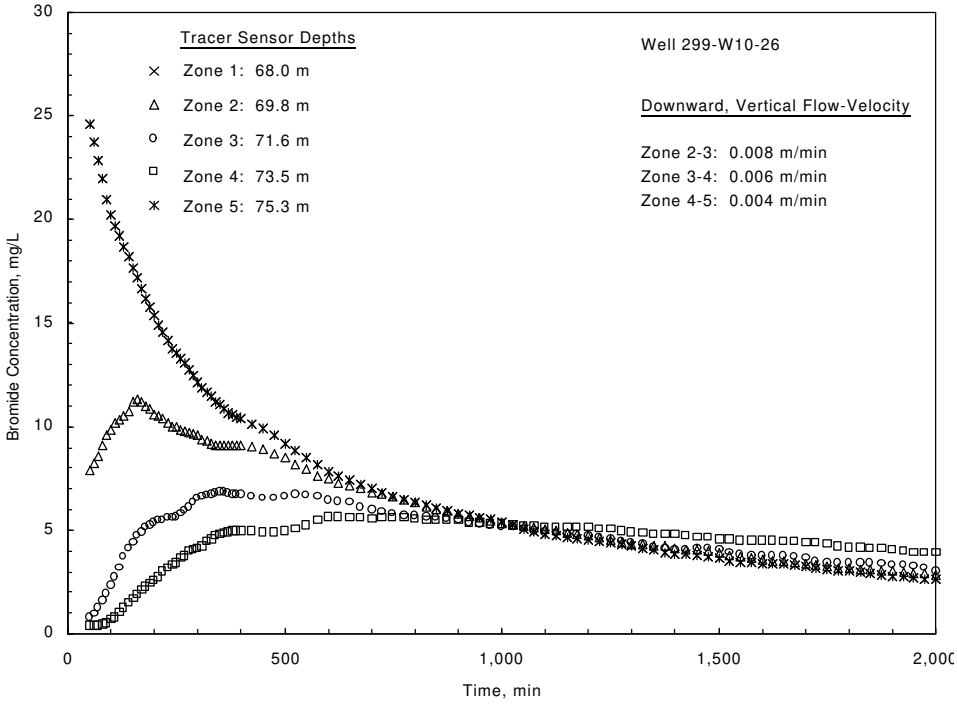

Figure 8.2. Tracer Concentration Versus Depth-Response Patterns Within Well 299-W10-26 During In-Well, Vertical Flow Testing and Calculated, Downward, Vertical Flow Velocities

The average vertical flow velocity was calculated by determining the depth to the center of the tracer mass within the well for selected test times. The slope of the linear regression of time versus the center of tracer mass provides the estimate of average, in-well, vertical flow. As shown in Figure 8.3, an average downward velocity of 0.005 m/min was calculated using the center-of-mass method.

Vertical flow measurements were obtained directly within well 299-W10-26 on January 19, 2000 using an EM flow meter. Flow-meter results reported in Waldrop and Pearson (2000) for three blank-joint sections within the well-screen section (i.e., at 68.6, 71.6, and 74.7 m below top of casing) provided velocity values between 0.003 and 0.006 m/min.

Table 8.1 summarizes the calculations determined within well 299-W10-26. As indicated, comparable velocities and consistent indications of downward-flow conditions within the well-screen section were indicated for all three methods. The fact that the flow-meter survey and vertical flow-tracer tests were conducted nearly 8 mo apart, and still provided consistent results, suggests that the vertical flow condition is a persistent characteristic.

8.2 Well 299-W14-13

Visual examination of the tracer concentration versus depth-response patterns (shown in Figure 8.4) for the tracer-dilution test conducted on April 30, 1999 (discussed in Section 5.3) indicates a significant

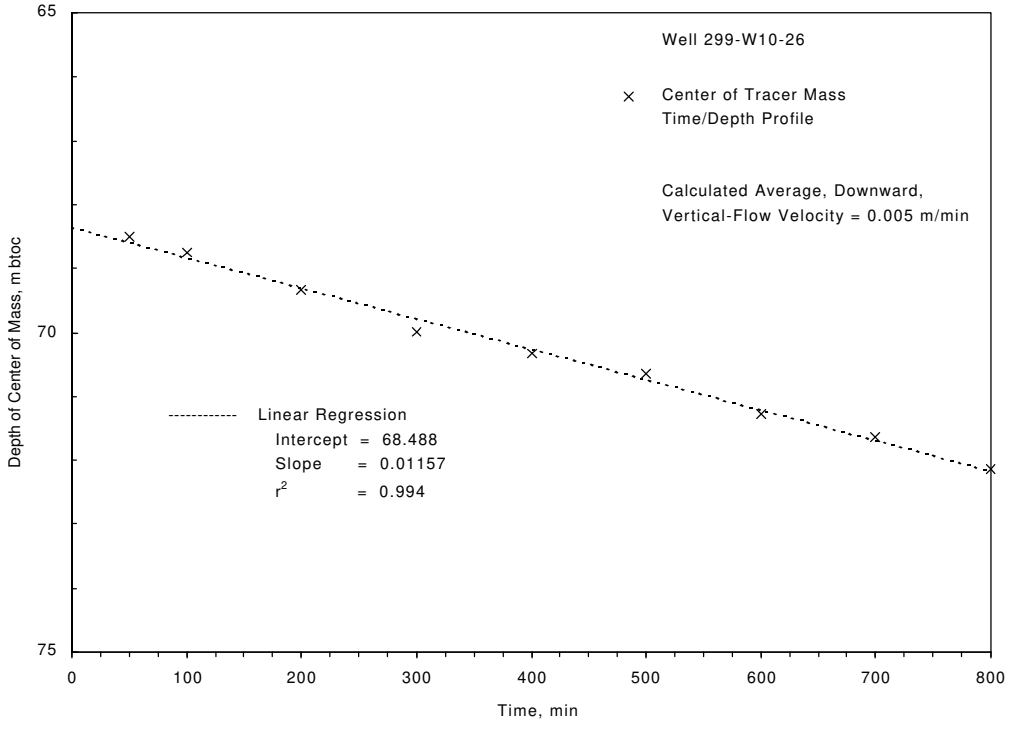

Figure 8.3. Calculated Average, In-Well, Downward, Vertical Flow Velocity Within Well 299-W10-26, Using Center-of-Mass Method (btoc = below top of casing)

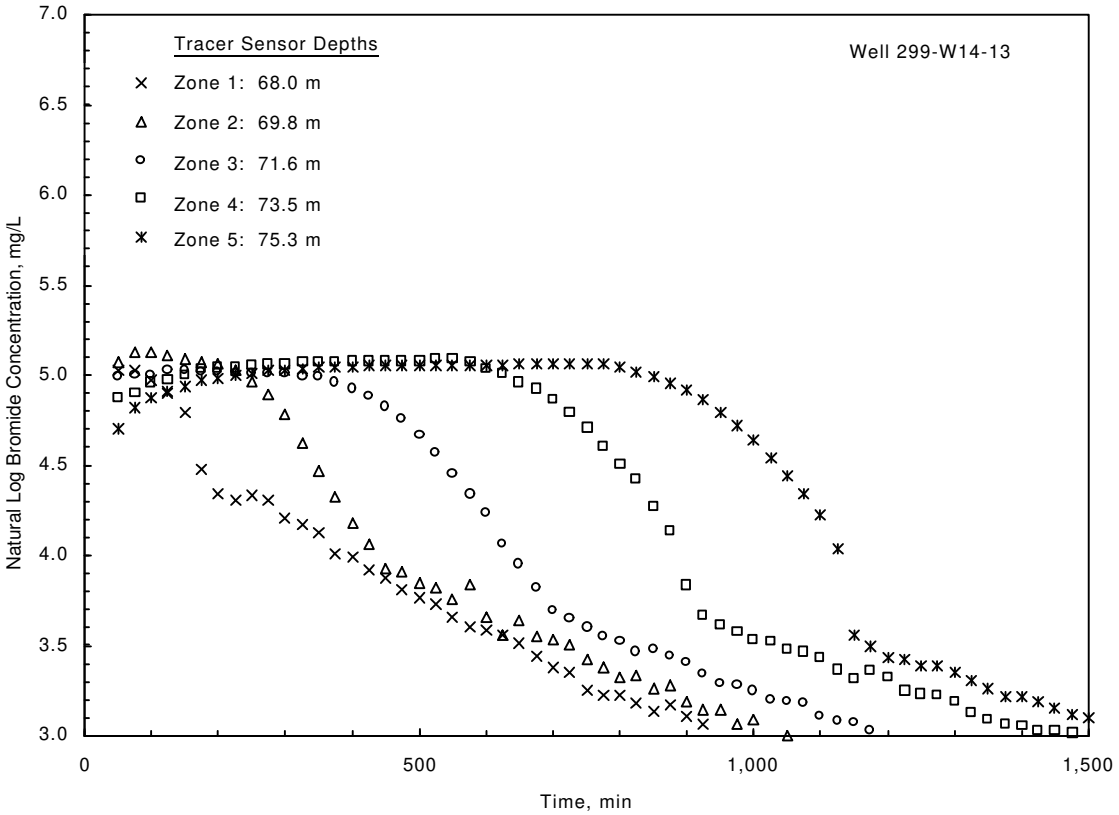

Figure 8.4. Tracer Concentration Versus Depth-Response Patterns Within Well 299-W14-13 During Tracer-Dilution Testing

vertical, downward-flow condition within the lower half of the well-screen section. Downward-flow velocities, ranging between 0.008 to 0.015 m/min, were calculated, based on arrival times of recognizable signatures between the lower three bromide probe sensors.

To corroborate vertical flow conditions within the well-screen section, a vertical flow-tracer test was conducted on May 7, 1999 (0928 Pacific daylight time) by introducing 0.766 L of tracer solution (containing 0.613 g of bromide) within the upper 1.5-m well-screen section. The tracer was introduced into the well using a 0.025-m polypropylene tube that was open at a depth of 65.9 m below top of casing. Efforts were made to maintain the tracer at the expected fluid-column temperature of ~17°C prior to its introduction. An electronic water-level sounder was attached to the tube for locating the depth of tracer introduction below the water level. A bottom-line static mixer was attached to the tube to enhance mixing when removing the tracer-delivery system from the well-water column.

Following tracer introduction, an equilibration time of 7 min was observed to allow for dissipation of the displaced water from the tube into the surrounding well-screen column. After the equilibration period, the tube was slowly raised out of the water column, causing emplacement and mixing of the 0.766 L of prepared tracer. The designed concentration within the well screen following mixing of the added tracer was ~50 mg/L.

Following mixing, an assembly of six bromide probe sensors, spaced at a uniform 1.83-m separation, was lowered into the well. Final depth settings for the sensors were 68.0, 69.8, 71.6, 73.5, 75.3, and 77.1 m below top of casing. The sensor at the bottom depth setting malfunctioned during the test and did not provide analyzable data. Each sensor had an attached plastic centralizer to keep it approximately centered within the well-screen section. Installation of the assembly was completed in ~37 min, following the mixing of the tracer within the well screen. The concentration measured within the top sensor depth following emplacement and equilibration (i.e., after ~45 min following initial mixing) was 17 mg/L.

Figure 8.5 shows the tracer versus time profiles for the various depth locations. Readings for the lowest depth setting (Zone 6, 77.1 m) were aberrant and could not be used in the vertical tracer analysis. The reason for the aberrant readings is unknown. Vertical flow velocities were calculated, based on the tracer peak arrival times between sensor-depth locations, divided by the distance spacing of 1.83 m. To aid in the identification of the tracer peak arrival times, linear-regression analysis of the tracer buildup and recovery limbs were employed for each sensor-depth location. The intersection of the buildup and recovery limb linear-regression lines provided the basis for the tracer peak arrival time determination. Linear-regression analysis was particularly useful for the lower sensor-depth settings, where tracer profiles were broad and arrival peak discernment less visually obvious. Calculated flow velocities within well 299-W14-13 were relatively uniform with depth within the well-screen section and ranged between 0.013 and 0.014 m/min.

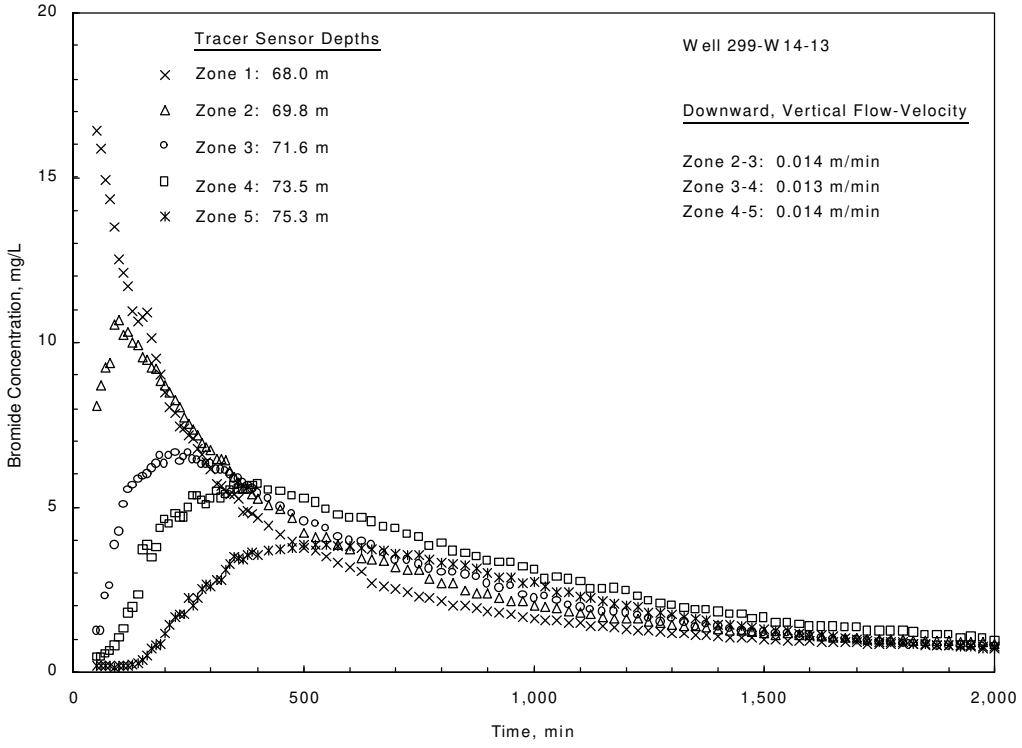

Figure 8.5. Tracer Concentration Versus Depth-Response Patterns Within Well 299-W14-13 During In-Well, Vertical Flow Testing and Calculated, Downward, Vertical Flow Velocities

The average vertical flow velocity was calculated by determining the depth to the center of the tracer mass within the well for selected test times. The slope of the linear regression of time versus the center of tracer mass provides the estimate of average, in-well, vertical flow. As shown in Figure 8.6, an average downward velocity of 0.012 m/min was calculated for this test method. The average velocity is slightly less than the individual depth versus vertical flow velocity measurements, based on the tracer peak arrival method. Part of the slight differences calculated between methods may be attributed to the center-of-mass method assumption (i.e., that the tracer mass remains in the well during the period of analysis). Loss of tracer mass from the wellbore to the surrounding aquifer would cause in-well, vertical, flow velocities to be lower than actual.

Vertical flow measurements were obtained directly within well 299-W14-13 on January 19, 2000 using an EM flow meter. Flow-meter results reported in Waldrop and Pearson (2000) for three blank-joint sections within the well-screen section (i.e., at 68.4, 71.5, and 74.5 m below top of casing) provided velocity values between 0.012 and 0.013 m/min.

Table 8.1 summarizes the calculations determined within well 299-W14-13. As indicated, comparable velocities and consistent indications of downward-flow conditions within the well-screen section were indicated for all three methods. The fact that the flow-meter survey and vertical flow-tracer tests were conducted nearly 8 mo apart, and still provided consistent results, suggests that the vertical flow condition is a persistent characteristic.

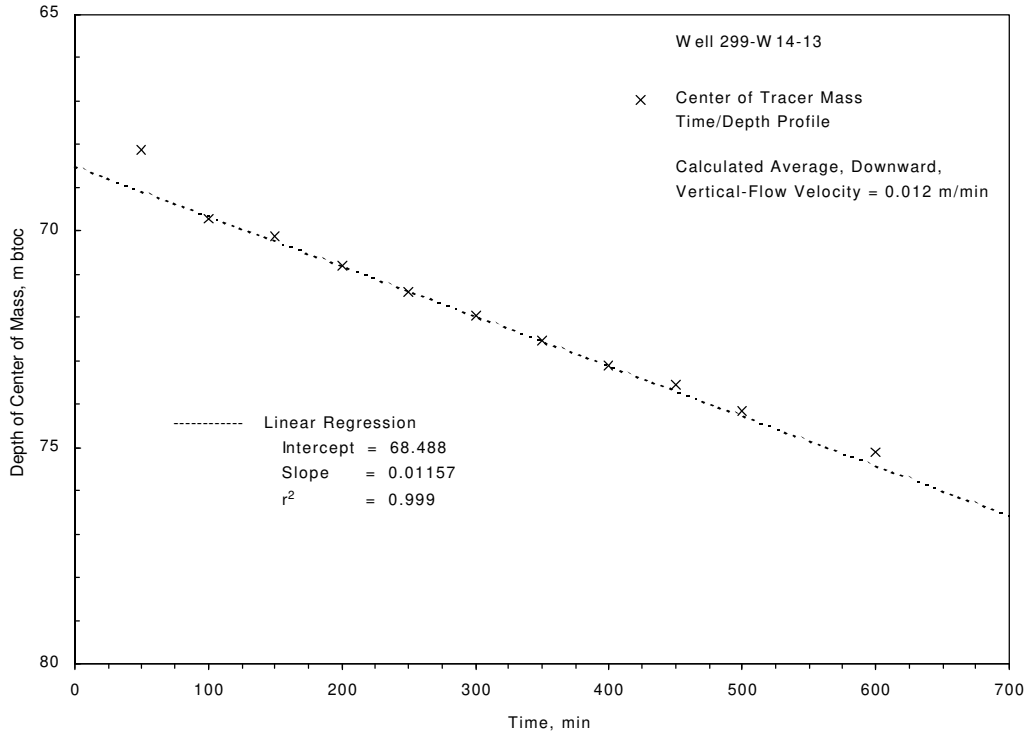

Figure 8.6. Calculated Average, In-Well, Downward, Vertical Flow Velocity Within Well 299-W14-13, Using Center-of-Mass Method (btoc = below top of casing)

9.0 Conclusions

The detailed hydrologic characterization of the Hanford Site's unconfined aquifer system conducted during FY 1999 included slug tests, single-well tracer tests (i.e. tracer-dilution; tracer-pumpback; and in-well, vertical flow-tracer tests), and constant-rate pumping tests. Hydraulic property estimates obtained from the detailed tests include hydraulic conductivity; transmissivity; specific yield; effective porosity; in-well, lateral, groundwater-flow velocity; aquifer-flow velocity; vertical distribution of hydraulic conductivity; and in-well, vertical flow velocity. In addition, local groundwater-flow characteristics (i.e., hydraulic gradient, flow direction) were determined for four sites where detailed well testing was performed.

9.1 Slug-Test and Constant-Rate Pumping Test Results

Slug-test results provided hydraulic conductivity estimates that range between 0.88 and 9.5 m/d for the nine 200-West Area wells and 24.2 m/d for the one 200-East Area well tested. Estimated values obtained using the Bouwer and Rice analytical method were generally lower and within 35% of the corresponding estimates obtained using the type-curve method. This is similar to findings of previous studies (e.g., Hyder and Butler 1995; Butler 1998) that evaluated the analytical performance of the Bouwer and Rice method. It should be noted that a wide range in hydraulic conductivity values is listed for the 200-West and 200-East Areas in several earlier reports (e.g., DOE/RL 1993; 200-West Area, 0.02 to 61 m/d). These results, however, were generally based on slug tests or single-well pumping tests, which did not rely on the more exacting analytical methods utilized in this report.

A comparison of the slug test-derived hydraulic conductivity estimates with values obtained from constant-rate pumping tests is shown in Table 9.1. As indicated, a close correspondence is evident between the two test methods. For the comparisons, slug-test estimates calculated using the type-curve method were either equivalent to or up to ~50% greater than pumping test-derived values. Slug-test estimates obtained using the Bouwer and Rice method ranged from ~30% lower to ~15% higher in comparison to their pumping test-derived counterparts. The estimate comparison exhibited falls within the error range commonly reported for slug tests in aquifer characterization studies (i.e., within a factor of ~2 or less [e.g., Butler 1996]). As noted in Butler (1998), the close correspondence between slug test and pumping test hydraulic conductivity estimates indicates that the formation tested can be represented as a homogeneous unit at the slug test or larger scale.

Analysis of the constant-rate pumping test results listed in Table 9.1 indicates that hydraulic property estimates for transmissivity ranged between 66 and 345 m^2/d (average 157 m^2/d). These values fall within to slightly below values recently calculated by Spane and Thorne (2000) for the central 200-West Area. Their estimates were based on the analysis of the induced areal composite pumping/injection effects of the 200-ZP-1 pump-and-treat system. The results from their study produced large-scale estimates, ranging between 230 and 430 m^2/d (average 325 m^2/d). As an additional source of comparison, large-scale transmissivity values of 300 and 327 m^2/d were reported in Newcomb and Strand (1953) and

Table 9.1. Hydraulic Property Summary for Slug- and Constant-Rate Pumping Tests

Waste Management Area	Well	Slug Test[(a)]	Constant-Rate Pumping Test		
		Hydraulic Conductivity, K_h, m/d	Hydraulic Conductivity, K_h, m/d	Transmissivity, T, m^2/d	Specific Yield, S_y
B-BX-BY	299-E33-44	22.0 - 24.2	-[(b)]	-	-
T	299-W10-23	1.62 - 2.35	-	-	-
	299-W10-24	1.04 - 1.68	1.22	66	0.11
TX-TY	299-W10-26	1.39 - 1.95	1.49	82	0.14
	299-W14-13	1.66 - 2.43	2.45	135	0.12
	299-W14-14	1.97 - 2.64	-	-	-
	299-W15-40	0.88 - 1.22	-	-	-
U	299-W19-41	1.18 - 1.69	-	-	-
	299-W19-42	7.06 - 9.50	6.12	345	0.17
216-U-12 Crib	299-W22-79	4.18 - 5.40	-	-	-

Note: Unless otherwise indicated, slug-test range represents the average analysis value for the Bouwer and Rice and type-curve methods. K_h = Assumes aquifer with uniform hydraulic conductivity value.

(a) Listed range represents the average K_h value obtained from the Bouwer and Rice and type-curve analysis methods.

(b) Constant-rate pumping test not conducted at the well site.

Wurstner et al. (1995), respectively, for the unconfined aquifer within the 200-West Area. These previously reported values were based on analyzing the areal growth and decline of the groundwater mound that developed in this area as a result of wastewater-disposal activities.

Comparison of the pumping test results in Table 9.1 also indicates a fairly close correspondence for specific yield, ranging between 0.11 and 0.17. These results coincide with the estimated values reported in Newcomb and Strand (1953) and Wurstner et al. (1995) of 0.11 and 0.17, respectively, for the 200-West Area. As mentioned previously, these earlier studies were based on analyzing the growth and decline of the groundwater mound beneath the 200-West Area that was associated with wastewater-disposal practices in the area.

9.2 Tracer-Dilution Test Results

Table 9.2 lists the tracer-dilution results for the four wells tested. As discussed in Section 5.0, two of the four sites exhibited in-well, vertical flow conditions that compromise the results of this characterization test. Average, in-well, flow velocities for the two sites not exhibiting in-well vertical flow (i.e., wells 299-W10-24 and -W19-42) ranged between 0.012 to 0.170 m/d. (Note: As shown in Equation [3.5] and discussed in Section 3.2.1, in-well flow velocity is related, but not equivalent, to actual groundwater-flow velocity within the aquifer.) The highest value of 0.170 m/d was calculated for well 299-W19-42, which is located in proximity (to the south) of the 200-ZP-1 pump-and-treat

Table 9.2. Tracer-Dilution Test Summary

Well	Test Interval, m, btoc(a)	Date Test Initiated	Total Dilution Time, t_d, min	Average Initial Tracer Concentration, C_o,[(b)] mg/L	Average Final Tracer Concentration, C_t,[(c)] mg/L	Average Flow Velocity, v_w, m/d	Range Flow Velocity, v_{wz},[(d)] m/d
299-W10-24	72.4 - 82.6	4/09/99	17,455	148	26	0.012	0.009 - 0.017[(e)]
299-W10-26	67.4 - 77.8	4/23/99	7,259	219	<1.0	vf[(f)] (0.086)	vf[(f)] (downward)
299-W14-13	67.1 - 77.9	3/26/99	8,575	VF[(g)]	VF[(g)]	VF[(g)]	VF[(g)] (downward)
299-W19-42	67.1 - 77.8	5/17/99	4,240	221	<1.0	0.170	0.149 - 0.181

(a) Below top of casing.
(b) Estimated initial tracer concentration based on linear back-projection of average well-screen conditions.
(c) Average observed well-screen tracer concentration at termination of test.
(d) Groundwater flow-velocity range within well determined from individual sensor-depth settings.
(e) Permeability profile indicates highest permeability (highest flow velocity) near middle of well screen; lowest permeability near top.
(f) Slight vertical flow conditions detected adversely affect tracer-test results; vertical flow direction indicated in parentheses.
(g) Significant vertical flow conditions that invalidate tracer-dilution test; vertical flow direction indicated in parentheses.

facilities. This well location is within the potential radius of influence distances reported in Spane and Thorne (2000) and, therefore, could produce elevated in-well flow velocities.

A comparison of the observed depth versus velocity profiles provided information about permeability distribution within the well-screen sections at the two well sites. At well 299-W10-24, the highest flow velocities (and inferred permeabilities) were exhibited near the middle of the screen, with lowest flow velocities indicated near the top. In contrast, for well 299-W19-42, relatively uniform depth versus velocity profiles were exhibited, indicating homogeneous permeability conditions throughout the well-screen section.

9.3 Tracer-Pumpback Test Results

Table 6.1 lists information pertaining to the tracer-pumpback tests performed. As noted previously, several wells exhibited vertical-flow conditions during the tracer-dilution tests. The fact that the tracer entered the aquifer within a small portion of the well screen seriously impacts the assumptions of the test. The tracer-pumpback results for those wells affected by vertical flow conditions are highly questionable and, therefore, should not be used for quantitative assessment. The estimates calculated from the tests, however, are provided in the table for comparison/informational purposes only.

Estimates for effective porosity ranged between 0.027 and 0.072. This range falls within, to slightly below, the range commonly reported for semiconsolidated to unconsolidated alluvial aquifers (0.05 to 0.30) and is slightly below the large-scale values for specific yield, S_y ($S_y \approx n_e$) of 0.11 and 0.17, derived from the constant-rate pumping tests. The reason for the slightly lower-than-expected estimated values is believed to be attributed to several of the test analysis deficiencies previously noted (e.g., wellbore effects, passive tracer injection).

Estimates for groundwater-flow velocity within the aquifer ranged between 0.029 and 0.419 m/d and generally fall within a factor of 2.5 of the calculated, in-well, flow velocities. As noted at well 299-W19-42, the observed estimate of 0.419 m/d at this well site may be elevated as a result of the effects imposed by operation of the adjacent 200-ZP-1 pump-and-treat system.

9.4 In-Well, Vertical Flow-Test Results

The tracer concentration versus depth-response patterns exhibited during the tracer-dilution tests conducted in wells 299-W10-26 and -W14-13 exhibited evidence of vertical flow conditions within the well-screen section. The cause of the induced flow conditions is not known but may be the result of either 1) proximity to local recharge areas, 2) use of relatively long well screens (i.e., 10 m) that intersect a heterogeneous formation, or 3) temporal effects from neighboring well-pumping/-sampling activities. To corroborate the downward vertical flow conditions calculated during the tracer-dilution tests, a follow-up, in-well, vertical, flow-tracer test and a direct, vertical, flow survey (Waldrop and Pearson 2000) were conducted at both well sites. The results of the calculations determined from the three methods are summarized in Table 8.1. As indicated in Table 8.1, consistent and comparable estimates were obtained using three methods, with well 299-W14-13 exhibiting higher velocities (0.011 to 0.012 m/min) than determined at well 299-W10-26 (0.003 to 0.005 m/min).

It should be noted that the existence of in-well vertical flow is not necessarily reflective of actual groundwater-flow conditions within the surrounding aquifer, but its presence has implications pertaining to the representativeness of groundwater samples collected from such monitor well facilities. The fact that the flow-meter survey and flow-tracer tests were conducted nearly 8 months apart, and still provided consistent results, suggests that the downward, vertical flow condition is a persistent characteristic at these well sites.

9.5 Groundwater-Flow Characterization Results

Table 9.3 lists results pertaining to the determination of groundwater-flow direction and hydraulic gradient conditions at the various sites during the period of tracer testing. Groundwater-flow direction and hydraulic gradient were calculated using the commercially available WATER-VEL (In-Situ, Inc. 1991) software program. Water-level elevations from neighboring, representative wells were used as input to the WATER-VEL program to calculate groundwater-flow direction and hydraulic gradient conditions during the detailed characterization period. The program uses a linear, two-dimensional trend surface (least squares) to randomly located hydrologic head or water-level elevation input data. This method is similar also to the linear approximation technique described by Abriola and Pinder (1982) and Kelly and Bogardi (1989). Reports that demonstrate the use of the WATER-VEL program for calculation of groundwater-flow velocity and direction on the Hanford Site include Gilmore et al. (1992) and Spane (1999).

The hydraulic gradient calculations listed in Table 9.3 were used in calculating the estimates of effective porosity and groundwater-flow velocity shown in Table 6.1. The indicated easterly and southerly groundwater-flow directions are consistent with generalizations presented in Hartman (1999) for these wells.

Table 9.3. Groundwater-Flow Characterization Results Based on Trend-Surface Analysis

Well	Measurement Date	Groundwater-Flow Direction[(a)]	Hydraulic Gradient, m/m	Wells Used in Analysis
299-W10-26	5/3/99	288°	0.00073	299-W10-17 299-W10-18 299-W14-12 299-W15-12 299-W15-22
299-W14-13	5/3/99	288°	0.00073	299-W10-17 299-W10-18 299-W14-12 299-W15-12 299-W15-22
299-W10-24	4/21/99	5°	0.00172	299-W10-8 299-W10-12 299-W10-22 299-W10-24 299-W11-23 299-W11-27
299-W19-42	5/20/99	14°	0.00184	299-W18-25 299-W18-30 299-W18-31 299-W19-12 299-W19-31 299-W19-32 299-W19-42

(a) 0 degrees East; 90 degrees North.

10.0 References

Abriola LM, and GF Pinder. 1982. "Calculation of velocity in three space dimensions from hydraulic head measurements." *Ground Water* 20(2):205-213.

Agarwal RG. 1980. "A new method to account for producing time effects when drawdown type curves are used to analyze pressure buildup and other test data." *SPE Paper 9289*, Society of Petroleum Engineers, Dallas Texas.

Bourdet DJ, A Ayoub, and YM Pirard. 1989. "Use of pressure derivative in well-test interpretation." *SPE Formation Evaluation* June 1989:293-302.

Bouwer H. 1989. "The Bouwer and Rice slug test – an update." *Ground Water* 27(3):304-309.

Bouwer H, and RC Rice. 1976. "A slug test for determining hydraulic conductivity of unconfined aquifers with completely or partially penetrating wells." *Water Resources Research* 12(3):423-428.

Brown DL, TN Narasimhan, and Z Demir. 1995. "An evaluation of the Bouwer and Rice method of slug test analysis." *Water Resources Research* 31(5):1239-1246.

Butler JJ, Jr. 1990. "The role of pumping tests in site characterization: some theoretical considerations." *Ground Water* 28(3):394-402

Butler JJ, Jr. 1996. "Slug tests in site characterization: some practical considerations." *Environmental Geosciences* 3(3):154-163

Butler JJ, Jr. 1998. *The design, performance, and analysis of slug tests*. Lewis Publishers, CRC Press, Boca Raton, Florida.

Butler JJ, CD McElwee, and W Liu. 1996. "Improving the quality of parameter estimates obtained from slug tests." *Ground Water* 34(3):480-490.

Connelly MP, JV Borghese, CD Delaney, BH Ford, JW Lindberg, and SJ Trent. 1992a. *Hydrogeologic model for the 200-East groundwater aggregate area*. WHC-SD-EN-TI-019, Rev. 0, Westinghouse Hanford Company, Richland, Washington.

Connelly MP, BH Ford, and JV Borghese. 1992b. *Hydrogeologic model for the 200-West groundwater aggregate area*. WHC-SD-EN-TI-014, Rev. 0, Westinghouse Hanford Company, Richland, Washington.

Cooper HH, Jr., and CE Jacob. 1946. "A generalized graphical method for evaluating formation constants and summarizing well-field history." *American Geophysical Union, Transactions* 27(4):526-534.

DOE/RL. 1993. *200 west groundwater aggregate area management study report*. DOE/RL-92-16, Rev. 0, U.S. Department of Energy, Richland Operations Office, Richland, Washington.

Drost W, D Klotz, A Koch, H Moser, F Neumaier, and W Rauert. 1968. "Point dilution methods of investigating groundwater flow by means of radioisotopes." *Water Resources Research* 4(1): 125-146.

Freeze RA and JA Cherry. 1976. *Groundwater*. Prentice-Hall, Englewood Cliffs, New Jersey.

Gephart RE, FA Spane, LS Leonhart, DA Palombo, and SR Strait. 1979. "Pasco Basin hydrology." In *Hydrologic studies within the Columbia plateau, Washington: An integration of current knowledge*, pp. III-1 to III-236. RHO-BWI-ST-5, Rockwell Hanford Operations, Richland, Washington.

Gilmore TJ, DR Newcomer, SK Wurstner, and FA Spane, Jr. 1992. *Calculation of groundwater discharge to the Columbia River in the 100-N area*. PNL-8057, Pacific Northwest Laboratory, Richland, Washington.

Graham MJ, GV Last, and KR Fecht. 1984. *An assessment of aquifer intercommunication in the B-Pond-Gable Mountain Pond area of the Hanford site*. RHO-RE-ST-12P, Rockwell Hanford Operations, Richland, Washington.

Güven O, RW Falta, FJ Molz, and JG Melville. 1985. "Analysis interpretation of single-well tracer tests in stratified aquifers." *Water Resources Research* 21(5):676-684.

Halevy E, H Moser, O Zellhofer, and A Zuber. 1966. "Borehole dilution techniques – a critical review." In *Isotopes in Hydrology,* International Atomic Energy Agency, Vienna, Austria.

Hall SH. 1993. "Single well tracer tests in aquifer characterization." *Ground Water Monitoring & Remediation* 13(2):118-124.

Hall SH, SP Luttrell, and WE Cronin. 1991. "A method for estimating effective porosity and ground-water velocity." *Ground Water* 29(2):171-174.

Hantush, MS. 1964. "Hydraulics of wells." *Advances in Hydroscience* (VT Chow, ed) 1:282-433, Academic Press, New York.

Hartman MJ, ed. 1999. *Hanford Site groundwater monitoring for fiscal year 1998*. PNNL-12086, Pacific Northwest National Laboratory, Richland, Washington.

Hyder Z and JJ. Butler, Jr. 1995. "Slug tests in unconfined formations: An assessment of the Bouwer and Rice technique." *Ground Water* 33(1):16-22.

In-Situ Inc. 1991. *WATER-VEL™ groundwater velocity*. ISI-GWV-2.21-1, Laramie, Wyoming.

Kearl PM, JJ Dexter, and JE Price. 1988. *Procedures, analysis, and comparison of groundwater velocity measurement methods for unconfined aquifers*. UNC/GJ-TMC-3, UNC Geotech, Grand Junction, Colorado.

Kelly WE, and I Bogardi. 1989. "Flow directions with a spreadsheet." *Ground Water – Computer Notes* 27(2):245-247.

Leap DI, and PG Kaplan 1988. "A single-well tracing method for estimating regional advective velocity in a confined aquifer: Theory and preliminary laboratory verification." *Water Resources Research* 24(7):993-998.

Lindsey KA. 1995. *Miocene- to Pliocene-aged suprabasalt sediments of the Hanford Site, south-central Washington*. BHI-00184, Bechtel Hanford Inc., Richland, Washington.

Lindsey KA, BN Bjornstad, JW Lindberg, and KM Hoffman. 1992. *Geologic setting of the 200-East area: An update*. WHC-SD-EN-TI-012, Rev. 0, Westinghouse Hanford Company, Richland, Washington.

Liu WZ, and JJ Butler, Jr. 1995. *The KGS model for slug tests in partially penetrating wells (Version 3.0)*. Kansas Geological Survey Computer Series Report 95-1, Lawrence, Kansas.

Michalski A. 1989. "Conductive slug tracing as a single-well test technique for heterogeneous and fractured formations." In *Proceedings of the Conference on New Field Techniques for Quantifying the Physical and Chemical Properties of Heterogeneous Aquifers, March 20-23, 1989, Dallas, Texas;* pp 247-263. National Water Well Association, Dublin, Ohio.

Michalski A, and GM Klepp. 1990. "Characterization of transmissive fractures by simple tracing of in-well flow." *Ground Water* 28(2):191-198.

Moench AF. 1997. "Flow to a well of finite diameter in a homogeneous, anisotropic water-table aquifer." *Water Resources Research* 33(6):1397-1407.

Molz FJ, JG Melville, O Güven, RD Crocker, and KT Matteson. 1985. "Design and performance of single-well tracer tests at the Mobile site." *Water Resources Research* 21(10):1497-1502.

Neuman SP. 1972. "Theory of flow in unconfined aquifers considering delayed response of the water table." *Water Resources Research* 8(4):1031-1045.

Neuman SP. 1974. "Effect of partial penetration of flow in unconfined aquifer considering delayed gravity response." *Water Resources Research* 10(2):303-312.

Neuman SP. 1975. "Analysis of pumping test data from anisotropic unconfined aquifers considering delayed gravity response." *Water Resources Research* 11(2):329-342.

Newcomb RC, and JR Strand. 1953. *Geology and ground-water characteristics of the Hanford Reservation of the U.S. Atomic Energy Commission, Washington*. Administrative Report WP-8, U.S. Geological Survey, Washington, D.C.

Novakowski KS. 1989. "Analysis of pulse interference tests." *Water Resources Research* 25(11):2377-2387.

Pickens JF, and GE Grisak. 1981. "Scale-dependent dispersion in a stratified granular aquifer." *Water Resources Research* 17(4):1191-1211.

Rasmussen TC, and LA Crawford. 1997. "Identifying and removing barometric pressure effects in confined and unconfined aquifers." *Ground Water* 35(3):502-511.

Reilly TE, OL Franke, and GD Bennett. 1989. "Bias in groundwater samples caused by wellbore flow." *Journal of Hydraulic Engineering* 115(2):270-276.

Resource Conservation and Recovery Act of 1976, as amended, Public Law 94-580, 90 Stat. 2795, 42 USC 6901 et seq.

Spane FA, Jr. 1993. *Selected hydraulic test analysis techniques for constant-rate discharge tests*. PNL-8539, Pacific Northwest Laboratory, Richland, Washington.

Spane FA, Jr. 1996. "Applicability of slug interference tests for hydraulic characterization of unconfined aquifer: (1) Analytical assessment." *Ground Water* 34(1):66-74.

Spane FA, Jr. 1999. *Effects of barometric fluctuations on well water-level measurements and aquifer test data*. PNNL-13078, Pacific Northwest National Laboratory, Richland, Washington.

Spane FA, Jr., and PD Thorne. 2000. *Analysis of the hydrologic response associated with shutdown and restart of the 200-ZP-1 pump-and-treat system*. PNNL-13342, Pacific Northwest National Laboratory, Richland, Washington.

Spane FA, Jr., and WD Webber. 1995. *Hydrochemistry and hydrogeologic conditions within the Hanford Site upper basalt confined aquifer system*. PNL-10817, Pacific Northwest Laboratory, Richland, Washington.

Spane FA, Jr., and SK Wurstner. 1993. "DERIV: A program for calculating pressure derivatives for use in hydraulic test analysis." *Ground Water* 31(5):814-822.

Spane FA, Jr., PD Thorne, and LC Swanson. 1996. "Applicability of slug interference tests for hydraulic characterization of unconfined aquifer: (2) Field test examples." *Ground Water* 34(5):925-933.

Theis CV. 1935. "The relationship between the lowering of the piezometric surface and the rate and duration of discharge of a well using ground-water storage." *American Geophysical Union, Transactions*, 2:519-524; reprinted in Society of Petroleum Engineers, "Pressure Transient Testing Methods", SPE Reprint Series (14):27-32, Dallas, Texas.

Thorne PD, MA Chamness, FA Spane, Jr., VR Vermeul, and WD Webber. 1993. *Three-dimensional conceptual model for the Hanford Site unconfined aquifer system, FY 93 status report*. PNL-8971, Pacific Northwest Laboratory, Richland, Washington.

Waldrop WR, and HS Pearson. 2000. *Results of field tests with the electromagnetic borehole flowmeter at the Pacific Northwest National Laboratory, Richland, Washington*. QEC-T-132, Quantum Engineering Corporation, Loudon, Tennessee.

Weeks EP. 1979. "Barometric fluctuations in wells tapping deep unconfined aquifers." *Water Resources Research* 15(5):1167-1176.

Williams BA, BN Bjornstad, R Schalla, and WD Webber. 2000. *Revised hydrogeology for the suprabasalt aquifer system, 200-East area and vicinity, Hanford Site, Washington*. PNNL-12261, Pacific Northwest National Laboratory, Richland, Washington.

Wurstner SK, PD Thorne, MA Chamness, MD Freshley, and MD Williams. 1995. *Development of a three-dimensional ground-water model of the Hanford Site unconfined aquifer system: FY 1995 status report*. PNL-10886, Pacific Northwest Laboratory, Richland, Washington.

Appendix

Barometric Corrected Water-Level Responses for Selected Wells Tested During Fiscal Year 1999

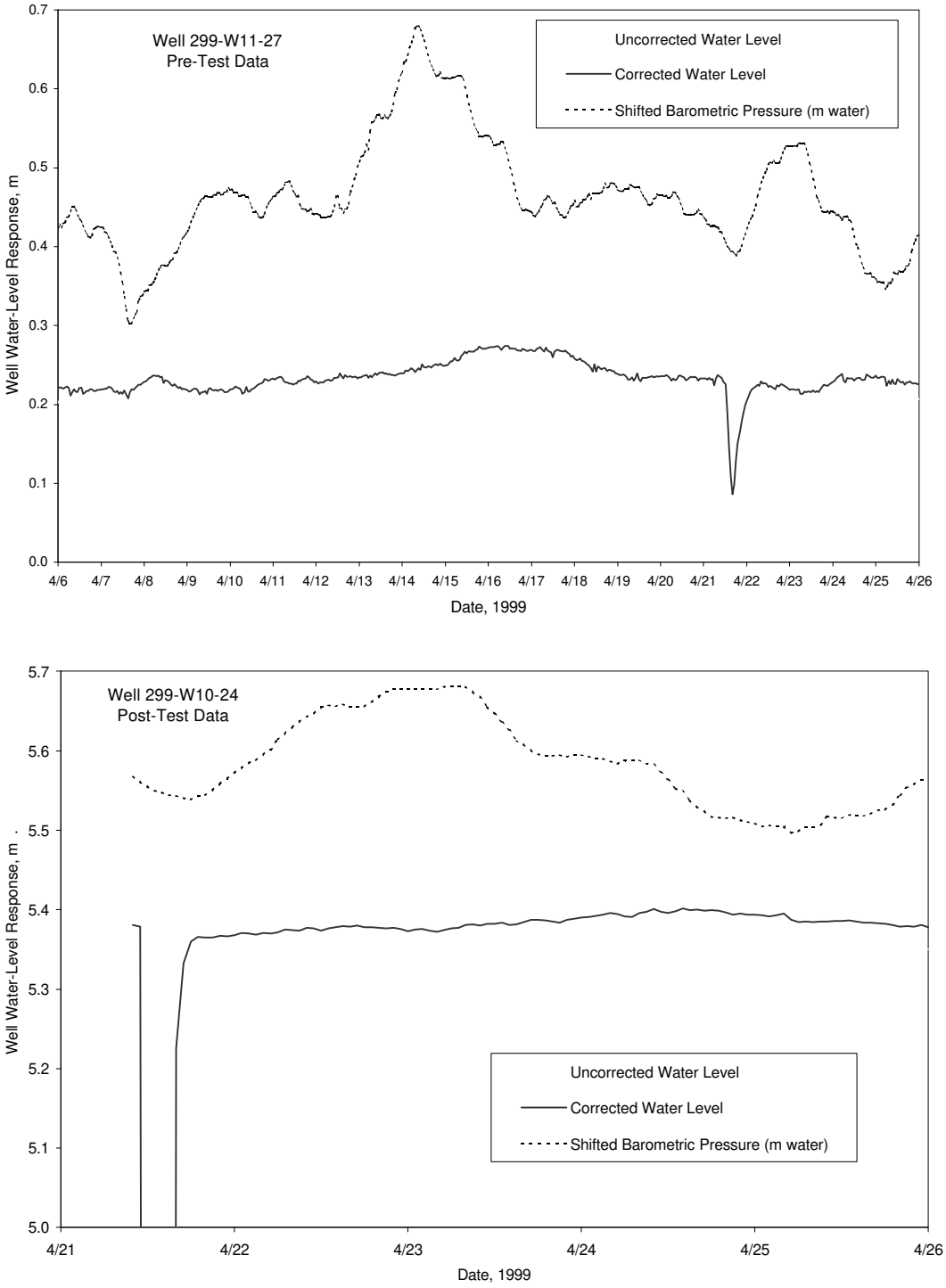

Figure A.1. Multiple-Regression, Model-Predicted, and Barometric Corrected Water-Level Responses for Wells 299-W11-27 and 299-W10-24

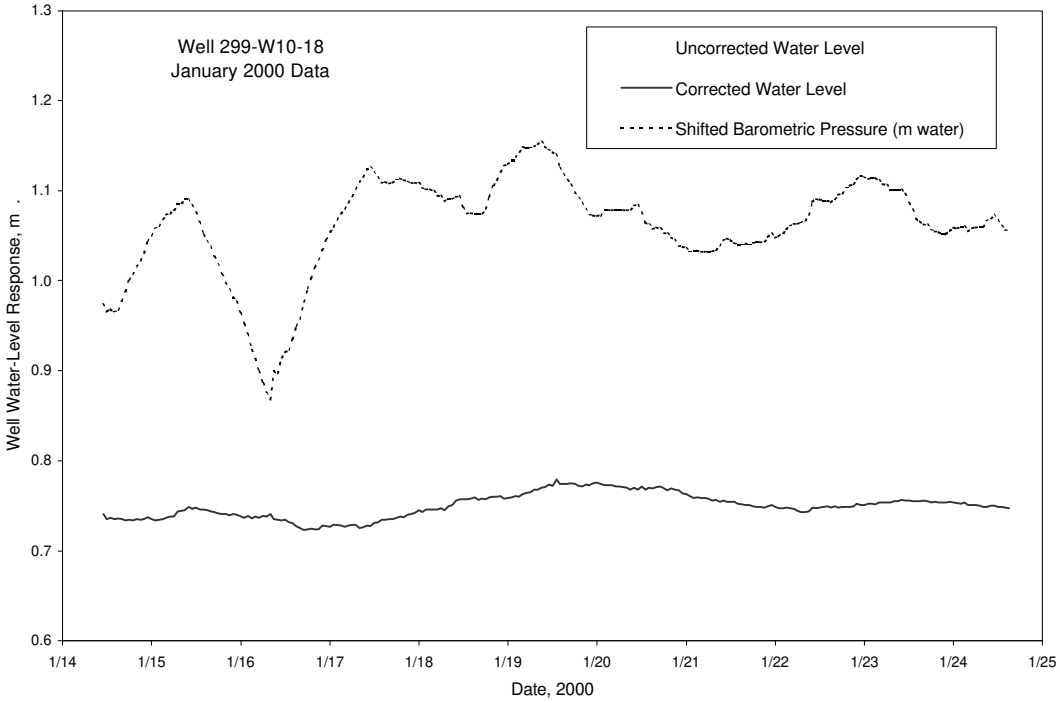

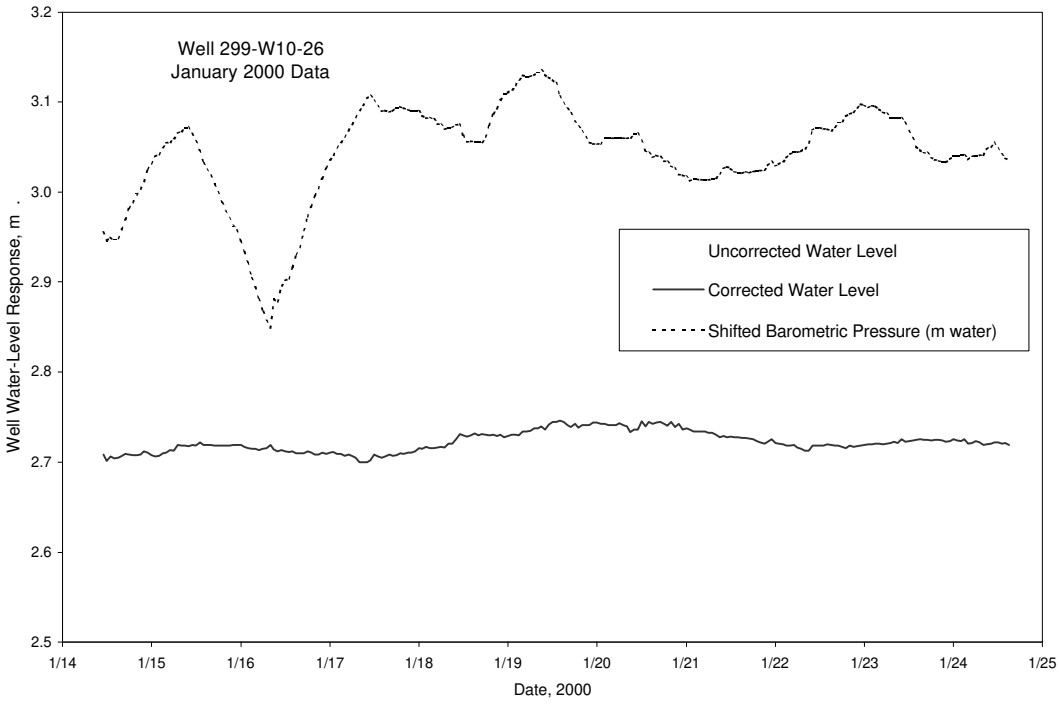

Figure A.2. Multiple-Regression, Model-Predicted, and Barometric Corrected Water-Level Responses for Well 299-W10-18 and 299-W10-26

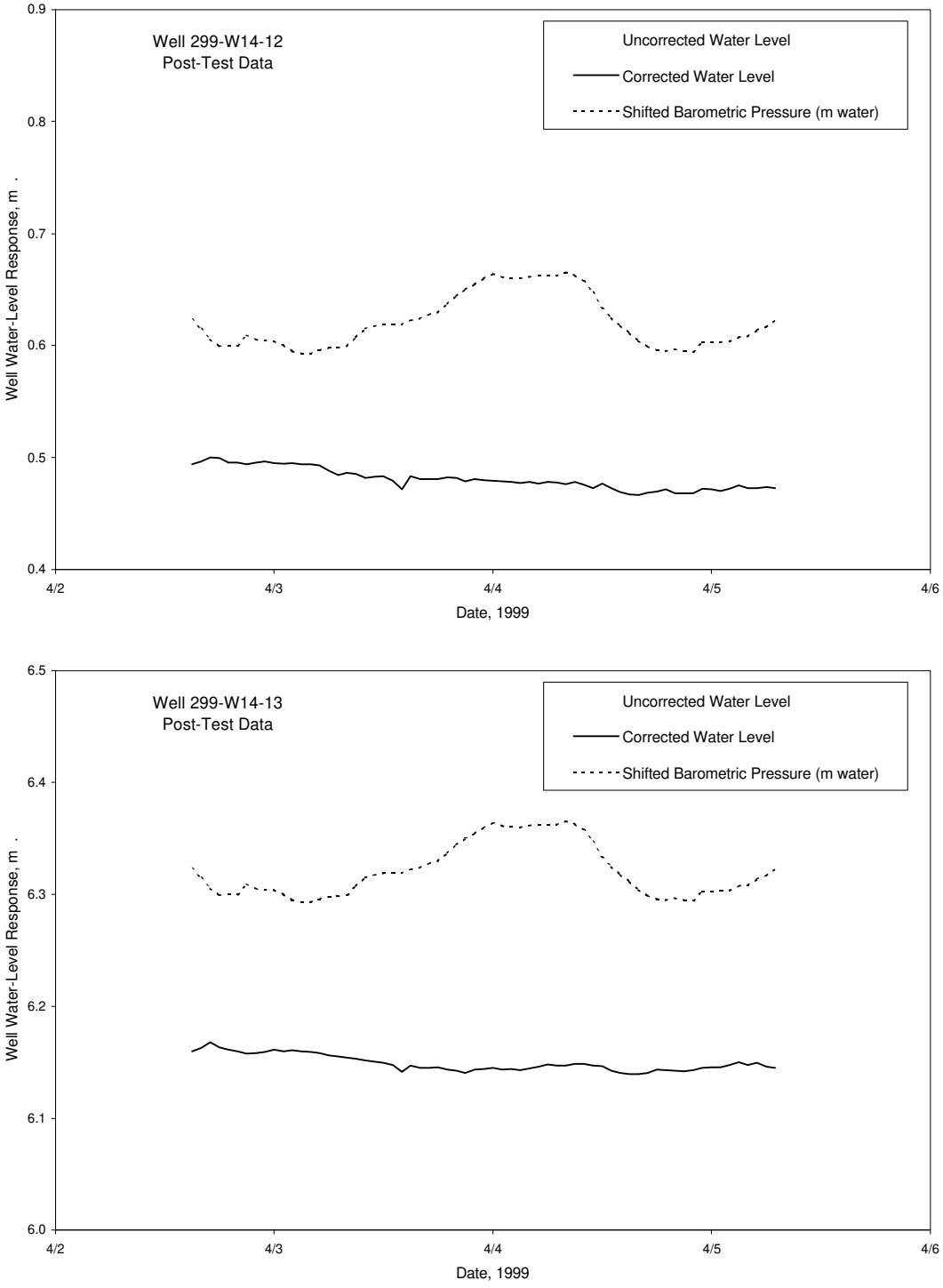

Figure A.3. Multiple-Regression, Model-Predicted, and Barometric Corrected Water-Level Responses for Well 299-W14-12 and 299-W14-13

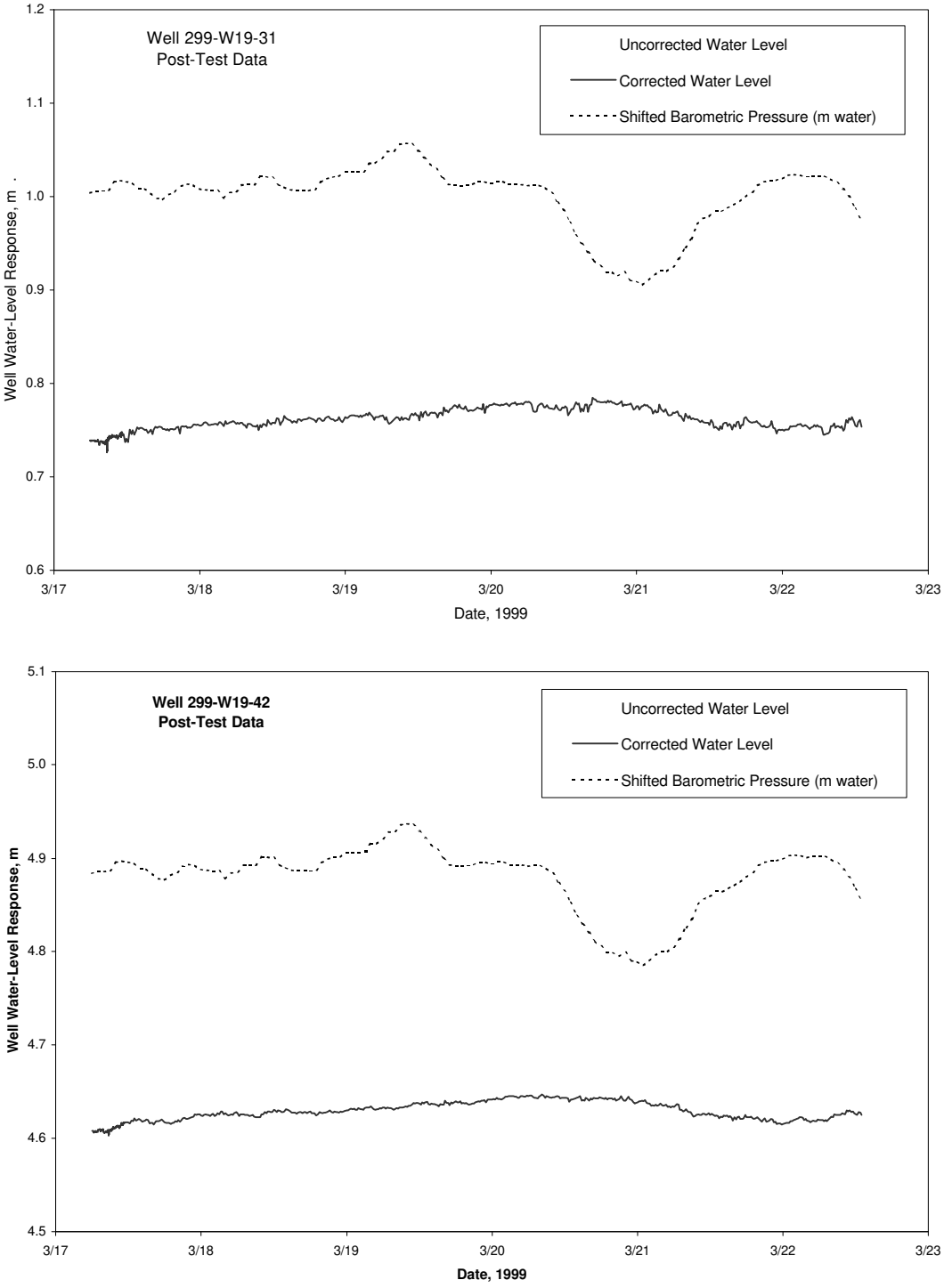

Figure A.4. Multiple-Regression, Model-Predicted, and Barometric Corrected Water-Level Responses for Well 299-W19-31 and 299-W19-42

Distribution

No. of Copies

OFFSITE

M. L. Blazek
State of Oregon Office of Energy
625 Marion Street N.E.
Salem, OR 97310

J. S. Bochmaier
U.S. Department of Energy
Forrestal Building, EH-412
1000 Independence Avenue, S.W.
Washington, D.C. 20585

J. Butler
Geohydrology Section
Kansas Geological Survey
University of Kansas
Lawrence, KS 66047

2 Confederated Tribes of the Umatilla Indian Reservation
P.O. Box 638
Pendleton, OR 97801
ATTN: W. Burke
S. Harris

R. A. Danielson
State of Washington Department of Health
2 South 45th Avenue
Yakima, WA 98908

B. W. Drost
Geological Survey
U.S. Department of the Interior
1201 Pacific Avenue, Suite 600
Tacoma, WA 98402

M. K. Harmon
U.S. Department of Energy
Cloverleaf Building, EM-44
19901 Germantown Road
Germantown, MD 20874-1290

No. of Copies

W. N. Herkelrath
Geological Survey
U.S. Department of the Interior
345 Middlefield Road, MS 496
Menlo Park, CA 94025

2 Idaho National Engineering and Environmental Laboratory
Lockheed Martin Idaho Technology Co.
P.O. Box 1625
Idaho Falls, ID 83415-2107
ATTN: J. M. Hubbell
J. B. Sisson

2 Nez Perce Tribe
Environmental Restoration/Waste Management
P.O. Box 365
Lapwai, ID 83540-0365
ATTN: S. Sobczyk
P. Sobotta

2 Schlumberger HydroGeological Technologies
6090 Greenwood Plaza Blvd.
Englewood, CO 80111
ATTN: R. Lewis
N. Clayton

2 State of Washington
Department of Health
Division of Radiation Protection
P.O. Box 47827
Olympia, WA 98504-7827
ATTN: D. McBaugh
G. Robertson

No. of Copies

3 Wanapum People
Grant County P.U.D.
P.O. Box 878
Ephrata, WA 98823
ATTN: R. Buck
L. Seelatsee
R. Tomanawash

2 Yakama Indian Nation
Environmental Restoration/Waste
Management Program
2808 Main Street
Yakima, WA 98903
ATTN: R. Jim
W. Rigsby

Foreign

M. Hagood
Schlumberger
Parkstraat 83
2514 JG The Hague
The Netherlands

12 **DOE Richland Operations Office**

H. L. Boston	H6-60
B. L. Foley	H0-12
M. J. Furman	H0-12
R. D. Hildebrand	H0-12
J. G. Morse	H0-12
J. P. Sands	H0-12
T. A. Shrader	H0-12
K. M. Thompson	H0-12
A. C. Tortoso	H0-12
R. M. Yasek	H6-60
Public Reading Room (2)	H2-53

4 **Bechtel Hanford, Inc.**

J. F. Armatrout	H0-19
B. H. Ford	H0-21
M. J. Graham	H0-09
G. B. Mitchem	H0-21

No. of Copies

ONSITE

5 **CH2M HILL Hanford, Inc.**

J. V. Borghese	H0-21
R. L. Jackson	H9-03
W. J. McMahon	H9-03
V. J. Rohay	H0-21
L. C. Swanson	H9-02

CH2M HILL Hanford Group

A. J. Knepp	H0-22

2 **State of Washington Department of Ecology**

D. Goswami	B5-18
A. Huckaby	B5-18

3 **U.S. Environmental Protection Agency**

D. R. Sherwood	B5-01

4 **Waste Management Federal Services, Inc., Northwest Operations**

D. R. Brewington	H1-11
M. G. Gardner	H1-11
D. E. Hollingsworth	H1-11
S. H. Worley	H1-11

4 **Waste Management Federal Services of Hanford, Inc.**

R. D. Haggard	G1-29
K. J. Lueck	S6-72
P. M. Olson	S6-72
R. W. Szelmeczka	S6-72

No. of Copies		
69	**Pacific Northwest National Laboratory**	
	J. G. Bush	K6-96
	D. B. Barnett	K6-81
	M. P. Bergeron	K9-36
	M. A. Chamness	K6-85
	C. R. Cole	K9-36
	P. E. Dresel	K6-96
	M. J. Fayer	K9-33
	M. D. Freshley	K9-36
	J. S. Fruchter	K6-96
	G. W. Gee	K9-33
	T. J Gilmore	K6-81
	M. J. Hartman	K6-96
	F. N. Hodges	K6-81
	V. G. Johnson	K6-96
	C. T. Kincaid	K9-33
	G. V. Last	K6-81
	T. L. Liikala	K6-96
	J. W. Lindberg	K6-81
	S. P. Luttrell (5)	K6-96
	J. P. McDonald	K6-96
	R. B. Mercer	K6-96
	L. F. Morasch	K6-86
	S. M. Narbutovskih	K6-96
	D. R. Newcomer	K6-96
	S. Orr	K9-33
	R. E. Peterson	K6-96
	S. P. Reidel	K6-81
	J. T. Rieger	K6-96
	R. G. Riley	K6-96
	R. Schalla	K6-96
	R. M. Smith	K6-96
	F. A. Spane, Jr. (15)	K6-96
	D. L. Stewart	K6-96
	M. D. Sweeney	K6-81
	P. D. Thorne (5)	K9-33
	E. C. Thornton	K6-96
	V. R. Vermeul	K6-96
	W. D. Webber	K6-96
	M. D. White	K9-36
	B. A. Williams	K6-81
	S. K. Wurstner	K9-36
	Information Release Office (7)	K1-06